Aalborg Universitet

AALBORG UNIVERSITY

DENMARK

D3.6 Relaying and Cooperative Communications Enhancements Based on Positioning Data (Final Report)

Nielsen, Jimmy Jessen; Ma, Yi; Majhi, Sudhan; Zhang, Yuanyuan; Raulefs, Ronald; Nasser, Youssef

Publication date:
2010

Document Version
Publisher's PDF, also known as Version of record

Link to publication from Aalborg University

Citation for published version (APA):
Nielsen, J. J., Ma, Y., Majhi, S., Zhang, Y., Raulefs, R., & Nasser, Y. (2010). *D3.6 Relaying and Cooperative Communications Enhancements Based on Positioning Data (Final Report)*.

ICT–217033 WHERE

D3.6 Version 1.0

Relaying and Cooperative Communications Enhancements Based on Positioning Data (Final Report)

Contractual Date of Delivery to the CEC: M28
Actual Date of Delivery to the CEC: 20.05.2010

Editor:	Yi Ma
Authors:	Yi Ma, Sudhan Majhi, Youssef Nasser, Jimmy Nielsen, Ronald Raulefs, Yuanyuan Zhang
Participants:	AAU, DLR, UoS, UR1
Work package:	WP3
Est. person months:	(Please fill in)
Security:	(Public)
Nature:	(RE)
Version:	1.0
Total number of pages:	76

Abstract:

This deliverable presents the performance evaluation and new approaches about location-aided cooperative communications. The investigation is performed for both the physical-layer and network-layer of wireless systems corresponding to WHERE scenarios C1-A and C2, respectively. For the physical-layer research, cooperative diversity-gain is analytically investigated for two typical relaying protocols, i.e. selective decode-and-forward (DF) and amplify-and-forward (AF), in various fading channels. It is shown that performance of cooperative communications is determined by several key parameters such as average signal-to-noise ratio (avg. SNR), user mobility and line-of-sight (LOS) condition. Those parameters can be obtained through intelligent exploitation of location information and finger-printing databases. The focus of network-layer research is on the throughput enhancement through employment of location-aided multi-hopping and node-selection schemes. Two link-quality estimation algorithms, i.e. the position-based and SNR-based algorithms, are investigated for DF-based multi-hop networks. Moreover, computer simulations are performed for practical wireless systems. It is shown that knowledge of location can effectively improve the network performance particularly for situations where the instantaneous channel knowledge is unavailable at both transmitters and relays.

Keyword list: Relaying, cooperative communications, positioning, decode-and-forward, amplify-and-forward, node selection, average signal-to-noise ratio (avg. SNR), finger-printing, database.

Disclaimer:

EXECUTIVE SUMMARY

Cooperative relaying turns out to be a promising technique to improve the efficiency and reliability of wireless networks. One of primary objectives of the WHERE project is to deliver efficient cooperative communication through exploitation of the location information. Key question this work seeks to address is: what is the efficient way of utilising the location-related information in cooperative communications? This question has been carefully investigated from both the physical-layer and network-layer aspects. In general, the results of this deliverable should serve as the final input to Task 3.3 of WP3. The focus of this deliverable is on two typical WHERE scenarios, i.e. C1-A and C2. In addition to a brief introduction to three classical relaying protocols, this deliverable includes three technical chapters:

Chapter 2 addresses the location-aided decode-and-forward (DF) cooperative relaying in the physical-layer aspect. Specifically, we investigated the outage performance of DF relaying over asymmetric fading channels. New cooperative strategies and multi-link adaptation approaches were proposed for multiuser incremental relaying protocols. Location information was used as a kind of side information that offered average channel gain or imperfect channel knowledge. The impact of location information on the DF performance has been investigated through both analytical analysis and computer simulations.

Chapter 3 addresses the location-aided amplify-and-forward (AF) cooperative relaying in the physical layer aspect. Specifically, we investigated the outage performance of AF relaying over asymmetric fading channels. New power allocation strategies have been proposed to improve the average sum-rate and outage performance of two-way AF relaying network. According to the scenario C1-A, the location information was used to obtain parameters such as avg. SNR for various wireless links and mobility information. Both analytical and simulation results have shown the significance of using location information in cooperative AF relaying protocols.

Chapter 4 presents the location-aided relay selection technique that was used to improve the network-layer throughput or physical-layer outage performance. The focus is to consider the impact of node movements and delays when assuming periodic collection of link SNR plus location measurements. Simulation results indicated that high accuracy positioning systems could be used to estimate the link quality sufficiently accurate to match the avg. SNR based approach. In addition, the outage probability is analyzed for the location-aided relay selection.

TABLE OF CONTENTS

AUTHORS

Partner	Name	Phone/Fax/e-mail
AAU		
	Jimmy Jessen Nielsen	Phone: +45 9940 9867 Fax: N/A e-mail: jjn@es.aau.dk
DLR		
	Ronald Raulefs	Phone: +49 8153 282803 Fax: +49 8153 281871 e-mail: Ronald.Raulefs@DLR.de
UoS		
	Yuanyuan Zhang	Phone: N/A Fax: N/A e-mail: yuanyuan.zhang@surrey.ac.uk
	Yi Ma	Phone: +44 1483 68 3609 Fax: +44 1483 68 6011 e-mail: y.ma@surrey.ac.uk
UR1		
	Sudhan Majhi	Phone: +33 22323 8703 Fax: N/A e-mail: sudhan.majhi@insa-rennes.fr
	Youssef Nasser	Phone: +33 22323 8758 Fax: N/A e-mail: youssef.nasser@insa-rennes.fr

LIST OF ACRONYMS AND ABBREVIATIONS

3GPP	3rd Generation Partnership Project
AF	Amplify and Forward
AP	Access Point
ARQ	Automatic Repeat reQuest
AWGN	Additive White Gaussian Noise
BER	Bit Error Ratio
BPS	Bits Per Symbol
BPSK	Binary Phase Shift Key
CRC	Cyclic Redundancy Check
CSI	Channel State Information
DF	Decode and Forward
FER	Frame Error Ratio
IR	Incremental Redundancy
LOS	Line Of Sight
MAC	Medium Access Control
MACS	Modulation Adaptive Cooperation Schemes
MD	Mobile Device
MRC	Maximum Ratio Combining
NE	Nash Equilibrium
NLOS	Non Line Of Sight
PDU	Protocol Data Unit
RCPC codes	Rate Compatible Punctured Convolutional codes
RD	Relay to Desintation
RSS	Received Signal Strength
SD	Source to Destination
SNR	Signal-to-Noise Ratio
SR	Source to Relay
STC	Space Time Code
TDMA	Time Division Multiple Access
TWRC	Two Way Relay Channel

1   INTRODUCTION

Channel fading, limited transmission power, user mobility and the lack of protection against interfering signals lead to high frame-error rates in cellular, ad-hoc and sensor networks [YH07], [GJ06]. The major obstacle for the next generation wireless networks requiring high bandwidth efficiency is signal fading due to multipath propagation. Frequency, time and spatial diversity, or hybrids of them have been used to mitigate the fading effects. Spatial diversity, while being more efficient in terms of bandwidth and delay, remains unattractive, since it calls for multiple antennas for transmission and/or reception, a requirement not always possible due to size, hardware or cost limitations.

While resolving the difficulties of installing multiple antennas on small communication terminals, cooperative communication has gained much interest by allowing a form of transmit diversity by cooperation between single-antenna users, creating a virtual antenna array [YH07], [NHCL05], [SSL05], and [IHL07]. Cooperative communication utilizes beamforming or space-time coding (STC) [SW08] to create a virtual MIMO system and involves multi layer design [NHH04b], [HL08]. A user cooperative region as defined in [WSL$^+$07] is the set of partners (relays) who will share and coordinate their resources to enhance the transmission quality leading to an improvement in the error probability or throughput for this user. In cooperative communication, relays forward the information to the receiver, which will then receive multiple replicas of the same information signal transmitted over independent fading channels [IHL07]. Because the channels are independent, the probability that all the signals will fade simultaneously is reduced considerably. The main differences between cooperative and non-cooperative systems are the use of multiple users' resources to transmit the data of a single source; and secondly, a proper combination of the multiple signals is made at the destination [HHCK07]. Note that cooperation does not cause a loss of efficiency in the system. Indeed, the spectral efficiency of each user improves due to the diversity achieved [NHH04b], [SSL07a].

Cooperative communication is a new communication paradigm promising significant capacity and multiplexing gain increase in wireless networks; it has also been shown to reduce the complexity of routing problems and realizing seamless networking [Rei08]. It is a very attractive technology for energy-constrained networks such as wireless sensor or robotic networks, where nodes are powered by batteries [LC06]. Several relaying schemes have been explored and are summarized in the following section.

1.1   Relaying schemes

Several cooperation techniques have been explored in the literature, namely Decode-and-Forward, Amplify-and-Forward, Coded Cooperation, Compress-and-Forward, etc. Most of those techniques adopt either Maximal Ratio Combining (MRC) or selective combining at the destination [HHCK07].

1.1.1   Amplify and Forward (AF)

In this case each relay amplifies and retransmits the received source signal to the destination. However, during this process noise and interference are also amplified [NHCL05], [ARDB08]. In AF, it is assumed that the receiver has knowledge of the inter-user channel coefficients to do optimal decoding; hence, some mechanism of exchanging this information must be incorporated, which introduces yet another challenge [NHH04b]. Signals of all users in AF are transmitted through orthogonal channels using TDMA, FDMA or CDMA schemes [HSL05].

1.1.2   Decode and Forward (DF)

also known as "demodulate-and-forward" or "detect-and-forward". In this case the relay decodes the received signal and re-encodes it with a potentially different code prior to retransmission. Error propagation, due to inaccurate decoding at the relay is a major drawback in DF, and hence the quality of the relay link, which is highly affected by interference, determines the quality of the decoding at the

relay [NHCL05]. In order to deal with interference, several strategies have been proposed such as "clean-and-forward" [NHCL05]. In order to cope with this problem, a new method is introduced, whereby transmission from the relay happens only if the decoding is reliable, which can be known by a using CRC check. Note that this should not present an additional overhead since most current and future wireless systems already employ CRC codes [NHH04b]. This hybrid version achieves the best performance. Another way of dealing with error propagation is the transmission from the relay only when the corresponding channel has a good SNR and refraining from transmitting when the SNR is low [NHH04b]. This scheme is known as Selective "Decode-and-Forward" (SDF). Another modification of DF is coded cooperation applying incremental redundancy. The source and the destination have a direct link plus an additional link through the relay. The relay decodes successfully the incoming data stream and forwards only the redundancy bits.

1.1.3   Compress and Forward (CF)

quantizes the data in one full block and forwards the analog signal. Usually Wyner-Ziv source coding is used for compression [Ros09].

1.1.4   Link-Adaptive Regeneration (LAR)

is a relaying strategy requiring simple average CSI knowledge of both the source-relay and relay-destination links [WCG06]. It can achieve full spatial diversity gain without the overhead of CRC codes. MRC at the destination is enough in this case to achieve full diversity. In diversity-achieving regenerative relaying strategies, LAR has been shown to outperform SDF [WCG06].

1.1.5   Some Remarks

Each of the schemes has its specific benefits as well as drawbacks. A practical comparison of DF and AF is offered in [YL05], using an approach based on error probability and mutual information. Both AF and DF are not very effective at low SNR [NHH04b], and this is due to the fact that their signaling is equivalent to repetition coding. The inter-user channel is a determining factor in comparing DF and AF schemes: When the inter-user channel is statistically worse than the two user channels, AF offers a higher capacity; otherwise, DF does [YL05]. However, for the worst case -which dominates the average performance of a system- AF and DF have been shown to be practically the same, and there's no practical benefit in considering a mixed-mode system. Coded cooperation however performs better than non-cooperative schemes at all SNRs, and better than other cooperative techniques for moderate to high SNR. On the other hand, coded cooperation unlike the AF and DF schemes is inherently integrated into channel coding [NHH04b].

Much of the works found in literature assume that the various nodes have partial knowledge of their channel state information (CSI) in the form of gain and/or phase information. Coherent reception requires the CSI. In interference-free schemes, the combiner output at the destination relies on Maximal Ratio Combining (MRC) to maximize the SNR statistic, while in interference-present schemes; the combiner output relies on Optimum Combining (OC) to maximize the SINR statistic [NHCL05].

In [YH07] a cooperative communication strategy for slow fading Ad-hoc networks is presented which increases the probability of successful transmissions and produces a significant performance gain. In this scheme, ACK/NAK feedback signals are used to acknowledge correct/incorrect reception similar to the Node Cooperative Stop and Wait (NCSW) and Cooperative MAC (CMAC) protocols. The main novelty of this strategy is the distinction made between cooperative and non-cooperative frames, the introduction of traffic categories at the node, where cooperative frames are given a high priority and finally the selection of the relaying node based on instantaneous channel conditions. In this case, a relaying node can become a partner only if it has already received a correct copy of the requested frame. Note that the drawback of distinguishing the two types of frames is the requirement for two MAC queues.

Another cooperative scheme, aiming at minimizing the total transmission time of a fixed amount of data is studied in [NVT08]. In this context two selection methods are proposed: Best expectation, which adaptively selects the optimal relay as a function of the instantaneous source-relay capacities, and Best-m where the source decides the optimal number of cooperative relays without relying on the network realization. The second, while resulting in a longer expected total transmission time, is simpler to implement. On the other hand, a two-stage cooperative communication protocol based on the use of timers is presented in [HL08].

Cluster-based cooperative communication -where nodes are aggregated into groups according to some criteria- is explored in [SSL05], [SGL06]. A model is presented which considers the effect of the random distribution of nodes across the network. It was shown that both the code structure and the nodes' distribution affect the diversity and coding gain of a system. Due to the mobility of the nodes, the number of nodes within a cluster is random, which reduces the diversity order [SSL05]. According to the presented protocol, a maximum of M nodes are assigned to help the source. The protocol consists of two phases: In phase 1 the relays are assigned for cooperation and the source transmits its data, while in phase 2 the relays which have been able to decode the message correctly retransmit it to the destination in a TDM manner, assuming perfect synchronization. However in practice, the lack of perfect delay synchronization among the cooperative nodes destroys the required STBC signal structure. A linear-prediction-based channel equalization technique to mitigate the effect of asynchronism is presented in [LC06].

In [LV05], cooperative communication over relay-based sensor networks, where no direct link between the sensors and destination is present, is studied. It was found that unless there is a perfect correlation between the transmit data; the gains of cooperation are very limited. Cooperation under such schemes at the physical layer showed to be able to provide large MIMO-like gains in throughput for the overall system [LV05].

A relay-based scheme where a fixed number of relays are utilized to design an OFDM cooperative protocol is presented in [SSL08]. This new protocol has been shown to achieve significant coverage extension in a WLAN scenario as compared to the direct transmission. In this scheme, the relay can help forward the data of multiple sources in one OFDM symbol, greatly improving the spectral efficiency, while still achieving full diversity at high SNR.

In [ISSL08], a cooperative scheme using AF and based on relay selection via available partial CSI at the source and relays is presented. This protocol achieves higher bandwidth efficiency while achieving the same diversity as that of conventional cooperative schemes. Partial CSI in this case expresses the instantaneous channel gain without the phase component. Cooperation decision is decided by comparing the source-destination channel gain and the optimal relay's metric and comparing it to the cooperation threshold. An SDF scheme, where the relay has a MAP-based receiver and the transmission is based on Log-Likelihood –Ratio (LLR) is presented in [PAR08]. This system achieved a performance of about 1dB worse than the optimum DF at considerably low implementation complexity. An approach in which the node positions and the channel fading states are assumed to be random is explored in [OAS07]. The proposed protocol requires minimal a priori knowledge of node positions and channel fading states. It further assumes that each node in the vicinity of the source knows its average link gain to the destination. In [SW08], a cooperative diversity based on modern error correction coding working with phase dithering is introduced. Unlike the traditional approaches, this method does not require knowledge of the number of transmitters, nor the CSI to be known at the transmitters' side.

Differential detection used along with diversity combining is known to provide a good tradeoff between performance and receiver complexity [HSL05]. A differential AF transmission scheme for a two-user cooperative communication system is presented in [HSL05]. The proposed scheme provides a better performance than direct transmission with either differential or coherent detection.

Relay selection has a significant impact on the performance of the system, and has been explored in [ZZC$^+$07]. Unlike most of the existing cooperation-based routing algorithms which are implemented by finding a shortest path route first, the Minimum Power Cooperative Routing (MPCR) introduced in [IHL07] makes full use of the cooperative communications while constructing the minimum-power route. In this algorithm, the minimum-power route from the source to the destination is constructed as a cascade

of the minimum-power single-relay building blocks, resulting in the least required transmit power among routing algorithms. Any distributed shortest-path algorithm can hence be used to find the optimal route with a polynomial complexity. This algorithm is implemented by letting each node calculate the costs of its outgoing links and then apply the Bellman-Ford algorithm. This results in a worst-case computational complexity at each node proportional to N^2. Another cooperative routing algorithm is the Cooperative Shortest Path (CSP), which chooses the next node in order to minimize the power transmitted by the last L nodes added to the route. Other similar routing algorithms which can be found in the literature include Relay-by-Flooding, Relay-Assisted and Relay-Enhanced routing [IHL07].

1.2   Effect of user mobility

Performance of wireless cooperative networks with a given number of users each moving according to the Random Waypoint mobility model has been studied in [WSL$^+$07]. In such a model, the mobility is characterized by a user moving with constant velocity from one point to another in a straight line. Performance degradation due to rapidly time varying channels in a repetition based coherent cooperative system is explored in [GJ06], along with several detection methods. It was shown that the performance of the system is affected much more by the mobility of source than the mobility of destination, despite the symmetry of the network.

Cooperative Communication advantages include: extension of the coverage at cell edge and to isolated areas, as well as penetration inside buildings and underground [Rei08], resistance to large scale shadowing, reduction in transmit power [HHCK07]. In resource constrained networks, cooperation can be exploited by an optimal allocation of power and bandwidth among the nodes based on the available CSI [HHCK07]. In [SSL07a] it was shown that the asymptotic performance of a simple cooperative scenario in which each relay combines the signals from the source and the previous relay is exactly the same as that for a much more complicated scenario in which each relay combines the signals from the source and all the previous relays.

A drawback of cooperative communication is the need of the mobiles to receive not only in the downlink band but also in the uplink band, thus requiring additional filtering and frequency conversion [NHH04b]. This is however not an issue for Ad-hoc wireless networks where users can receive and transmit on the same frequency band. For CDMA systems, transmit signals can be up to 100 dB above the level of receive signals, which is beyond the isolation achievable by existing direction couplers [NHH04b]. On the other hand, in the case where the detection by the partner node(s) is unsuccessful, the cooperation can be detrimental. Since cooperation involves the interaction between multiple users, it requires a cross-layer approach [HHCK07].

In slow fading environment, the CSI is acquired by using pilot symbols, which is not possible for fast fading environments. Also leads to poor spectral and energy efficiency. Processing and computing power in cooperative communication, usually neglected so far, was explored in [SWL06].

1.3   Using Location Information in Cooperative Communication

In [ZR03], a forwarding technique (GeRaF) based on geographical locations of the nodes is presented. This protocol is a best-effort one, where the relay node is not known a priori by the sender, but decided after the transmission has taken place. It is assumed that each node knows (perfectly) its position and the position of the destination node, and that a channel contention scheme exists to determine the forwarding node. In this scheme, each relay, assuming knowledge of its own location information, could assess its proximity toward source and destination and based on that proximity, contend for the channel with the rest of the relays [BKRL06a].

Note however that while solving the problem of relay scheduling, (GeRaF) does not achieve the diversity advantage of the other cooperative networks. This is due to the fact that each potential relay only receives a single version of the message, either from the source or from the current relay [BKRL06a], [ZV05]. A method to introduce a diversity effect to GeRaF is explained in [ZV05]; it relies on the nodes

keeping previously received information concerning each active message until it is able to decode the message correctly, then it can act as a relay and forward the message. Other routing protocols based on geographic information include GPSR, GEAR, LAR and DREAM [ZR03].

1.4   Overview of different chapters

This deliverable includes three technical chapters as follows:

Chapter 2 addressed the location-aided decode-and-forward (DF) cooperative relaying in the physical-layer aspect. Specifically, we investigated the outage performance of DF relaying over asymmetric fading channels. New cooperative strategies and multi-link adaptation approaches were proposed for multiuser incremental relaying protocols. Location information was used as a kind of side information that offered average channel gain or imperfect channel knowledge. The impact of location information on the DF performance has been investigated through both analytical analysis and computer simulations.

Chapter 3 addressed the location-aided amplify-and-forward (AF) cooperative relaying in the physical layer aspect. Specifically, we investigated the outage performance of AF relaying over asymmetric fading channels. New power allocation strategies have been proposed to improve the average sum-rate and outage performance of two-way AF relaying network. According to the scenario C1-A, the location information was used to obtain parameters such as avg. SNR for various wireless links and mobility information. Both analytical and simulation results have shown the significance of using location information in cooperative AF relaying protocols.

Chapter 4 presented the location-aided relay selection technique that was used to improve the network-layer throughput or physical-layer outage performance. The analysis was conducted by calculating the actual link quality via bit level simulations and using this as a reference to evaluate the performance of both location-based and avg. SNR based relay decision algorithms. Simulation results indicated that high accuracy positioning systems could be used to estimate the link quality sufficiently accurate to match the avg. SNR based approach.

2   LOCATION-AIDED DECODE-AND-FORWARD RELAYING

2.1   Coded Cooperation in Multiple-Access Incremental Relaying

Cooperative communications presents a distributed way of creating spatial diversity in wireless networks. This is especially attractive for mobiles due to the limited size constraints. We intend to look into cooperative coded communications with two sources using incremental redundancy (IR) at one relay. The required IR bits are selected based on the chosen base rate at the source and its channel conditions. For this we use the Nash equilibrium to find a fair distribution of the load between source and relay.

2.1.1   Introduction

Cooperative communication has been shown to be an effective technique that enables mobile terminals to share their antennas, thus creating virtual MIMO systems that reap the benefits of spatial transmit diversity in wireless networks. This is especially useful when size, cost, and hardware limitations deny wireless devices the luxury of having multiple transmit antennas [SEA03c]. As opposed to pure relay networks, nodes in cooperative networks act as both sources as well as relays. In other words, a node not only transmits its own information, but also helps others transmit theirs. The transmission process can be divided into two phases [HN02]. In the first phase, each node transmits its information to both the destination and other nodes, which act as potential future relays. In the second phase, the relay processes the message received from the source and forwards it to the designated destination. Processing strategies at the relay include simple forwarding, amplification and forwarding, either with fixed or variable amplification, and decoding and forwarding [HN02]. In this phase, the original source could send more messages, act as a relay for other sources, or simply remain silent. A novel technique in cooperative communication is to use the relay to transmit incremental redundancy information related to the source message. In this model, the source sends a punctured version of its codeword to both the relay and the destination. Consequently, the relay decodes the source codeword, then calculates and sends the destination the incremental redundancy bits that were punctured out by the source. The destination then combines the bits received from both nodes and decodes accordingly. This model reaps the improvement in bit error ratio (BER) and frame error ratio (FER) experienced in the previous cooperative techniques, and in addition increases throughput as a beneficial consequence of puncturing. The latter is achieved through using rate compatible punctured convolutional codes (RCPC) [Hag88] at the source node. Several questions arise within this framework. What is the optimal puncturing rate to be used by the source? What is the cost demanded by the relay for assisting the source and how does that affect the original choice of the puncturing rate? How much redundancy information should the relay send to the destination? In Section 2.1.2, the system model and operation are explained in details. The game-theoretic approach is outlined in Section 2.1.3. In Section 2.1.4 the transmission scheme from the transmitter to the receiver is presented followed by Section 2.1.5 which shows simulation results.

2.1.2   System Model

In the system model presented in Figure 2.1, we consider a situation where a single node (relay) is offering its services to relay information for the two other source nodes (S1 and S2), where the channels used are additive white gaussian noise (AWGN) channels. The fraction of bits the relay transmits on behalf of a source node sets the load balance between the two. Thus, each source node demands from the relay an amount of bandwidth that would optimally balance the load in a manner that maximizes throughput and minimizes the transmit error rate. But, in a multi-source system such as the one we have, sources compete to get the requested bandwidth from the relay which in turn charges a price in return for its services. This competition can be modeled as a strategic game for which Nash Equilibrium exists [Jr.50]. Thus, the equilibrium strategy for each node defines the optimal bandwidth to be allocated to it by the relay given the system conditions, and the transmission load will be distributed accordingly. In the cooperative technique discussed in this paper, the source transmits a punctured [Hag88] version of its codeword to
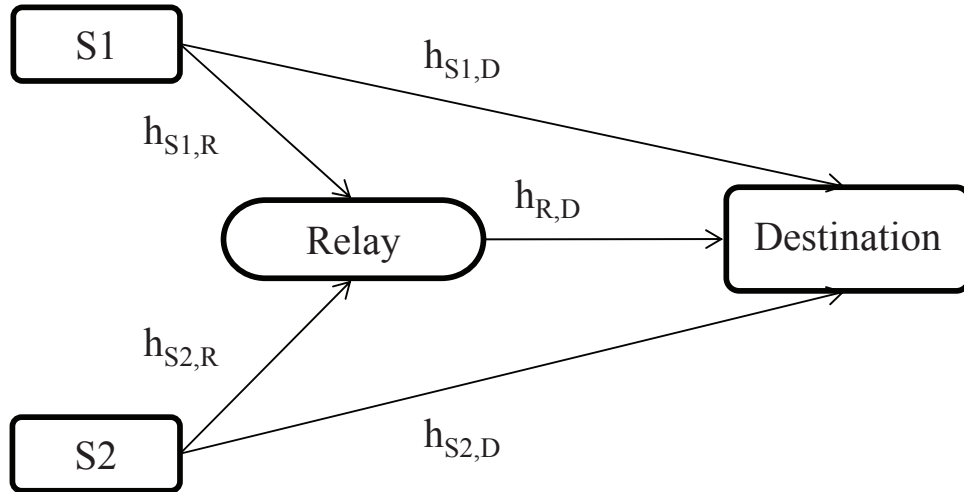
Figure 2.1: A system model with one relay node and two source nodes

both the relay and the destination. It is then the relay's job to calculate the missing redundancy bits and adaptively send them to the destination. Furthermore, the puncturing rate at the source is determined by the equilibrium bandwidth allocated to it by the relay, where a higher puncturing rate implies shifting more load to the relay and vice versa.

2.1.3 *Game-Theoretic Resource Allocation*

To determine the optimal bandwidth allocation scheme, game theory is an efficient tool to model how selfish nodes interact with each other. Moreover, relaying entails the expenditure of valuable resources. Thus the relay naturally asks for a price in return for its services. The pricing function used by the relay to charge the users is defined as:

$$C(W) = b \sum_{i=1}^{N} W_i \tag{2.1}$$

Where b is a non-negative constant and W_i is the strategy adopted by source S_i, i.e. the amount of bandwidth that source S_i wishes to buy given the current price and the strategies adopted by other users. Given the current price C, each selfish user strives to adopt the strategy that maximizes his own utility. Owing to the fact that the total price is determined by the strategies of all users, the resource competition among them is a strategic game for which Nash Equilibrium exists. We define that the utility function of a user is directly proportional to the throughput and inversely proportional to the energy consumption. The energy consumption is linked to a dedicated location that is known at the mobile and shared with the relay and/or the destination.

Thus it is expressed as $u = T/p$, where p is the transmit power and T is the throughput expressed as:

$$T = W f(\gamma) \frac{L}{M}, \tag{2.2}$$

where W is the bandwidth, L is the number of source information bits which are packed in a frame of M bits. $f(\gamma)$ characterizes the probability of a correct reception of a frame and is approximated as $f(\gamma) = [1 - BER(\gamma)]^M$ where γ denotes the SNR of the corresponding channel [GM00] and the location of the desired source. Hence, the utility function of S_i is expressed as:

$$U_i = \frac{T_{s_i,d_i}(p_i, W - W_i) + T_{s_i,r_i,d_i}(p_i, W_i)}{p_i} - CW_i \tag{2.3}$$

Substituting (2.1) and (2.2) into (2.3), we express the S_i's utility function as:

$$U_i = \frac{LW}{Mp_i}f(\gamma_{s_i,s_i}) + \frac{LW_i}{Mp_i}\Delta f(\gamma_{s_i,d_i}) - W_i[b\sum_{j=1}^{N} W_j] \tag{2.4}$$

where $\Delta f(\gamma_{s_i,d_i}) = f(\gamma_{s_i,r_i,d_i}) - f(\gamma_{s_i,d_i})$. Each user strives to maximize his utility function by buying the optimal amount of bandwidth from the source [ZCZ$^+$09]:

$$\frac{\partial U_i}{\partial W_i} = \frac{L}{Mp_i}\Delta f(\gamma_{s_i,d_i}) - [b\sum_{j=1}^{N} W_j + bW_j] = 0 \tag{2.5}$$

To find the Nash Equilibrium (NE), we need to solve N equations of the form of (2.5). This requires the solution to be developed in a centralized manner since each user should possess knowledge of the others' strategies.

In [ZCZ$^+$09] a decentralized mechanism is developed to find the NE in a distributed manner according to the following strategy update function

$$W_i(t+1) = W_i(t) + \Theta_i W_i(t)\frac{\partial U_i}{\partial W_i}, \tag{2.6}$$

Where Θ_i represents the speed with which S_i adjusts his strategy, and $W_i(t+1)$ is the updated strategy of S_i at time $t+1$. This strategy update function is based on the marginal profit function in microeconomics, depending solely on the pricing information from the relay. The key point in this algorithm is that each user's NE strategy must ensure $\frac{\partial U_i}{\partial W_i}$ to be zero at every instant. The optimal bandwidth W_i obtained at the NE defines the level of cooperation with the relay. Since the relay's job is forwarding the bits that were punctured out at the source node, the NE strategy W_i consequently defines the puncturing scheme to be used at the source node. The latter chooses from amongst a set of puncturing schemes [Lee94] in which each scheme corresponds to a cooperation level.

2.1.4   Adaptive Coded Cooperation

In what follows, we will focus on a single source node – relay node pair.

Transmission at the Source Node

After setting the load balance between the source and the relay and consequently the puncturing rate at the source, the latter sends its codewords according to the transmission processes depicted in Figure 2.2. At the termination of this process, both the relay and the destination will possess the encoded and punctured version of the source information bits.

Processing at the Relay Node

As is explained in the upper part of Figure 2.3, the relay uses the codeword received from the source to retrieve the original information bits through decoding and consequently calculates the incremental redundancy bits for the encoding scheme used. The relay's job now is to send the destination the missing redundancy bits that were punctured out by the source. Note that the relay does not send the redundancy bits in full, but rather incrementally upon receiving feedback from the destination.

Combining at the Destination

At the final stage of the process, the destination uses the inputs from the source and the relay to calculate the log likelihood ratios (LLR) of the bits in each message. The destination now possesses both components of the original message. The first is obtained directly from the source, and the other incremental
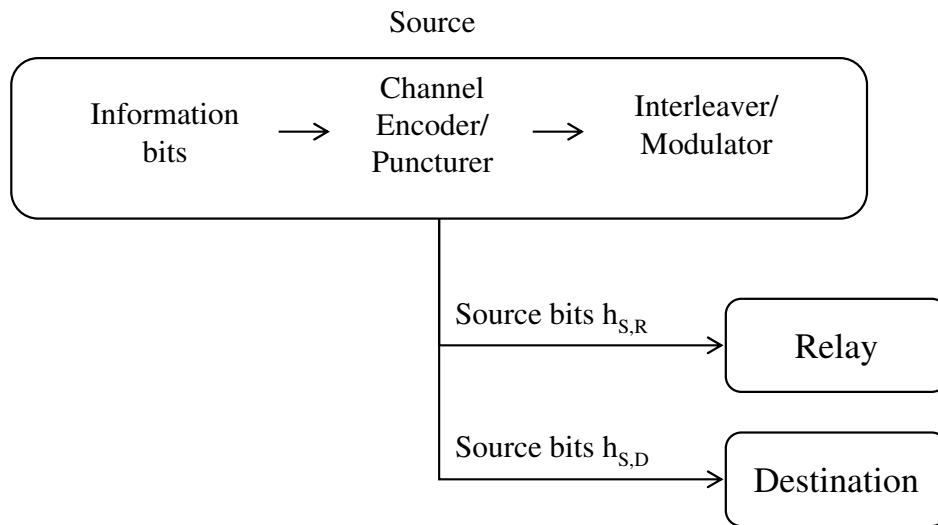
Source

Figure 2.2: The transmission method at the source node.

redundancy component is obtained from the relay. The destination now combines these inputs according to the original puncturing scheme to obtain a whole codeword expressed in terms of the log-likelihood ratios of its individual bits. This codeword is fed into a decoder that generates the original information bits. Note that the relay could send 1) the whole range of redundancy bits right from the start or 2) could transmit them incrementally (as it is originally planned) depending on the feedback from the destination to the relay. Alternatively the relay station could exploit the location information of the mobile and with this the channel condition of $h_{Si,D}$. Knowing the condition at the relay allows to assess the required redundancy bits that are required at the destination. This saves the required feedback between the destination and the relay and additional time slots for transmitting additional redundancy bits from the relay station to the final destination.

The IR scheme that would would start sending no redundancy bits per codeword. The destination thus decodes the input using the source bits while inserting dummy bits in place of the bits that where punctured out. The destination also predicts an acceptable correctness rate based on a weighted mean of and with the weights being based on the load share of each node. Latter is signified by the puncturing scheme and amount of incremental redundancy sent by the relay. If the decoding results were satisfactory, evident by achieving a better correctness than the one predicted, the destination proceeds using only the source bits, thus saving bandwidth and power for the relay. Otherwise, the destination asks the relay to increase the number of redundancy bits sent per codeword for the upcoming frames. The destination continues asking for a higher level of incremental redundancy bits for the upcoming frames until the correctness rate requirement is satisfied. This way, the relay does not have to send all incremental redundancy bits in the not infrequent case where the destination could decode using partial incremental redundancy at a satisfactory correctness rate. This process is also illustrated in Figure 2.3.

2.1.5   Simulation Results

We simulated a two user system as shown in Figure 2.1 that competes for the access to the relay station. The bandwidth size W is 10 MHz, and we use a convolutional channel code of rate $\frac{1}{2}$ of memory eight. Table 2.1 shows the different puncturing schemes that are used for adaptive incremental redundancy. The modulation scheme is 4-QAM. We compare in the following with a fixed coding rate three standard amplify and forward algorithms (AF), as well as a decode and forward scheme.

For the cooperative scheme using incremental redundancy adaptively we use the following parameter: The speed adjustment parameter is $\Theta = 0.01$ and the initial strategy adopted by each user is $W_i(t = 0) =$

Relay

Source bits $\longrightarrow$ De-Interleaver/ Demodulator $\longrightarrow$ Decoder

Interleaver Modulator $\longleftarrow$ Encoder $\longleftarrow$ Calculate IR bits

Relay bits: $h_{R,D}$

Increase IR level if needed

Destination

Relay bits $\rightarrow$ De-Interleaver/ Demodulator $\rightarrow$ LLR Decoder   Evaluate FER

Source bits $\rightarrow$ De-Interleaver+ Demodulator (obtain LLR) $\rightarrow$ Combine LLR $\rightarrow$ Decoder
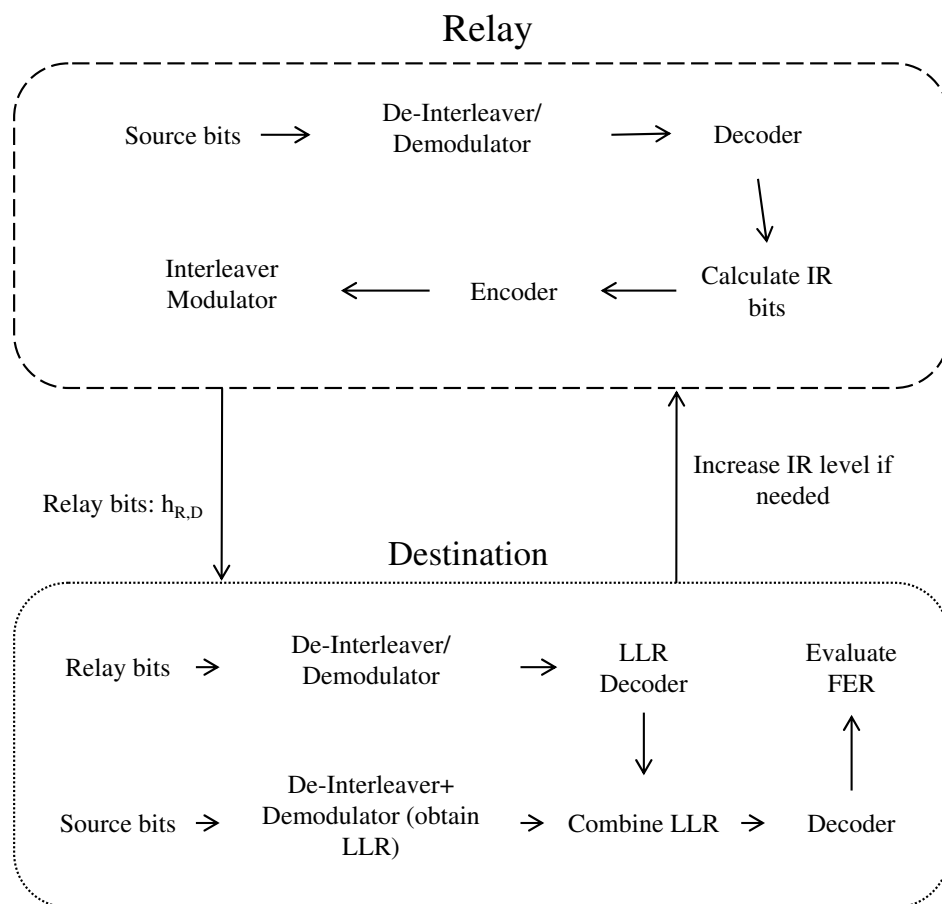
Figure 2.3: The combination process at the final destination.

Table 2.1: Various puncturing schemes to choose for each node S_i.

base code rate	Puncturing scheme
$\frac{1}{2}$	111111111111
$\frac{3}{5}$	011110111111
$\frac{2}{3}$	011110101111
$\frac{3}{4}$	011110100111
$\frac{6}{7}$	011110100110

$2 * 10^4$ Hz. For the pricing function in (2.1), we used $b = 10^{-5}$. The bit error rate function used is $BER = Q(\sqrt{(2 * Eb/N0)})$ where Q is the Q function, and Eb/N0 is the the energy per bit to noise power spectral density ratio.

Figure 2.4 shows a comparison between the various cooperative communication techniques in terms of BER for varying SNR. Amplify and forward techniques fare slightly better than simple forwarding. In addition, the results clearly show that techniques involving decoding at the destination have a superior performance to those where processing at the relay is limited to fixed or variable amplification. Interestingly, the adaptive incremental redundancy (IR) technique discussed has a superior performance to both AF, fixed amplification (AFFIXED) and variable amplification (AFVARIABLE) techniques, and comes close to matching the performance of the decode and forward(DF) technique, although it uses significantly less bits than the latter. The adaptive IR technique also operates with variable redundancy bits depending on the request from the destination. Please note this is not reflected in Figure 2.4 as the signal energy in the SNR is represented by the energy of the data symbol. The relative throughput of Figure 2.5 reflects the adaptive code rate.

The fort of the adaptive IR technique, in addition to achieving BER improvement, is the allowing a remarkably higher throughput for both the source and the destination compared to other cooperative methods. Using adaptively a code rate from table 2.1 allows to use the available spectrum W_i efficiently. Figure 2.5 shows the percentage of the redundancy bits saved by the adaptive IR technique for the whole system (source and relay) compared to traditional techniques that involve transmitting the whole code-word by the source and relay node. The 100% level is taken to be the case of sending only information bits without neither channel encoding nor cooperation. Although this has the highest throughput level, it is of course significantly prone to error due to the absence of an error correcting code and cooperation. It is worthy of notice that the adaptive IR techniques saves at least half the bits sent by other cooperative methods. Furthermore, for higher levels of Eb/N0, the adaptive IR technique achieves saving levels of up to 71%, which means sending less bits than the encoded non-cooperative technique while reaping the benefits of cooperation.

2.1.6   Conclusion

In this work we presented an adaptive incremental redundancy technique for cooperative communication networks. This technique operates within a game-theoretic approach that is used to optimize the level of cooperation between nodes. Moreover, the relay adapts the level of redundancy sent based on feedback from the destination. The location information of the mobile could be used by the relay to assess if or if not IR bits are required at the destination. We showed that this technique provides noticeable error rate improvement, and more interestingly, significantly enhances throughput. As the key benefits are a) using the relay helps the source to operate with a much higher code rate, b) the destination needs to receive less bits to successfully decode the bit stream of the source and c) the relay itself only needs to transmit the redundant data bits that are required. All this encourages the usage of incremental redundancy by

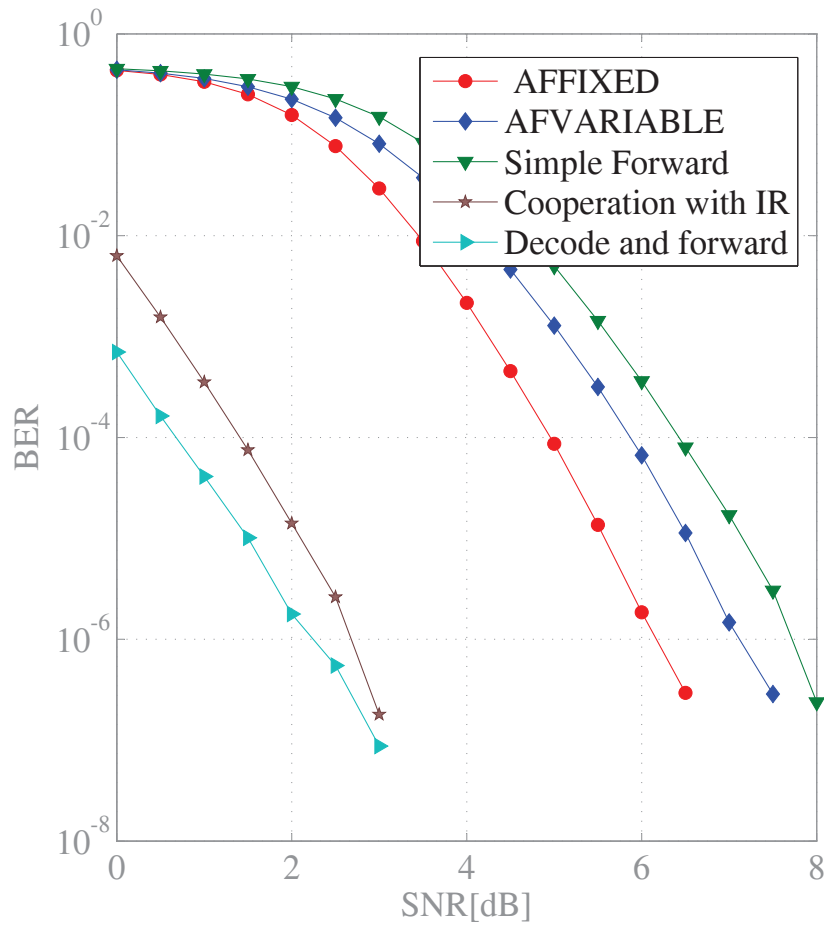Figure 2.4: BER of different relaying techniques - SNR[dB] reflects the energy of the data symbol versus the noise.
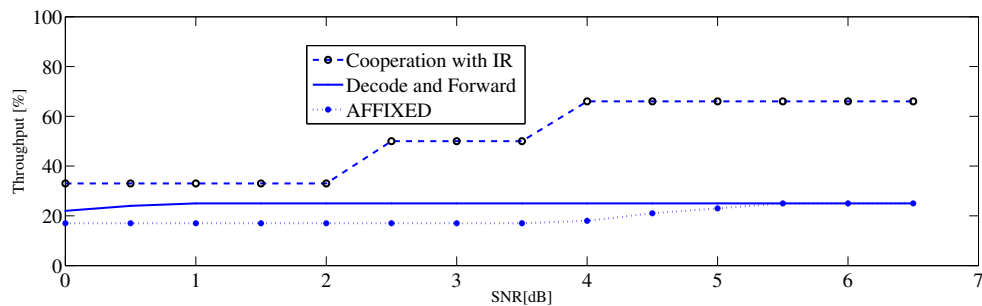

Figure 2.5: Comparison of analog (amplify and forward) and digital (decode and forward) decoding relay schemes: The effective throughput is significantly higher for the cooperative adaptive incremental redundancy (IR) scheme and also exploits higher modulation more effectively.

applying the NE over standard decode and forward relays together with location information combined with the derived knowledge of the wireless channel between the mobile and the destination.

2.2 Outage Performance of DF Relaying over Asymmetric Environments

2.2.1 Motivation and Approach

In practice, relay (R) nodes are usually located at different geographical locations and different distances with respect to source (S) and destination (D). One link may be in line of sight (LOS) situation and other links could be in non-LOS (NLOS) situation. For example, fixed relay nodes are used to forward source's data to the specific region (e.g. tunnel, behind building) and they often use directional antenna. So the R-D link is likely to be in LOS situation. However, we cannot assume such a situation for all other links, specially when D is in a shadowing region with respect to S. In other words, one link may undergo Rician distribution and other links may undergo Rayleigh distribution. Such scenario is referred to as asymmetric fading channel. This channel scenario can also be seen in cooperative cognitive radio where secondary terminals work as relaying nodes. In addition, all the links, i.e., S to i^{th} relay (S-R_i) and i^{th} relay to D (R_i-D), may be independent but non-identically distributed (i.n.d) fading channels. An asymmetric channel can be identified based on the positioning information of two nodes and corresponding signal strength between the link.

The outage probability of relaying networks over symmetric fading channel, in which all the links undergo the same fading distribution, is provided in several works [HKA07], [ZAL06], [ZZZ09]. The outage probability for repetition-based decode-and-forward (DF) relaying over Rayleigh fading channel is provided in [LTW04a] and [ZAL05] for high SNR and arbitrary SNR, respectively. The similar outage performance analysis over Nakagami-m fading channel is provided in [SSA06]. The asymmetric fading channel, mix of Rayleigh and additive white Gaussian noise, is introduced in [KS09]. The performance of amplify-and-relaying (AF) relaying over asymmetric fading, mix of Rician and Rayleigh, is provided in independent work in [SLL^{+}09], [SKS09]. However, to our knowledge, no work in the literature has provided any closed form expression of the outage probability for repetition-based relaying over asymmetric fading channel.

In this section, we provide a complete study of outage performance of the repetition-based DF relaying over asymmetric fading channels. The outage probability over independent identically distributed (i.i.d) is provided at arbitrary SNR. The outage probability over independent but non-identically distributed (i.n.d) is provided only at high SNR regime to simplify the mathematical formulation. In this work, we adopted DF relaying networks over two different scenarios called asymmetric channel I and asymmetric channel II. We show through analytical and simulation studies that the outage performance is better when the relay is in LOS situation with respect to the source rather than to the destination for the large number of relay nodes scenarios and the outage performance is better when relay is in LOS with respect to the destination rather than to the source for the small number of relay node environment. In the other words, asymmetric channel II has better outage performance than asymmetric channel I for large number of relay nodes environment and asymmetric channel I has better outage performance than asymmetric channel II for the small number of relay nodes environment.

2.2.1.1 Signal model of repetition-based DF relaying

In this framework, we consider a general two hop DF relaying network consisting of S, M relays, R_i, $i = 1, 2, \ldots, M$., and D. We assume that D performs maximal ratio combining at the receiver [KT08].

For the repetition-based relaying, we assume that the network has $M + 1$ time slots. In the first time slot, S broadcasts the signal to D and all R_i. After the successful decoding at R_i, it forwards the source's data to D at $(i + 1)^{\text{th}}$ time slot. So, all the channels are orthogonal to each other. Although its spectral efficiency is lower than that of conventional communications, it has $(M + 1)^{\text{th}}$ order diversity gain.

In the first time slot, the received signals at D and R_i are given as

$$y_{sd} = \sqrt{p_s}h_{sd}x + \eta_d \qquad (2.7)$$

$$y_{sr_i} = \sqrt{p_s}h_{sr_i}x + \eta_{r_i} \qquad (2.8)$$

where x is the signal transmitted by S, we omit time t in x for simplicity, p_s is the transmitted power by S, η_d and η_{r_i} are the zero mean and unit variance complex Gaussian random variables representing noise at D and R_i, respectively. The fading coefficients of S-D and S-R_i links are h_{sd} and h_{sr_i}, respectively.

The received signal at D from R_i at the $(i+1)^{\text{th}}$ time slot is given by

$$y_{r_id} = \sqrt{p_s}h_{r_id}x' + \eta_d \qquad (2.9)$$

where x' is the signal transmitted by R_i, h_{r_id} is the fading coefficient of R_i-D link. We have used equal power allocation at all nodes.

2.2.1.2 Channel model of asymmetric fading channel

For simplicity reasons, we use different notations of the random variables for different fading distributions. For Rayleigh fading channel, let $\gamma_{ab} = p_a|h_{ab}|^2$ be the instantaneous signal power of a-b link, it follows the exponential distribution. For Rician fading channel, the instantaneous signal power is denoted as ξ_{ab}, it follows the noncentral Chi-square distribution. The probability density function (PDF) of γ_{ab} and ξ_{ab} are expressed respectively as

$$f_{\gamma_{ab}}(z) = \frac{1}{\bar{\lambda}_{ab}}e^{-z/\bar{\lambda}_{ab}} \qquad (2.10)$$

$$f_{\xi_{ab}}(\xi) = \frac{K_{ab}+1}{\bar{\xi}_{ab}}e^{-\xi(K_{ab}+1)/\bar{\xi}_{ab}-K_{ab}}I_0\left(\sqrt{\frac{4K_{ab}(K_{ab}+1)\xi}{\bar{\xi}_{ab}}}\right) \qquad (2.11)$$

where $I_0(.)$ is the 0th order modified Bessel function of first kind, $\bar{\lambda}_{ab} = E\{\gamma_{ab}\}$, $\bar{\xi}_{ab} = E\{\xi_{ab}\}$, and K_{ab} is the Rician factor.

Although there are several possibilities of asymmetric fading channel, in this framework, we assume two asymmetric fading channels: namely asymmetric channel I and asymmetric channel II, shown in Fig. 2.6. For the asymmetric channel I, we assume that S-D and R-D links undergo Rician distribution and S-R link undergoes as Rayleigh distribution. For the asymmetric channel II, S-D and R-D links undergo Rayleigh distribution and S-R link undergoes Rician distribution. Of course, there are 2^3 transmission scenarios to be compared in such asymmetric environment. However, the idea here is not only to give a general framework of the outage probability but also to analyze if it is worth to locate D (respectively R) in LOS environment with respect to S. The particular asymmetric channel model can be configured based on the knowledge of LOS and NLOS situation of the links. The LOS and NLOS can be known by using the positioning information of the two nodes and corresponding signal strength between the nodes.

2.2.2 *Repetition-based DF Relaying*

In repetition-based DF relaying process, first, each relay node checks the received SNR with a predefined threshold value. If the received SNR of the relay node is greater than a predefined threshold value, the relay node is assumed to be decoded perfectly.

We assume that the network has M relay nodes. We define an instantaneous set $\mathscr{D}_l, l \in \{1,2,\ldots,M\}$ as the set of relay nodes at one instant which have successfully decoded the data or equivalently the information rate I_i of S-R_i is greater than a given system data rate R. The number of decoded relay nodes in $\mathscr{D}_l$ is denoted as $|\mathscr{D}_l|$. It has l relay nodes. This data rate R is defined as the minimum rate required by the different links to work properly. This set is defined as

$$\mathscr{D}_l = \{i : I_i > R\} \qquad (2.12)$$

Figure 2.6: Different asymmetric fading channel of a cooperative relaying network

The mutual information of the repetition-based DF relaying networks is

$$I = \frac{1}{M+1} \log_2 \left(1 + \frac{p_s |h_{sd}|^2}{N_0} + \sum_{i \in \mathscr{D}_l} \frac{p_s |h_{r_i d}|^2}{N_0} \right) \tag{2.13}$$

By using the total probability theory, the outage probability of the repetition-based DF relaying can be defined as [LTW04a, eq. (7)]

$$
\begin{aligned}
p_{out} &= Pr[I < R] \\
&= \sum_{l=0}^{M} Pr[I < R | |\mathscr{D}_l| = l] Pr[|\mathscr{D}_l| = l]
\end{aligned}
\tag{2.14}
$$

The probability of outage given that the network has l decoded relays is given by

$$Pr[I < R | |\mathscr{D}_l| = l] = Pr \left[\frac{p_s |h_{sd}|^2}{N_0} + \sum_{i \in \mathscr{D}_l} \frac{p_s |h_{r_i d}|^2}{N_0} < \gamma \right] \tag{2.15}$$

where $\gamma = (2^{(M+1)R} - 1)/\gamma_0$, $1/N_0 = \gamma_0$. From (2.12), (2.14) and (2.15) it is clear that the probability $Pr[|\mathscr{D}_l| = l]$ depends on the fading distribution of the S-R links, and the conditional probability $Pr[I < R | |\mathscr{D}_l| = l]$ depends on the fading distribution of the S-D links, S-R links and the number of relay nodes in $\mathscr{D}_l$. In the next section, we evaluate the outage probabilities over the two different asymmetric fading channels, shown in Fig. 2.6.

2.2.2.1 Asymmetric channel I:

For the asymmetric channel I, S-R link experiences Rayleigh distribution and S-D and R-D links experience Rician distribution. From (2.15) it is clear that the conditional probability $Pr[I < R | |\mathscr{D}_l| = l]$ is the cumulative distribution function (CDF) of $\xi_{sd} + \sum_{i \in \mathscr{D}_l} \xi_{r_i d}$ which is the sum of $(l + 1)$ noncentral Chi-square random variables.

The distribution of ξ_{ub} over i.n.d fading channel can be evaluated at high SNR regime. By using the initial value theorem (IVT), the Laplace transform (LT) of PDF of ξ_{sd} or $\xi_{r_i d}$ can be written as

$$\mathscr{L}(f_{\xi_{sd}}(\xi)) = \frac{1}{s} f_{\xi_{sd}}(0) \tag{2.16}$$

Now by using the multiplication properties of LT, the LT of the PDF of ξ_{ub} over i.n.d fading channel can be written as

$$\mathscr{L}(f_{\xi_{ub}}(\xi)) = \frac{1}{s^{l+1}} f_{\xi_{sd}}(0) \prod_{i \in \mathscr{C}_l} f_{\xi_{r_i d}}(0) \tag{2.17}$$

where the last equality is obtained due to $f_{\xi_{r_id}}(0)$ is the same for all i. The PDF of γ_{ub} is obtained by applying the inverse LT on the above, which yields

$$f_{\xi_{ub}}(\xi) = \frac{1}{l!} f_{\xi_{sd}}(0) \prod_{i \in \mathscr{D}_l} f_{\xi_{r_id}}(0) \xi^l \tag{2.18}$$

The CDF of ξ_{ub} or the equivalent conditional probability is derived by integrating the above, which gives

$$Pr[I < R || \mathscr{D}_l|] = \frac{1}{(l+1)!} f_{\xi_{sd}}(0) \prod_{i \in \mathscr{D}_l} f_{\xi_{r_id}}(0) \xi^{l+1} \tag{2.19}$$

Although the channel is asymmetric fading, the probability $Pr[|\mathscr{D}_l| = l]$ depends only on the fading distribution of the S-R link. The relay node R_i belongs to the set $\mathscr{D}_l$ if the received SNR of S-R_i link is greater than the predefined threshold value γ. Since S-R_i is Rayleigh distribution, the probability that a relay belongs to $\mathscr{D}_l$ can be computed as

$$\begin{aligned} Pr[i \in \mathscr{D}_l] &= Pr[\gamma_{sr_i} > \gamma] \\ &= e^{-\gamma/\bar{\lambda}_{sr_i}} \end{aligned} \tag{2.20}$$

The number of relay nodes in $\mathscr{D}_l$ is equivalent to the number of successive received SNR of S-R_i, ($i = 1, 2, ..., M$) links. Since S-R link has M sub-links, the number of successful links can be any number between 0 to M. The probability that l relay nodes are decoded is obtained as

$$Pr[|\mathscr{D}_l| = l] = \binom{M}{l} \prod_{i \in \mathscr{D}_l} \left(e^{-\gamma/\bar{\lambda}_{sr_i}} \right) \prod_{i \notin \mathscr{D}_l} \left(1 - e^{-\gamma/\bar{\lambda}_{sr_i}} \right) \tag{2.21}$$

Finally, substituting (2.19) and (2.21) in (2.14), the outage probability of repetition-based DF relaying over asymmetric and i.n.d fading channel is given by

$$p_{out} = \sum_{l=0}^{M} \binom{M}{l} \prod_{i \in \mathscr{D}_l} \left(e^{-\gamma/\bar{\lambda}_{sr_i}} \right) \prod_{i \notin \mathscr{D}_l} \left(1 - e^{-\gamma/\bar{\lambda}_{sr_i}} \right) \frac{(K_{sd}+1)}{(l+1)! \bar{\xi}_{sd} e^{K_{sd}}} \prod_{i \in \mathscr{D}_l} \frac{(K_{r_id}+1)}{\bar{\xi}_{r_id} e^{K_{r_id}}} \gamma^{l+1} \tag{2.22}$$

Since the above outage probability is obtained based on IVT, this analytical model is valid at medium and high SNR regime.

For i.i.d fading channel, the outage probability can be computed for arbitrary SNR values. If $\gamma_{sum} = \gamma_{sd} + \sum_{i=1}^{l} \gamma_{r_id}$ is a sum of $(l+1)$ i.i.d. random variables of the PDF given in (2.10). The LT of the PDF of random variable γ_{sum} is obtained by applying [AS64, eq.(29.3.8)] and the shifting property of the LT as

$$\begin{aligned} \mathscr{L}\{f_{sum}(\xi)\} &= \left(\int_0^\infty e^{-s\xi} f_\xi(\xi) d\xi \right)^{l+1} \\ &= (K+1)^{l+1} e^{-(l+1)K} \left(\frac{1}{\bar{\xi}s + K + 1} \right)^{l+1} e^{\frac{(l+1)K(K+1)}{\bar{\xi}s+K+1}} \end{aligned} \tag{2.23}$$

The PDF of γ_{sum} is obtained by applying the inverse LT and its shifting property on (2.23) as [AS64, eq.(29.3.81)]

$$f_{sum}(y) = \left(\frac{K+1}{\bar{\xi}} \right)^{(l+2)/2} e^{-(l+1)K - \frac{(K+1)y}{\bar{\xi}}} \left(\frac{y}{(l+1)K} \right)^{l/2} I_l \left(2\sqrt{\frac{(l+1)K(K+1)y}{\bar{\xi}}} \right) \tag{2.24}$$

The conditional probability $Pr[I < R || \mathscr{D}_l| = l]$ or CDF of γ_{sum} is computed by integrating (2.24) and

substituting $(l+1)K = b^2/2$ and $(K+1)y/\bar{\xi} = x^2/2$. The conditional probability is obtained as

$$
\begin{aligned}
Pr[I < R||\mathscr{D}_l|=l] &= \int_0^{\sqrt{2(K+1)\gamma/\bar{\xi}}} x\left(\frac{x}{b}\right)^l e^{-\frac{x^2+b^2}{2}} I_l(bx)dx \\
&= 1 - \int_{\sqrt{2(K+1)\gamma/\bar{\xi}}}^{\infty} x\left(\frac{x}{b}\right)^l e^{-\frac{x^2+b^2}{2}} I_l(bx)dx \\
&= 1 - Q_{l+1}\left(\sqrt{2(l+1)K}, \sqrt{\frac{2(K+1)\gamma}{\bar{\xi}}}\right)
\end{aligned}
$$

(2.25)

where $Q_M(,)$ is the Mth order Marcum Q-function.

For the i.i.d fading channel, we assume that all the sub-links of S-R have the same mean power i.e. $\bar{\lambda}_{sr_i} = \bar{\lambda} \; \forall i$. Since S-R experiences Rayleigh distribution, $Pr[|\mathscr{D}_l| = l]$ can be written as

$$
Pr[|\mathscr{D}_l| = l] = \binom{M}{l}\left(e^{-\gamma/\bar{\lambda}}\right)^l \left(1 - e^{-\gamma/\bar{\lambda}}\right)^{M-l}
$$

(2.26)

Now by substituting (2.25) and (2.26) in (2.14), the outage probability for i.i.d fading can be expressed as

$$
p_{out} = \sum_{l=0}^{M} \binom{M}{l}\left(e^{-\gamma/\bar{\lambda}}\right)^l \left(1 - e^{-\gamma/\bar{\lambda}}\right)^{M-l} \left(1 - Q_{l+1}\left(\sqrt{2(l+1)K}, \sqrt{\frac{2(K+1)\gamma}{\bar{\xi}}}\right)\right)
$$

(2.27)

where $Q_M(,)$ is the Mth order Marcum Q-function and $\bar{\lambda}$, $\bar{\xi}$ and K are the Rayleigh mean, Rician mean and Rician factor respectively for i.i.d fading channel.

For this asymmetric channel I, when a relay R_i belongs to $\mathscr{D}_l$, the S-R_i link is not in outage case. The signal transmitted from $R_i \in \mathscr{D}_l$ to D has less chance to be in outage in the $(i+1)^{\text{th}}$ time slot due to the presence of LOS component in the R_i-D links. Since the S-D link is also in LOS situation, the sum of the signals of S-D and R_i-D, $(i = 1,2,...,l)$ links has less chance to be in outage. The outage in the system is introduced mainly due to the Rayleigh fading nature of S-R_i link which shrinks the number of relay nodes in in $\mathscr{D}_l$. Hence, the number of relay nodes in $\mathscr{D}_l$ does not increase simply with the number of relays nodes in the network.

2.2.2.2 Asymmetric channel II:

In this asymmetric channel, we assume that the S-R link experiences Rician distribution and the S-D and R-D links experience Rayleigh distribution. In this scenario, the conditional probability is nothing but a CDF of the random variable $\gamma_{sum} = \gamma_{sd} + \sum_{i \in \mathscr{D}_l} \gamma_{r_id}$, sum of $(l+1)$ i.n.d exponential random variables. By substituting $K_{sd} = 0$ in $f_{\xi_{sd}}(0)$ and $K_{r_id} = 0$ in $f_{\xi_{r_id}}(0)$, from (2.19), the conditional probability can be obtained for asymmetric channel II as

$$
Pr[I < R||\mathscr{D}l| = l] = \frac{1}{(l+1)!\lambda_{sd}} \prod_{i \in \mathscr{D}_l} \frac{1}{\lambda_{r_id}} \gamma^{l+1}
$$

(2.28)

Since S-R link experiences Rician distribution, the probability that a relay R_i belongs to $\mathscr{D}_l$ is given by

$$
\begin{aligned}
Pr[i \in \mathscr{D}_l] &= 1 - \int_0^{\gamma} \frac{K_{sr_i}+1}{\bar{\xi}_{sr_i}} e^{-\xi(K_{sr_i}+1)/\bar{\xi}_{sr_i}-K_{sr_i}} I_0\left(\sqrt{\frac{4K_{sr_i}(K_{sr_i}+1)\xi}{\bar{\xi}_{sr_i}}}\right) d\xi \\
&= Q_1\left(\sqrt{2K_{sr_i}}, \sqrt{\frac{2(K_{sr_i}+1)\gamma}{\bar{\xi}_{sr_i}}}\right)
\end{aligned}
$$

(2.29)

where the last identity is obtained by substituting $\xi(K_{sr_i}+1)/\bar{\bar{\xi}}_{sr_i} = x^2/2$ and $K_{sr_i} = b^2/2$ in the above integration. Therefore, the probability that l relay nodes are decoded is obtained as

$$Pr[|\mathscr{D}_l| = l] = \binom{M}{l} \prod_{i \in \mathscr{D}_l} Q_1\left(\sqrt{2K_{sr_i}}, \sqrt{\frac{2(K_{sr_i}+1)\gamma}{\bar{\bar{\xi}}_{sr_i}}}\right) \prod_{i \notin \mathscr{D}_l}\left(1 - Q_1\left(\sqrt{2K_{sr_i}}, \sqrt{\frac{2(K_{sr_i}+1)\gamma}{\bar{\bar{\xi}}_{sr_i}}}\right)\right)$$

(2.30)

By substituting (2.28) and (2.30) in (2.14), the outage probability of repetition-based DF relaying over this asymmetric and i.n.d fading channel can be expressed as

$$p_{out} = \sum_{l=0}^{M} \binom{M}{l} \prod_{i \in \mathscr{D}_l} Q_1\left(\sqrt{2K_{sr_i}}, \sqrt{\frac{2(K_{sr_i}+1)\gamma}{\bar{\bar{\xi}}_{sr_i}}}\right) \prod_{i \notin \mathscr{D}_l}\left(1 - Q_1\left(\sqrt{2K_{sr_i}}, \sqrt{\frac{2(K_{sr_i}+1)\gamma}{\bar{\bar{\xi}}_{sr_i}}}\right)\right)$$
$$\frac{1}{(l+1)!\lambda_{sd}} \prod_{i \in \mathscr{D}_l} \frac{1}{\lambda_{r_id}}\gamma^{l+1}$$

(2.31)

For asymmetric channel II, $\gamma_{sum} = \gamma_{sd} + \sum_{i=1}^{l}\gamma_{r_id}$ is a sum of $(l+1)$ i.i.d. random variables of the PDF given in (2.10). By substituting $K = 0$ in the previous case of asymmetric channel I, the CDF of the random variable γ_{sum} or equivalent conditional probability is derived as

$$Pr[I < R||\mathscr{D}_l| = l] = \left(1 - e^{-\gamma/\bar{\lambda}}\sum_{i=0}^{l}\frac{(\gamma)^i}{i!\bar{\lambda}^i}\right)$$

(2.32)

Since S-R experiences Rician distribution in asymmetric channel II, the probability of l nodes in $\mathscr{C}$ over i.i.d fading channel is derived from (2.30) by substituting $K_{sr_i} = K$ as

$$Pr[|\mathscr{D}_l|] = \binom{M}{l} Q_1\left(\sqrt{2K_{sr_i}}, \sqrt{\frac{2(K_{sr_i}+1)\gamma}{\bar{\bar{\xi}}_{sr_i}}}\right)^l\left(1 - Q_1\left(\sqrt{2K_{sr_i}}, \sqrt{\frac{2(K_{sr_i}+1)\gamma}{\bar{\bar{\xi}}_{sr_i}}}\right)\right)^{M-l}$$

(2.33)

By substituting (2.32) and (2.33) in (2.14) the outage probability for this asymmetric and i.i.d fading channel can be written as

$$p_{out} = \sum_{l=0}^{M} \binom{M}{l} Q_1\left(\sqrt{2K}, \sqrt{\frac{2(K+1)\gamma}{\bar{\bar{\xi}}}}\right)^l\left(1 - Q_1\left(\sqrt{2K}, \sqrt{\frac{2(K+1)\gamma}{\bar{\bar{\xi}}}}\right)\right)^{M-l}$$
$$\times \left(1 - e^{-\gamma/\bar{\lambda}}\sum_{i=0}^{l}\frac{(\gamma)^i}{i!\bar{\lambda}^i}\right)$$

(2.34)

For this asymmetric channel II, the number of relay nodes in $\mathscr{D}_l$ is likely higher than that of asymmetric channel I due to the presence of LOS component in S-R_i link. The transmitted signal from $R_i \in \mathscr{D}_l$ to D has higher chance to be in outage in the $(i+1)^{\text{th}}$ time slot due to NLOS situation of the R_i-D links. Again, since transmitted signal in S-D link is also in NLOS situation, the outage of the system is mostly due to the NLOS situation of both S-D and R_i-D links. However, this outage can be compensated by the large number of relay nodes in $\mathscr{D}_l$. Since S-R_i link experiences LOS signal, the number of relay nodes in $\mathscr{D}_l$ increases with the number of relay nodes in the network. Therefore, for the large number of relay nodes, instantaneous SNR at D increases just with the large number of active R_i-D links. So, asymmetric channel II provides better outage performance than the asymmetric channel I for the large number of relay nodes in the network. However, this is not possible for asymmetric channel I because the number of active R_i-D links is very small due to the bottleneck of S-R_i link.

2.2.3   Simulation Results

In this section, the outage performance for repetition-based DF relaying is provided over two scenarios: i.n.d and i.i.d fading channels. For i.n.d fading channel, we assume that $\bar{\lambda}_{ab}$ and K_{ab} are uniformly distributed in [2,3] and [3,4], respectively. The LOS component is derived for a given value of K_{ab} and $\bar{\gamma}_{ab}$. For i.i.d fading channel, we assume that the mean $\bar{\lambda} = 2.5$ and Rician factor $K = 3.5$. The number of relay nodes is set to 3 and 8.

Fig. 2.7 shows the analytical ((2.22) and (2.31)) and Monte-Carlo outage performance for i.n.d fading channel over the two asymmetric channel scenarios. As expected the analytical results converge to the Monte-Carlo simulation for high SNR value ((2.22) and comments thereafter). Fig. 2.8 shows the analytical ((2.27) and (2.34)) and Monte-Carlo outage performance for i.i.d fading channel over the same asymmetric channels. As expected the analytical results match exactly to the Monte-Carlo simulations for any value of SNR.
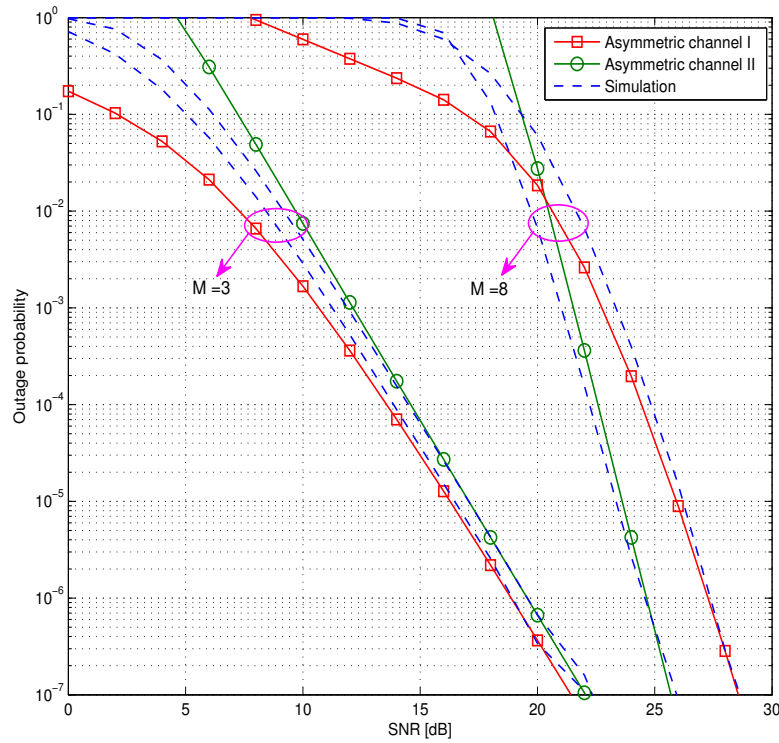

Figure 2.7: The outage performance of scenario I and scenario II over i.n.d fading channel for arbitrary SNR.

For both the i.n.d and i.i.d fading channel scenarios, the outage performance is provided for small (M=3) and large (M=8) number of relay nodes. Due to the presence of LOS components in S-D and R_i-D links, asymmetric channel I has better outage performance than that of asymmetric channel II when the number of relay nodes is small. However, when the number of relay nodes becomes large, asymmetric channel II shows better outage performance than that of asymmetric channel I over the same fading parameters. Indeed, when S-R_i link experiences LOS signal in asymmetric channel II, the number of relay nodes in $\mathscr{D}_l$ increases with the number of relay nodes in the network, thus, $\sum_{i \in \mathscr{D}_l} \gamma_{r_i d}$ increases in R_i-D link and leads to better outage performance. However, this is not possible in asymmetric channel I. In fact, in asymmetric channel I, the number of active R_i-D links is very small due to the bottleneck of S-R_i link. It implies that for the large number of relay nodes it is better to have LOS situation of S-R_i link in order to achieve better outage performance than having a LOS component of other links.
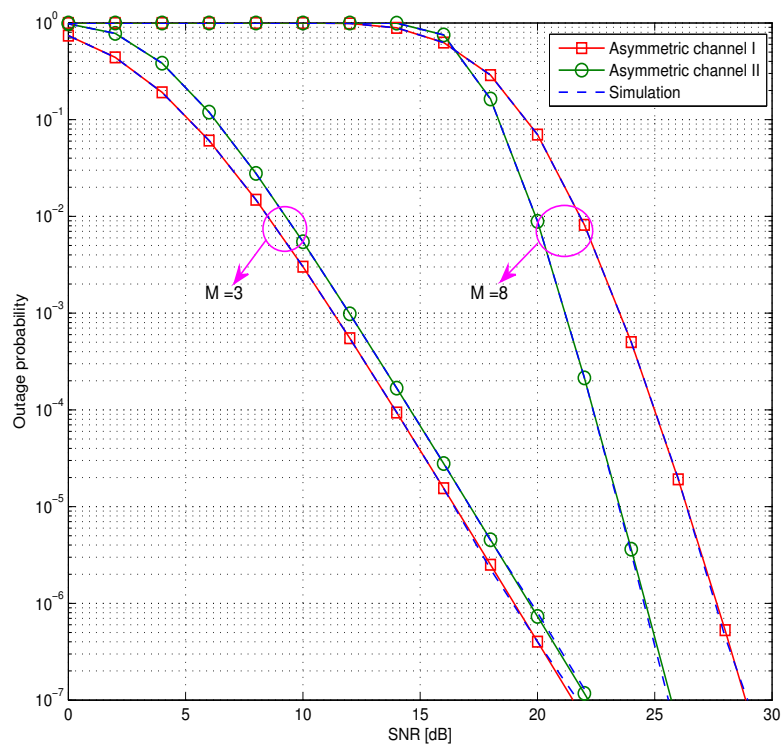
Figure 2.8: The outage performance of scenario I and scenario II over i.i.d fading channel for high SNR regime.

2.2.4 Conclusions

In this letter, we have analyzed the outage probability of repetition-based DF relaying over two asymmetric channel scenarios. The asymmetric channel scenarios (LOS and NLOS) can be identified through positioning information of two nodes and corresponding signal strength between the nodes. We show through analytical and the Monte-Carlo studies that the outage performance is better when the relay is in LOS situation with respect to the source rather than to the destination for the large number of relay nodes and the outage performance is better when relay is in LOS with respect to the destination rather than to the source for the small number of relay node environment. In the other words, asymmetric channel II has better outage performance than asymmetric channel I for large number of relay nodes environment and asymmetric channel I has better outage performance than asymmetric channel II for the small number of relay nodes environment.

2.3 Modulation-Adaptive Cooperation in Rayleigh Fading Channels with Imperfect CSI

2.3.1 Motivation and Approaches

Cooperative communication is an efficient way to provide spatial diversity without the requirement of multiple antennas at users [LTW04b]- [NHH04a]. When first proposed, the system is operated by allowing the cooperative nodes a fair opportunity to transmit messages through their own channels. With the development of sophisticated channel estimation and feedback techniques, some forms of channel state information (CSI) are available to the transmitters. Thus, the radio resource can be dynamically allocated among the senders to improve the communication efficiency.

Based on various cooperation protocols and network configurations, many resource allocation strategies have been proposed. Among these strategies, the power allocation is performed based on average channel SNR in [LBC$^+$05] [SSL07b], in which the resource allocation is in fact mainly affected by long-term and average properties of the channel. However, in wireless communications, the instantaneous channel gains are various because of shadowing and small scale fading. Perfect instantaneous CSI is assumed to be available at all senders in [BHW07]- [MYT08] to achieve better BER or higher data rate. The feedback cost is huge if CSI is estimated at receiver and sent back to all possible senders each time the channel changes. In our previous work [ZMT08], a class of novel modulation-adaptive cooperation schemes (MACSs) are proposed, in which perfect CSI is only needed at relays. The proposed schemes can significantly improve the throughput compared with conventional DF relaying systems.

Due to the transmission delay and the processing delay both at the transmitter and receiver, perfect CSI is not always available at transmitter. CSI feedback at the transmitter may become outdated, unless the channel variations are sufficiently slow [DHHH00]. Noisy or quantized channel prediction [SG02] are also very common in practical systems. So further investigation of modulation-adaptive cooperation with partial or imperfect CSI at the transmitter side is of great importance.

Here, we design the modulation-adaptive schemes in a relay network accommodating a source-destination pair and parallel relays with imperfect feedback. In a slowly time-varying channel, we use delayed CSI at the transmitter side to model the imperfect feedback. Our contributions can be summed up as follows. First, we develop our previous work with perfect CSI in [ZMT08] to current channel and feedback settings. The performance of this scheme shows no severe degradation because of the feedback delay. Second, a new adaptive-modulation scheme with adaptation at both the source and relay is proposed. With the delayed CSI of their own channels to destination at the source and relay, the proposed scheme can further improve the system performance in terms of throughput over fixed DF relaying and our previous scheme. Finally, we provide a discussion about how to use the location information in the proposed scheme.

2.3.2   System model and channel characterization

2.3.2.1 System model

Consider a relay network with a source-destination pair and K relay nodes employing Decode-and-Forward (DF) relaying protocol, as shown in Fig. 2.9.
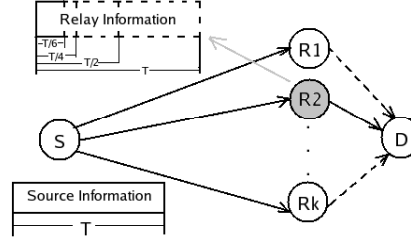

Figure 2.9: Block diagram of opportunistic DF relaying network, T: the duration of source frame, S: Source, D: Destination, R: Relay.

Without loss of generality, the nodes are supposed to transmit in time-orthogonal channels. In conventional DF cooperation, relays decode the data received from the source and transmit to destination one by one, in the same coding and modulation mode (referred as fixed DF in this report). In our previous work [ZMT08], we proposed a class of modulation-adaptive cooperation schemes (MACSs), and the transmission is completed in two phases in the following manner.

Phase I: the source transmits data in a fixed low-order modulation (BPSK for example). Both the destination and relays try to decode the data separately. If destination can decode the data correctly (judged by CRC), the transmission goes into the non-cooperation mode. Then the source starts a new transmission block. Or else, the 2nd phase of transmission is carried on.

Phase II: among the relays who have correctly decoded the data from the source, the one with the highest SNR of relay-destination link, is selected to forward data to destination. Adaptive modulation is used at the selected relay based on the CSI feedback. As an example in Fig. 2.9, only the 2nd relay is selected to forward data. If no relay is able to recover data from the source correctly, the source retransmits itself in this phase.

The channel fading coefficients between source and destination, source to the ith relay, ith relay to the destination are denoted by $h_{s,d}$, $h_{s,i}$ and $h_{i,d}$, respectively. The additive independent, zero-mean complex Gaussian noise at each channel is denoted by $n_{s,d}$, $n_{s,i}$, $n_{i,d}$ with variance $\mathcal{N}_0$, respectively. In Phase I, the destination receives $y_{s,d}$,

$$y_{s,d} = h_{s,d}x_s + n_{s,d} \tag{2.35}$$

and the ith relay receives $y_{s,i}$,

$$y_{s,i} = h_{s,i}x_s + n_{s,i} \tag{2.36}$$

During Phase II, if the ith relay is selected to transmit, the signal received at the destination $y_{i,d}$ is

$$y_{i,d} = h_{i,d}x_i + n_{i,d} \tag{2.37}$$

In our previous work [ZMT08], the mapping constellation is fixed for x_s. But for x_i, the constellation size is adjusted with respect to the CSI of RD link. Using the proposed MAP detection, the destination combines signals with different modulation formats, $y_{s,d}$ and $y_{i,d}$, to make the final decision.

For fixed DF cooperation, if the time duration of each phase is T, the total transmission takes $(K+1)T$. In our precious schemes, at most 2 phases are needed. Adaptive modulation can reduce the duration of the 2nd phase to T/2, T/4, T/6, respectively, if QPSK, 16QAM and 64QAM are used. This is reflected in Fig 2.9. Simulations show the proposed schemes significantly improve the throughput.

2.3.2.2 Slowly Time-varying Channel Model

The channel considered here is made up of both path loss and small-scale fading. The path loss between the transceiver pair is modeled by

$$L = G/d_{t,r}^{\alpha} \tag{2.38}$$

where $d_{t,r}$ is the distance between the transmitter and receiver, G is a constant that depends on the environment and α is the path loss exponent. For the free space path loss, we can choose $\alpha = 2$ and $G = G_t G_r \lambda^2/(4\pi)^2$, G_t and G_r are antenna gains at transmitter and receiver, respectively, and λ is the wavelength [Rap01].

Different from flat fading channels considered in most work in this area, here we model the channels and imperfect feedback as slowly time-varying Rayleigh fading channels and outdated CSI with the following assumptions [SG02]:

AS1): The channels $h_{s,d}$, $h_{s,i}$ and $h_{i,d}$ are independent Rayleigh fading channels with mean related to path loss and variance of $\sigma_{h_{s,d}}^2$, $\sigma_{h_{s,i}}^2$ and $\sigma_{h_{i,d}}^2$ respectively, and fixed during a whole cooperative transmission of one block.

AS2): Without loss of generality, the channel between each transmitter and receiver pair is modeled as slowly time-varying fading channel according to Jakes' model with Doppler spread f_d; thus we have $E\{h^*(t)h(t+\tau)\} = J_0(2\pi f_d \tau)$ (we omit the footnotes as it's general assumption for all channels), where τ is the time delay, and $J_0(\cdot)$ is the zeroth order Bessel function of the first kind.

AS3): Channel estimation is used at the receiver providing perfect CSI at the receiver side. To enable adaptive modulation, the receiver feeds the estimated CSI back to the transmitter. As is commonly assumed, we suppose that the feedback channel is error-free, which can be ensured by coding and ARQ protocol.

Based on AS1) to AS3), the transmitter obtains an unbiased channel estimation $\bar{h}$ based on partial CSI received from receiver through the feedback channel; before updated feedback arrives, the transmitter treats $\bar{h}$ as deterministic, and it relies on an estimation of the true channel h, which is formed as

$$h = \bar{h} + \varepsilon \tag{2.39}$$

where, ε is zero-mean complex Gaussian with mean σ_ε^2, independent of the channel coefficients. The deterministic pair $(\bar{h}, \sigma_\varepsilon^2)$ parameterizes the partial CSI, which is updated regularly given feedback information from the receiver. The partial CSI parameters $(\bar{h}, \sigma_\varepsilon^2)$ can be provided in many different ways with realistic consideration. In this report, we use delayed CSI as specified in [SG02].

Let $\hat{h}$ denote the channel feedback from receiver to transmitter. Notice that both h and $\hat{h}$ are complex Gaussian vectors, drawn from the same distribution $\mathscr{CN}(1, \sigma_h^2)$. It can be shown that $E\{h\hat{h}\} = \rho \sigma_h^2$, where the correlation coefficient $\rho = J_0(2\pi f_d \tau)$ determines the feedback quality. The minimum mean-square error (MMSE) estimator of h based on $\hat{h}$ is given by $E\{h|\hat{h}\} = \rho \hat{h}$, with estimation error having variance $\sigma_h^2(1-|\rho|^2)$. Thus, for each realization of $\hat{h}$, the transmitter obtains

$$\bar{h} = \rho \hat{h}, \sigma_\varepsilon^2 = \sigma_h^2(1-|\rho|^2) \tag{2.40}$$

2.3.3 Modulation adaptive cooperation design

As only one relay is selected to do the transmission, the parallel relay system with multiple relays is equivalent to the single relay system except the relay selection part, which is out of the scope of this report. Then the system can be simplified as shown in Fig. 2.10. Here we propose two modulation-adaptive transmission schemes providing delayed CSI available at relay only, at both source and relay, respectively.

2.3.3.1 Adaptive modulation at relay only

This contribution is an extension of our previous work by considering the delayed CSI. Let $\bar{\gamma}_{s,d}$, $\bar{\gamma}_{s,r}$ and $\bar{\gamma}_{r,d}$ denote the estimated received SNR of SD, SR and RD link. $\bar{P}_{s,d}^b$ and $\bar{P}_{s,r}^b$ denote the estimated block
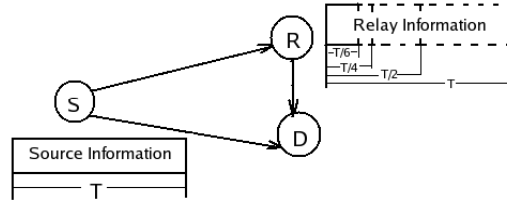
Figure 2.10: A single relay cooperative model

error rate for SD and SR link, and $\bar{P}_{s,d}$ and $\bar{P}_{r,d}$ are estimated BER of SD and RD link, respectively. The estimated BER of combined SD and RD link is $\bar{P}_{srd}$, and $\bar{P}'_{s,d}$ is the SNR if source retransmits in Phase II. For fair comparison with conventional DF system, we suppose the total transmission bits number is fixed, and adaptive modulation is to choose M_i-QAM to minimize the transmission time. The overall BER is constraint to BER_0. The transmission time normalized by the duration of first frame is $\{(1 - \bar{P}^b_{s,d}) + \bar{P}^b_{s,d}[(1 - \bar{P}^b_{s,r})(1 + 1/\log_2(M_i)) + 2\bar{P}^b_{s,r}]\}$.

Thus, the objective function is

$$\min_i\{(1 - \bar{P}^b_{s,d}) + \bar{P}^b_{s,d}[(1 - \bar{P}^b_{s,r})(1 + 1/\log_2(M_i)) + 2\bar{P}^b_{s,r}]\} \tag{2.41}$$

with constraint

$$\bar{P}_e = \bar{P}^b_{s,d}[(1 - \bar{P}^b_{s,r})\bar{P}_{srd}(M_i) + \bar{P}^b_{s,r}\bar{P}'_{s,d}] \leqslant BER_0 \tag{2.42}$$

Because relay is only used when destination fails and relay success in Phase I, $\bar{P}^b_{s,d} = 1$ and $\bar{P}^b_{s,r} = 0$. Then the problem can be simplified as

$$\max_i M_i \tag{2.43}$$

with constraint

$$\bar{P}_{srd}(M_i) \leqslant BER_0 \tag{2.44}$$

For this constraint, the channel information of SD link is needed at the relay as well. Here, we assume that the relay knows only the RD channel. The link adaptation scheme is restricted by the following constraint

$$\bar{P}_{r,d}(M_i) \leqslant BER_0 \tag{2.45}$$

The simulation results in [ZMT08] show the performance with constraint (2.45) is quite close to the one using (2.44).

Refer to [GC97], the BER of M-QAM modulation transmission over AWGN channel can be written as,

$$P(M_i) \approx 0.2\exp(-g_i\frac{E_s}{N_0}) \tag{2.46}$$

where, $g_i = \frac{3}{2(M_i-1)}$ for $M_i \geqslant 4$ and $g_1 = 1$ for BPSK. The M_i-QAM adaptive modulation is to divide the channel fading levels into several consecutive and non-overlapping fading regions R_i associated with M_i. Each R_i corresponds to the interval $\gamma \in [\gamma_i, \gamma_{i+1})$. If adaptive modulation among BPSK, QPSK, 16QAM and 64QAM is considered, substituting (2.46) into (2.45), we get the following boundaries,

$$\gamma_i = -\ln(5BER_0) \cdot 2(M_i - 1)/3, (i = 2, 3, 4),$$
$$\gamma_1 = 0, \gamma_5 = \infty \tag{2.47}$$

If the estimated SNR $\bar{\gamma}_{r,d}$ at relay falls into the set $[\gamma_i, \gamma_{i+1})$, relay chooses the modulation with rate i, and $M_i = 2^i$.

2.3.3.2 Adaptive modulation at both source and relay

If CSI is available at the source, not only the relay but also the source can dynamically change the constellation size. Denote M_i^s and M_i^r to be the constellation size for source and relay, respectively. While maintaining the overall BER no larger than BER_0, our target is to minimize the normalized transmission time as

$$\min_i \{(1 - \bar{P}_{s,d}^b)/i_s + \bar{P}_{s,d}^b[(1 - \bar{P}_{s,r}^b)(1/i_r + 1/i_s) + 2\bar{P}_{s,r}^b/i_s]\} \tag{2.48}$$

The BER constraint for the whole transmission is,

$$\bar{P}_e = \bar{P}_{s,d}^b(M_i^s)[(1 - \bar{P}_{s,r}^b(M_i^s))\bar{P}_{srd}(M_i^s, M_i^r)$$
$$+ \bar{P}_{s,r}^b(M_i^s)\bar{P}_{s,d}'(M_i^s)] \leqslant BER_0 \tag{2.49}$$

and if the transmission in Phase I fails at destination, the BER constraint becomes,

$$\bar{P}_{srd}(M_i^r, M_i^s) \leqslant BER_0 \tag{2.50}$$

To optimize both M_i^s and M_i^r together based on these equations is very complexity. Even if the optimal solution is mathematically traceable, M_i^s and M_i^r are functions of $h_{s,d}$, $h_{s,r}$, and $h_{i,d}$. This requires the CSI of both its own channel and the channels of the other nodes, which results in more feedback cost. Here we design a simpler solution in two steps that the source and the relay can determine their modulation locally.

Step 1. source chooses the maximum M_i^s to ensure SD link can achieve the target BER:

$$\bar{P}_{s,d}(M_i^s) \leqslant BER_0 \tag{2.51}$$

If the SD link is reliable, the destination can receive the data correctly, and transmission changes to non-cooperative communication. Thus only one phase is needed and the efficiency is improved. Now the problem for SD channel is a similar problem with traditional non-cooperative system. The adaptation regions are acquired as in (2.47). If the estimated SNR $\bar{\gamma}_{s,d}$ at source falls into the set $[\gamma_i, \gamma_{i+1})$, the modulation mode with transmission rate i is used, and $M_i^s = 2^i$.

Step 2. With similar consideration, relay chooses the maximum modulation order that can support target BER_0 for RD link. This optimization can be solved with the same boundaries described in (2.47). If the estimated SNR $\bar{\gamma}_{r,d}$ at the relay falls into the set $[\gamma_i, \gamma_{i+1})$, the modulation mode with transmission rate i is selected, and $M_i^r = 2^i$.

2.3.4 Performance Analysis

The overall average BER and throughput in terms of average bits per symbol (BPS) are two performance evaluation parameters we are interested in. Take the whole transmission for the first scheme to consideration, there are three possibilities for the transmission.

1) The transmission in Phase I is correctly received at destination with probability P_1,

$$P_1 = 1 - P_{s,d}^b = 1 - \int_0^\infty [1 - (1 - P_{s,d}(\gamma_{s,d})^B)]p(\gamma_{s,d})d\gamma_{s,d} \tag{2.52}$$

where B is the block size, $p(\gamma_{s,d})$ is the pdf of $\gamma_{s,d}$. In this case, there is no error.

2) The transmission to both relay and destination fails in Phase I, thus source retransmits in Phase II. This happens with probability

$$P_2 = P_{s,d}^b P_{s,r}^b \tag{2.53}$$

The average BER in this case is

$$P_{s,d}' = \int_0^\infty 0.2 \exp(-2\gamma_{s,d})p(\gamma_{s,d})d\gamma_{s,d} \tag{2.54}$$

3) The relay decodes correctly and transmits in Phase II. The probability for this case is $(1 - P_1 - P_2)$. With diversity combining detection proposed in [ZMT08], the average BER can be calculated as,

$$P_{srd} = \int_0^{\infty} \sum_i \bar{P}_{srd}(i) p(\gamma_{s,d}) d\gamma_{s,d} \tag{2.55}$$

For each modulation, $\bar{P}_{srd}(i) = \int_{\gamma_i}^{\gamma_{i+1}} \bar{P}_{srd}(i, \bar{\gamma}_{r,d}) p(\bar{\gamma}_{r,d}) d\bar{\gamma}_{r,d}$. The received SNR is linked with channel coefficients by $\gamma_{r,d} = |h_{r,d}|^2 \gamma$, and γ is transmit SNR. For a given realization of $\bar{h}_{r,d}$, the true channel gain $h_{r,d}$ can be viewed as a Gaussian random variable with non-zero mean and variance $(1 - \rho^2)\sigma_{r,d}^2$. The BER averaged over all possible realization of $h_{r,d}$ is,

$$\bar{P}_{srd}(i, \bar{\gamma}_{r,d}) = E_{h_{r,d}}\{P_{srd}(g_i, \bar{h}_{r,d}, h_{r,d})\}, \tag{2.56}$$

where $P_{srd}(g_i, \bar{h}_{r,d}, h_{r,d}) = 0.2 \exp[-(g_i |h_{r,d}|^2 + |h_{s,d}|^2)\gamma]$ is the instantaneous BER for each realization of $h_{r,d}$.

The overall BER is then,

$$P_e = P_1 \cdot 0 + P_2 \cdot P'_{s,d} + (1 - P_1 - P_2)P_{srd} \tag{2.57}$$

Substituting (2.52)-(2.56) to (2.57), we can get the exact expression of the overall BER.

Provided the probabilities of all the 3 possible cases in the transmission, the average bits per symbol (BPS) is a direct derivation.

$$S = P_1 \cdot 1 + P_2 \cdot 1/2 + (1 - P_1 - P_2) \sum_i \Pr(i)(\frac{1}{1 + 1/i}) \tag{2.58}$$

where $i = \log_2(M_i)$, $\Pr(i) = \int_{\gamma_i}^{\gamma_{i+1}} p(\bar{\gamma}_{r,d}) d\bar{\gamma}_{r,d}$ is the probability for relay to use modulation with rate i. From a long-term point of view, $\bar{\gamma}_{r,d}$ can be roughly seen as $\rho^2 \gamma_{r,d}$. When $\rho = 1$, it's equivalent to perfect CSI, and it can be mathematically proved that with $\rho < 1$, the average BPS is smaller than that with $\rho = 1$. This will be shown in the simulation results in next section.

The performance analysis for the 2nd proposed scheme is similar and further discussion is omitted here.

2.3.5 Simulation Results

In this section, we present simulation results for the proposed schemes. The basic settings for simulation are as follows:

Carrier Frequency:	5GHz
Velocity of user:	3m/s
Maximum Doppler:	50Hz
Symbol Duration:	$2\mu s$
Source Frame size:	192 symbols
Target BER:	1e-3
Coding:	16-bit CRC with generator polynomial coefficients 15935 (hexadecimal notation).

The average SNR of SD link is ranging from 0 to 20dB, and the average SNR of RD link is 20dB higher, assuming the relay is 10 times close to destination than source. For fair comparison and to reflect the improvement by adaptive modulation (not CRC), we use CRC for fixed DF in the simulation as well (referred as 'DF with CRC' in the figures).

Adaptive modulation at relay only

We consider the performance of single relay system as an example to see how much delayed CSI can affect the performance of the proposed scheme. The simulation results are shown in Fig. 2.11 and Fig. 2.12.
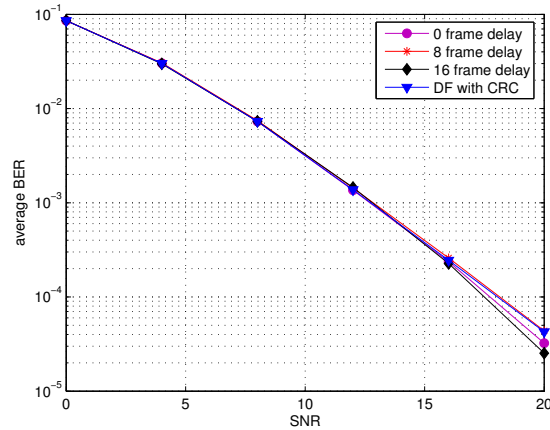

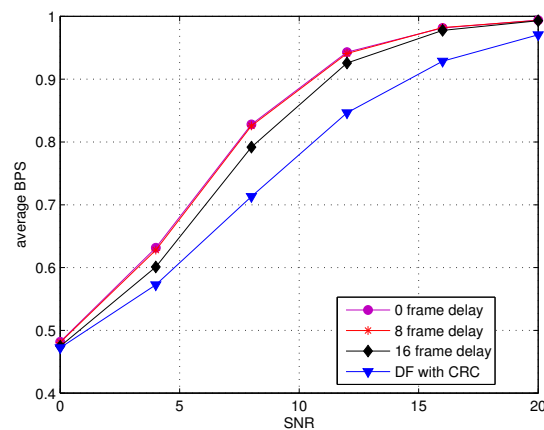Figure 2.11: BER performance vs. delay for CSI at relay only

Figure 2.12: BPS performance vs. location for CSI at relay only

Different delay of feedback is considered, 0, 8, 16 frames, where 0 frame delay is equivalent to perfect CSI at relay. The proposed scheme has close BER performance to fixed DF with CRC, but higher BPS. Equivalently, the proposed scheme can provide significant throughput improvement over fixed DF when their BER is at the same level. For simulations with delayed CSI, the BER performance is nearly the same with no delay, because of the constraint of target BER in our algorithm. At the same time the throughput improvement is still observable. Even if the CSI is delayed by 16 frames, the proposed scheme can provide higher throughput than fixed DF relaying. This shows the proposed scheme is robust to CSI delay in this slowly time-varying channel to some extent.

Adaptive modulation at both relay and source

From the results, shown in Fig. 2.13 and Fig. 2.14, we can observe that the throughput improvement is even higher, improved from 1 to nearly 2.5 bits/symbol. This is because when SD link is good enough, only one phase with high-order modulation is enough. The small feedback delay (such 8 frame delay)

doesn't have a severe impact on the performance as well. Even the throughput with 16 frame delay is still slightly higher than fixed DF with CRC.
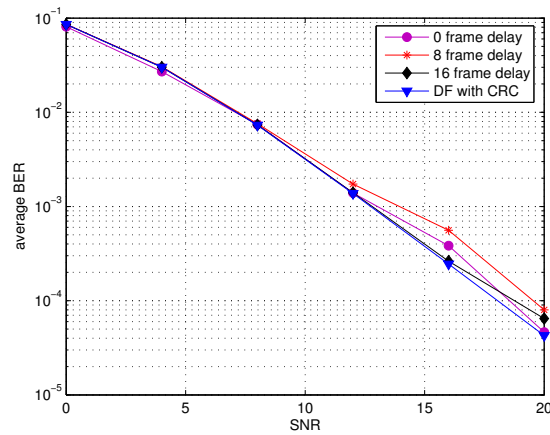
Figure 2.13: BER performance vs. delay for CSI at both source and relay
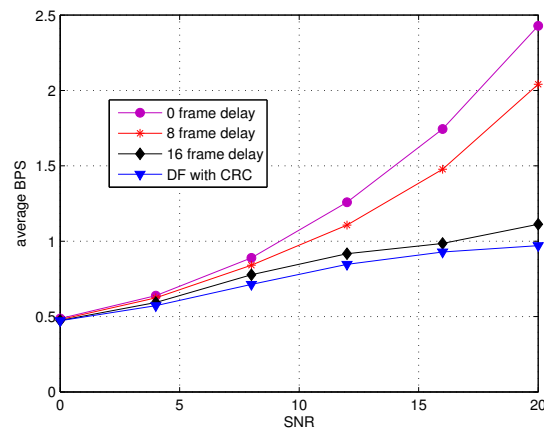
Figure 2.14: BPS performance vs. delay for CSI at both source and relay

2.3.6   *Conclusion and Discussion about Location-Aided Aspects*

2.3.6.1 Conclusion

We have addressed the adaptive modulation design for cooperative systems under slowly time-varying Rayleigh fading channels with imperfect CSI. Providing delayed CSI at the relay only or both source and relay, we designed the modulation-adaptive cooperation schemes, respectively. Simulation results show that the proposed design can significantly improve the throughput while keeping BER at the same level with fixed DF cooperation. In addition, CSI delay doesn't have severe impact on the performance.

2.3.6.2 How to use the location information

We answer this question from the following two aspects:

1. The real-time location information of relays and mobile terminals serves as an index to the location-related fingerprint database. Therefore, the relays are able to obtain the partial CSIs between the base-station (destination) and relays, and a mobile terminal can know the partial CSI between itself and the base-station. The accuracy of partial CSIs (i.e. ε) is related to the mobility, the fingerprint database, and the localization accuracy. Moreover, the base-station can predict the next position of relays (if they are mobiles) and mobile terminals so as to further improve the accuracy of partial CSIs.

2. In the proposed schemes, adaptive modulation is performed individually at the relays and the mobile terminal. Therefore, the proposed multilink adaptation approaches do not require CSI between a mobile terminal and a relay station. This distinctive feature reduces the demand to the fingerprint database, since the database usually cannot provide such a CSI for mobile relays.

3   LOCATION-AIDED AMPLIFY-AND-FORWARD RELAYING

3.1   Power Allocation for Two-Way AF Relaying

3.1.1   Motivation and Approaches

Since 1960s Shannon's ground-breaking work about the two-way channel [Sha61], a lot of research efforts have been paid to find the fundamental capacity limit of this special communication model. However, the capacity for this seemingly simple channel has not been found to this date. Recently, there are increasing research activities towards the combination of two-way channel and relay channel, namely, two-way relay channel (TWRC) or bidirectional relaying [RW07] [PY07]. In the TWRC system, bidirectional communication between two users can enjoy improved spectral efficiency compared with the traditional one-way relay channel [RW07]. The achievable rate of the system is investigated for relaying protocols including amplify-and-forward (AF), and decode-and-forward (DF) for deterministic channels in [PY07]. For more efficient use of the power resource, the power allocation has been exploited. In [AVM09] [HZL08], the power allocation is to maximize the system capacity and achievable rate for the deterministic channel; while a fixed power allocation ratio independent of channel quality is given to improve the upper bound of the average sum rate in [HTHC08].

In this subsection, we add to this area by investigating power allocation strategies for AF bidirectional relaying system under total power constraint[1]. Requiring knowledge of only the channel variance, these power allocation strategies are applicable even under rapidly time-varying channels. First, a power allocation strategy is proposed to maximize the upper bound of the average sum rate in high average SNR region. Second, to avoid one of the terminals suffering from severe outage, the outage probability of each individual terminal is derived, which can't be optimized at the same time. Accordingly, a power allocation strategy is proposed to make a trade-off between these two terminals. It is noticed in the numerical results that the proposed strategies outperform the traditional equal power allocation in the average sum rate and outage probability. Finally, we provide a discussion about how to use the location information in the proposed scheme.

3.1.2   System Model

Consider a three-node bidirectional relaying system consisting of two terminals, S_1 and S_2, one relay, R. In Phase I, S_1 and S_2 transmit their signals simultaneously to the relay R and the received signal at R is given by

$$y_R = h_1 x_1 + h_2 x_2 + n_R \qquad (3.1)$$

where x_1 and x_2 are the transmitted signals with transmit power P_s from S_1 and S_2 respectively, h_1 and h_2 are independent complex Rayleigh fading channel gains of channels from S_1 and S_2 to R, respectively, and n_R is the complex Additive White Gaussian Noise (AWGN) with noise power N_0. The channel variances of these two channels are g_1 and g_2, respectively. The channels are assumed to be invariant for the consecutive two phases.

At the relay, with amplification factor α, the received signal is broadcast to both terminals in Phase II. Then, the received signal at terminal $S_{t,t=1,2}$ is,

$$y_t = h_t(\alpha y_R) + n_t \qquad (3.2)$$

With the knowledge of its own signal at each terminal, the self-interference part can be subtracted from y_t resulting

$$\widetilde{y}_t = \alpha h_1 h_2 x_k + \alpha h_t n_R + n_t \qquad (3.3)$$

---

[1]The total power constraint is widely considered in relay networks to provide useful insight into the relay optimization [GCN08] [LLG06].

where $k = 2$ for $t = 1$ and $k = 1$ for $t = 2$, α is chosen subject to the power at relay P_r as [HTHC08],

$$\alpha = \sqrt{\frac{P_r}{|h_1|^2 P_s + |h_2|^2 P_s + N_0}} \tag{3.4}$$

Then the received SNR for signals from S1 and S2 are,

$$\gamma_1 = \frac{|h_1|^2 |h_2|^2 \gamma_s \gamma_r}{|h_1|^2 \gamma_s + |h_2|^2 (\gamma_s + \gamma_r) + 1}, \tag{3.5}$$

$$\gamma_2 = \frac{|h_1|^2 |h_2|^2 \gamma_s \gamma_r}{|h_2|^2 \gamma_s + |h_1|^2 (\gamma_s + \gamma_r) + 1}, \tag{3.6}$$

respectively, where $\gamma_s = P_s/N_0$ and $\gamma_r = P_r/N_0$. In most early publications, it is assumed all the three nodes transmit with the same power, $P_s = P_r$, referred as equal power allocation in this section. However, the performance of this system can be improved by allocating power among these nodes. Next we propose two different power allocation strategies with the total power constraint $2P_s + P_r = P_0$ in high average SNR range.

3.1.3   Power Allocation Strategies

3.1.3.1 Average Sum Rate

Define $R_t \overset{\Delta}{=} \log_2 (1 + \gamma_t)$. The average sum rate of the bidirectional AF relaying is given by

$$\begin{aligned} E[R] &= E[R_1] + E[R_2] \\ &= E[\log_2(1 + \gamma_1)(1 + \gamma_2)], \end{aligned} \tag{3.7}$$

where $E[\cdot]$ denotes the expectation. The optimization problem is to solve the following cost function

$$\max \left(E[\log_2(1 + \gamma_1)(1 + \gamma_2)] \right), \text{s.t.} \quad 2P_s + P_r = P_0. \tag{3.8}$$

However, optimization based on $E[R]$ is still an open mathematical problem to this date. Alternatively, we can reduce the optimization problem by maximizing the following upper bound

$$\begin{aligned} E[R] &\leq \sum_{t=1}^{2} \log_2(1 + E[\gamma_t]) \\ &\leq \log_2 \left(1 + \frac{g_1 g_2 \gamma_s \gamma_r}{g_1 \gamma_s + g_2 (\gamma_s + \gamma_r) + 1} \right) \\ &\quad + \log_2 \left(1 + \frac{g_1 g_2 \gamma_s \gamma_r}{g_2 \gamma_s + g_1 (\gamma_s + \gamma_r) + 1} \right) \end{aligned} \tag{3.9}$$

where the 1st step follows Jensen's inequality, and the 2nd step follows the computation of average SNR in [DH05]. In the high SNR region ($g_t \gamma_j >> 1, j = s, r$), this upper bound can be approximately written into

$$E[R] \leq \log_2 \left(\frac{g_1^2 g_2^2 \gamma_s^2 \gamma_r^2}{(g_1 \gamma_s + g_2 (\gamma_s + \gamma_r))(g_2 \gamma_s + g_1 (\gamma_s + \gamma_r))} \right). \tag{3.10}$$

Then, our objective reduces to maximize (3.10) subject to the total power constraint in (3.8). Due to the employment of Jensen's inequality, the upper bound (3.10) is not tight enough. Optimization based on (3.10) does not offer an optimum solution to (3.8). On the other hand, our numerical results in Sec. 3.1.4 show that the proposed optimization scheme outperforms the state-of-the-art power allocation schemes in terms of average sum rate.

Define a parameter $\beta\,(0 < \beta < 0.5)$, as the power ratio allocated to each terminal over the total power P_0. Thus, each terminal transmits with power $P_s = \beta P_0$, and relay with power $P_r = (1-2\beta)P_0$. Let $\gamma_0 = P_0/N_0$ denote the total transmit SNR, thus, $\gamma_s = \beta\gamma_0$, $\gamma_r = (1-2\beta)\gamma_0$. Substituting β into (3.10), our power allocation strategy is to determine the optimal β which can maximize the following as,

$$\max_{\beta} \frac{\beta^2(1-2\beta)^2 g_1^2 g_2^2 \gamma_0^2}{(\beta g_1 + (1-\beta)g_2)((1-\beta)g_1 + \beta g_2)}, \text{s.t.} 0 < \beta < 0.5. \tag{3.11}$$

By taking the first order derivation of this function with respect to β, it can be proved via standard analysis of continuous functions that the optimal solution to (3.11) exists and is in the area $\beta \in (0.1910, 0.25]$. In practice, the optimal β can be calculated numerically. Contrastively, β is fixed $1/3$ in equal power allocation; the power allocation suggested in [HTHC08] is equivalent to $\beta = 0.1910$, but our analysis suggests better performance can be achieved with $\beta \in (0.1910, 0.25]$.

3.1.3.2 Outage Probability

In some cases, the sum rate of the system is able to satisfy certain requirement, with one direction transmission at high data rate and the other direction in outage. With this consideration, to improve the outage probability of individual terminals is important. In this section, we derive the average outage probability of each terminal and propose the power allocation to make a balance of the two terminals in terms of the individual outage probability.

The outage probability is the probability for each terminal's instantaneous rate R_t falls below the threshold rate R_0 as $P_{out,t} = \Pr\{R_t \leq R_0\}$. Take terminal S_1 as an example, its outage probability is given as,

$$P_{out,1} = \Pr\left[\log_2\left(1 + \frac{\beta(1-\beta)|h_1|^2|h_2|^2\gamma_0}{\beta|h_1|^2 + (1-\beta)|h_2|^2}\right) \leq R_0\right]. \tag{3.12}$$

Equivalently, we have

$$P_{out,1} = \Pr\left[\frac{2\beta|h_1|^2(1-\beta)|h_2|^2}{\beta|h_1|^2 + (1-\beta)|h_2|^2} \leq \frac{2(1-\beta)(2^{R_0}-1)}{(1-2\beta)\gamma_0}\right]. \tag{3.13}$$

Note that the term at the left side of '$\leq$' is the harmonic mean of two random variables, $\beta|h_1|^2$ and $(1-\beta)|h_2|^2$. Using Theorem 1 in [HA02], the outage probability can be expressed as,

$$P_{out,1} = 1 - \delta K_1(\delta)\exp\left(-\frac{\mu}{2}\left(\frac{1}{\beta g_1} + \frac{1}{(1-\beta)g_2}\right)\right) \tag{3.14}$$

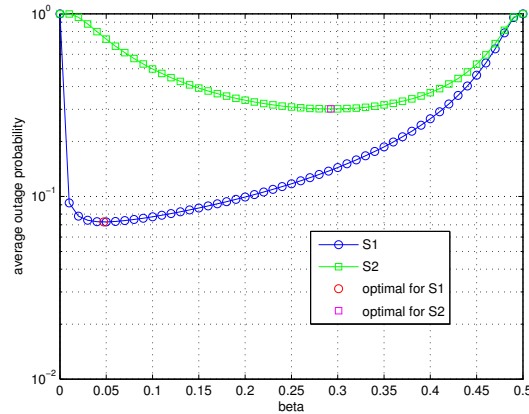
Figure 3.1: The relationship of individual average outage probability with β ($g_1 > g_2$)

where $\mu = \frac{2(1-\beta)(2^{R_0}-1)}{(1-2\beta)\gamma_0}$, $\delta = \mu\sqrt{\frac{1}{\beta(1-\beta)g_1g_2}}$, $K_1(x)$ is the 1st order Bessel function of the 2nd kind. When x is small, $K_1(x) \approx 1/x$, which is true in high average SNR region, i.e., $\gamma_0 \gg 1$. Thus, the outage probability can be further simplified into,

$$P_{out,1} = 1 - \exp\left(-\frac{u(1-\beta)}{1-2\beta}\left(\frac{1}{\beta g_1} + \frac{1}{(1-\beta)g_2}\right)\right) \tag{3.15}$$

with $u = \frac{2^{R_0}-1}{\gamma_0}$ as a constant. Similarly, the outage probability for S_2 is

$$P_{out,2} = 1 - \exp\left(-\frac{u(1-\beta)}{1-2\beta}\left(\frac{1}{\beta g_2} + \frac{1}{(1-\beta)g_1}\right)\right) \tag{3.16}$$

Both $P_{out,1}$ and $P_{out,2}$ are convex functions of β, thus the optimal β to minimize them are $\beta_{opt,1} = \frac{2g_2-\sqrt{2g_2^2+2g_1g_2}}{g_2-g_1}$ and $\beta_{opt,2} = \frac{2g_1-\sqrt{2g_1^2+2g_1g_2}}{g_1-g_2}$, respectively. However, $\beta_{opt,1}$ and $\beta_{opt,2}$ are different, thus the outage probability for the two terminals can't be optimized simultaneously with the same β. This is shown in Fig. 3.1. The outage probability is convex for both terminals, with the minimum point at $\beta_{opt,1}$ and $\beta_{opt,2}$, respectively.
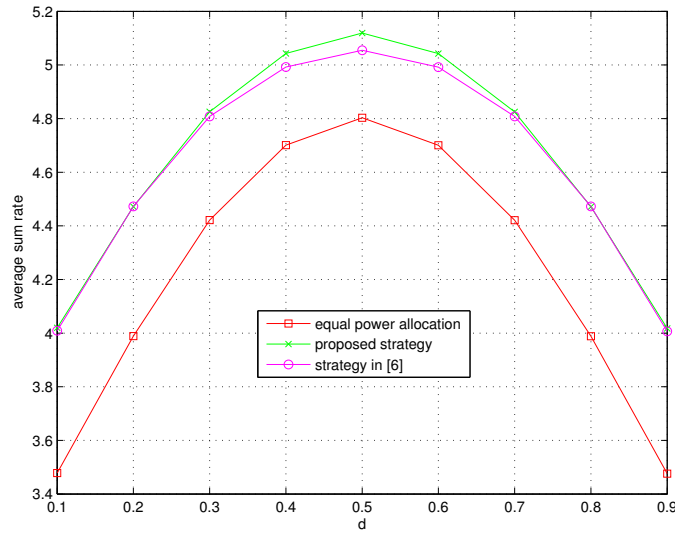

Figure 3.2: Average sum rate versus normalized distance (γ_0=10dB)

To keep both terminals' outage probability at a considerable level, we propose to choose β_{pro} as the optimal β for the terminal with larger outage probability as a trade-off solution to balance the outage performance of the two terminals. For example in Fig. 3.1, $\beta_{pro} = \beta_{opt,2}$, and mathematically it is to find β_{pro} to the following,

$$\min\max\{P_{out,1}, P_{out,2}\}, \text{s.t.} \quad 0 < \beta < 0.5. \tag{3.17}$$

With this power allocation, both $P_{out,1}$ and $P_{out,2}$ are increasing functions versus β in $[\beta_{pro}, 0.5)$; the terminal with larger outage probability is optimized and the other's outage probability is already at a relatively low level.

3.1.4   Numerical Results

In this section, computer simulations are performed to present the performance of the proposed power allocation strategies. The total average SNR is set to be γ_0=10dB and 20dB, respectively, and the relay
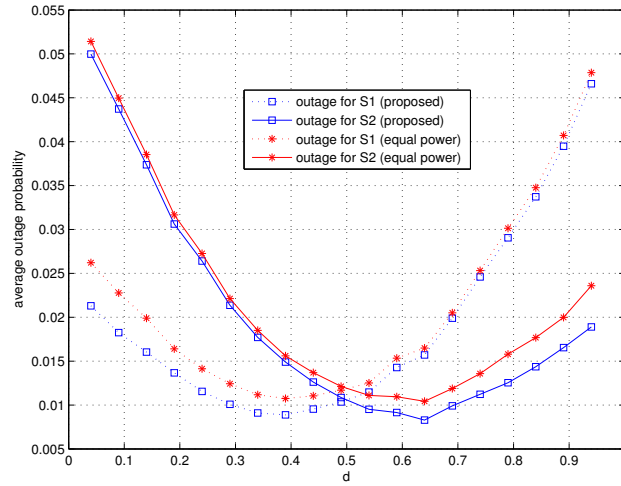
Figure 3.3: Average outage probability versus normalized distance (γ_0=20dB)

is assumed to be located on the line that passes through S_1 and S_2. The distance between S_1 and S_2 is normalized to 1, and the normalized distance from S_1 to R is d. Thus the channel variances of the two channels are $g_1 = d^{-3}$, and $g_2 = (1-d)^{-3}$, respectively.

Fig. 3.2 shows the average sum rate versus d. The proposed power allocation strategy is compared with the power allocation strategy in [HTHC08], and equal power allocation. The proposed one provides significant improvement over the equal power allocation, and is slightly better than in [HTHC08], which is in line with our analytical results. Fig. 3.3 compares the two terminals' average outage probability of the 2nd proposed power allocation strategy with equal power allocation (threshold rate $R_0 = 1$). The individual outage probability with the proposed power allocation strategy for either S_1 or S_2 is lower than with equal power allocation. The performance gain is larger when the relay is close to one terminal ($d \to 0$ or $d \to 1$).

3.1.5   Conclusion and Discussion about Location-Aided Aspects

3.1.5.1 Conclusion

This subsection has presented simple power allocation strategies for bidirectional AF-relaying system. With the only requirement of the channel variance, the proposed strategies aimed to improve the average sum rate and individual average outage probability under Rayleigh fading channels, respectively. Numerical results have shown visible improvement over the equal power allocation.

3.1.5.2 Discussion about Location-Aided Aspects

The proposed power-allocation approaches only require statistical channel quality information, and thus are suitable for high-mobility environments. More importantly, it would be more reasonable for the location-related fingerprint database to provide the statistical channel knowledge rather than the instantaneous channel knowledge.

3.2   Outage Performance of AF Relaying over Asymmetric Environments

The objective of this section is to investigate the outage probability of AF relaying over asymmetric fading channels as done in section 2.2. This part analyzes the scenarios where the relay nodes are located at different positions and then, affected by different fading distributions. From the general point of view,

Figure 3.4: Different asymmetric fading channels of a cooperative networks.

as in section 2.2, these distributions could be independent but non-identical. The lower bound of outage probability is derived at high SNR regime. The performance is provided for both the repetition-based and opportunistic relaying.

3.2.1 *Repetition Based AF Relaying*

The repetition-based AF relaying is introduced in [LTW04a]. Due to the higher degree of freedom of repetition-based relaying and easy to implement for AF relaying, it gained its own importance in cooperative communications. The equivalent instantaneous end-to-end SNR for repetition-based AF relaying is given as [ZAL06]

$$\gamma = \frac{P_s|h_{sd}|^2}{N_{sd}} + \sum_{i=1}^{M} \frac{\frac{P_s|h_{sr_i}|^2}{N_{sr_i}}\frac{P_s|h_{r_id}|^2}{N_{r_id}}}{\frac{P_s|h_{sr_i}|^2}{N_{sr_i}} + \frac{P_s|h_{r_id}|^2}{N_{r_id}} + 1} \tag{3.18}$$

The upper bound of instantaneous SNR for the above can be written as

$$\gamma_{max} = P_s|h_{sd}|^2\gamma_0 + \sum_{i=1}^{M} \min\left(P_s|h_{sr_i}|^2\gamma_0, P_s|h_{r_id}|^2\gamma_0\right) \tag{3.19}$$

where $\gamma_0 = 1/N_o$ is proportional to the system SNR.

In the following section, we provide the lower bound of outage probability of the opportunistic AF relaying for different asymmetric fading channels shown in Fig. 3.4. The asymmetric channels described in this section are totaly different scenarios than the section 2.2.

3.2.1.1 Asymmetric channel I:

For the asymmetric channel I, S-D link experiences Rayleigh fading distribution and S-R and R-D links experience Rician fading distribution, so (3.19) can be written as

$$\gamma_{max} = \gamma_0\gamma_{sd} + \gamma_0\xi_{sum} \tag{3.20}$$

where $\gamma_{ab} = P_a|h_{sd}|^2$ is the exponential distribution, $\xi_{sum} = \sum_{i=1}^{M}\xi_{min,i}$, $\xi_{min,i} = \min(\xi_{sr_i}, \xi_{r_id})$, ξ_{sr_i} and ξ_{r_id} are the random variables of noncentral Chi-square distribution. The corresponding outage probability can be defined as

$$p_{out} \quad = \quad Pr[\gamma_{ub} < \gamma] \tag{3.21}$$

where $\gamma_{ub} = \gamma_{max}/\gamma_0$, $\gamma = (2^{(M+1)R} - 1)/\gamma_0$. The outage probability provided in (3.21) is equivalent to the CDF of γ_{ub}. The direct evaluation CDF of γ_{ub} is complicated, so we use IVT. Therefore, this derived

analytical results are valid for high SNR regime. To evaluate this, first CDF of $\xi_{min,i}$ needs to be evaluated. The CDF of the random variable $\xi_{min,i}$ can be written as

$$F_{\xi_{min,i}}(\gamma) = 1 - (1 - Pr[\xi_{sr_i} < \gamma])(1 - Pr[\xi_{r_id} < \gamma])$$

$$= 1 - Q_1\left(\sqrt{2K_{sr_i}}, \sqrt{\frac{2(K_{sr_i}+1)\gamma}{\bar{\xi}_{sr_i}}}\right) Q_1\left(\sqrt{2K_{r_id}}, \sqrt{\frac{2(K_{r_id}+1)\gamma}{\bar{\xi}_{r_id}}}\right) \qquad (3.22)$$

where $Q_1(,)$ is the Marcum Q-function of first order. The PDF of $\xi_{min,i}$ is obtained by differentiating the above equation. It can be expressed as

$$f_{\xi_{min,i}}(\gamma) = Q_1\left(\sqrt{2K_{sr_i}}, \sqrt{\frac{2(K_{sr_i}+1)\gamma}{\bar{\xi}_{sr_i}}}\right) f_{\xi_{r_id}}(\gamma) + Q_1\left(\sqrt{2K_{r_id}}, \sqrt{\frac{2(K_{r_id}+1)\gamma}{\bar{\xi}_{r_id}}}\right) f_{\xi_{sr_i}}(\gamma) \qquad (3.23)$$

The LT of the random variable $\gamma_{ub} = \gamma_{sd} + \xi_{sum}$ is obtained by using IVT at high SNR regime. Since $\gamma \to 0$ as $\gamma_0 \to \infty$, we can write

$$\lim_{s \to \infty} s\mathscr{L}(f_{\gamma_{sd}}(\gamma)) = \lim_{\gamma \to 0} f_{\gamma_{sd}}(\gamma) \qquad (3.24)$$

This implies

$$\mathscr{L}(f_{\gamma_{sd}}(\gamma)) = \frac{1}{s} f_{\gamma_{sd}}(0) \qquad (3.25)$$

Similarly the LT of the PDF of random variable ξ_{sum} can be expressed as

$$\mathscr{L}(f_{\xi_{min,i}}(\gamma)) = \frac{1}{s} f_{\xi_{min,i}}(0) \qquad (3.26)$$

Now by using the multiplication properties of LT, the LT of the PDF of random variable γ_{ub} for i.n.d fading channel can be written as

$$\mathscr{L}\left(f_{\gamma_{sd}}(\gamma)\right) = \frac{1}{s^{M+1}} f_{\gamma_{sd}}(0) \prod_{i=1}^{M} f_{\xi_{min,i}}(0) \qquad (3.27)$$

The PDF of random variable γ_{ub} is obtained by applying the ILT on the above

$$f_{\gamma_{ub}}(\gamma) = \frac{1}{M!} \gamma^M f_{\gamma_{sd}}(0) \prod_{i=1}^{M} f_{\xi_{min,i}}(0) \qquad (3.28)$$

By integrating the above and substituting the value of $f_{\gamma_{sd}}(0)$ and $f_{\xi_{min,i}}(0)$, the outage probability can be expressed as

$$p_{out} = \frac{1}{(M+1)!\bar{\gamma}_{sd}} \prod_{i=1}^{M} \left(\frac{(K_{sr_i}+1)}{\bar{\xi}_{sr_i} e^{K_{sr_i}}} + \frac{(K_{r_id}+1)}{\bar{\xi}_{r_id} e^{K_{r_id}}}\right) \gamma^{M+1} \qquad (3.29)$$

3.2.1.2 Asymmetric channel II:

For asymmetric channel II, S-D and D-R links experience Rician fading distribution and S-R link experiences Rayleigh fading channel. For this scenario, we use $\xi_{sd} = P_s|h_{sd}|^2$, $\xi_{sr_i} = P_s|h_{sr_i}|^2$ and $\gamma_{r_id} = P_s|h_{r_id}|^2$. The end-to-end instantaneous SNR can be expressed as

$$\gamma_{ub} = \gamma_0 \xi_{sd} + \gamma_0 g_{sum} \qquad (3.30)$$

where $g_{sum} = \sum_{i=1}^{M} g_{min,i}$ and $g_{min,i} = \min(\xi_{sr_i}, \gamma_{r_id})$. Similarly as the previous section, the PDF of $g_{min,i}$ is expressed as

$$f_{g_{min,i}}(\gamma) = Q_1\left(\sqrt{2K_{sr_i}}, \sqrt{\frac{2(K_{sr_i}+1)\gamma}{\bar{\xi}_{sr_i}}}\right) f_{\gamma_{r_id}}(\gamma) + f_{\xi_{sr_i}}(\gamma)\left(1 - F_{\gamma_{r_id}}(\gamma)\right) \qquad (3.31)$$

where $F_{\gamma_{r_id}}(\gamma)$ is the CDF of the random variable γ_{r_id}.

Similarly as previous, the PDF of γ_{ub} for this asymmetric channel can be derived as

$$f_{\gamma_{ub}}(\gamma) = \frac{1}{M!}\gamma^M f_{\xi_{sd}}(0)\prod_{i=1}^{M} f_{g_{min,i}}(0) \tag{3.32}$$

By integrating (3.32), the outage probability for the asymmetric channel II can be expressed as

$$p_{out} = \frac{1}{(M+1)}\frac{(K_{sd}+1)}{\bar{\xi}_{sd}e^{K_{sd}}}\prod_{i=1}^{M}\left(\frac{(K_{sr_i}+1)}{\bar{\xi}_{sr_i}e^{K_{sr_i}}}+\frac{1}{\bar{\gamma}_{r_id}}\right)\gamma^{M+1} \tag{3.33}$$

3.2.2   Opportunistic AF Relaying

In this section, we analyze the outage probability of opportunistic AF relaying over the same asymmetric fading scenario. For the relay selection, we use maximum SNR approach provided in [BSW07]. The equivalent instantaneous end-to-end SNR for opportunistic AF relaying is given as [ZAL06]

$$\gamma = \frac{P_s|h_{sd}|^2}{N_{sd}} + \max_{i=\{1,2,...,M\}}\frac{\frac{P_s|h_{sr_i}|^2}{N_{sr_i}}\frac{P_s|h_{r_id}|^2}{N_{r_id}}}{\frac{P_s|h_{sr_i}|^2}{N_{sr_i}}+\frac{P_s|h_{r_id}|^2}{N_{r_id}}+1} \tag{3.34}$$

The upper bound of instantaneous SNR for the expression above (3.34) can be written as

$$\gamma_{max} = P_s|h_{sd}|^2\gamma_0 + \max_{i=\{1,2,...,M\}}\min\left(P_s|h_{sr_i}|^2\gamma_0, P_s|h_{r_id}|^2\gamma_0\right) \tag{3.35}$$

3.2.2.1 Asymmetric channel I:

In asymmetric channel I, the outage performance can be expressed as

$$p_{out} = Pr[\gamma_{ub} < \gamma] \tag{3.36}$$

where $\gamma_{ub} = \gamma_{max}/\gamma_0$, $\gamma = (2^{2R}-1)/\gamma_0$, $\xi_{max} = \max(\xi_{min,1},\xi_{min,2},...,\xi_{min,M})$ and $\xi_{min,i} = \min(\xi_{sr_i},\xi_{r_id})$.

The CDF of the random variable ξ_{max} for i.n.d fading channel can be expressed as

$$F_{\xi_{max}}(\gamma) = \prod_{i=1}^{M}F_{\xi_{min,i}}(\gamma) \tag{3.37}$$

and the corresponding PDF of ξ_{max} is obtained as

$$f_{\xi_{max}}(\gamma) = \sum_{i=1}^{M}f_{\xi_{min,i}}(\gamma)\prod_{\substack{j=1\\j\neq i}}^{M}F_{\xi_{min,j}}(\gamma) \tag{3.38}$$

Since $F_{\xi_{min,i}}(0) = 0$, the $(M-1)$th order derivative of (3.38) at high SNR, i.e., at $\gamma = 0$ for $\gamma_0 \to \infty$, can be derived as

$$\frac{\partial^{M-1}}{\partial\gamma^{M-1}}f_{\xi_{max}}(\gamma)\Big|_{\gamma=0} = M!\prod_{i=1}^{M}f_{\xi_{min,i}}(0) \tag{3.39}$$

By using LT of M$^{\text{th}}$ order differentiation, we can write

$$\mathscr{L}\left(\frac{\partial^{M-1}}{\partial\gamma^{M-1}}f_{\xi_{max}}(\gamma)\right) = s^{M-1}\mathscr{L}\left(f_{\gamma_{max}}(\gamma)\right) - s^{M-2}f_{\gamma_{max}}(0) - ... - f_{\gamma_{max}}^{(M-2)}(0) \tag{3.40}$$

Since $f_{\gamma_{max}}(0) = f_{\gamma_{max}}^{(1)}(0) = ... = f_{\gamma_{max}}^{(M-2)}(0) = 0$, by using the IVT of LT, we can write

$$\mathcal{L}\left(f_{\gamma_{max}}(\gamma)\right) = \frac{1}{s^M} \frac{\partial^{M-1}}{\partial \gamma^{M-1}} f_{\xi_{max}}(\gamma)\Big|_{\gamma=0} \qquad (3.41)$$
$$\lim s \to \infty$$

The LT of the PDF of random variable $\gamma_{ub} = \gamma_{sd} + \xi_{max}$ over i.n.d can be written as

$$
\begin{aligned}
\mathcal{L}(f_{\gamma_{ub}}(\gamma)) &= \mathcal{L}(f_{\gamma_{sum}}(\gamma))\mathcal{L}(f_{\gamma_{max}}(\gamma)) \\
&= \frac{1}{s^{M+1}} f_{\gamma_{sd}}(0) \frac{\partial^{M-1}}{\partial \gamma^{M-1}} f_{\xi_{max}}(\gamma)\Big|_{\gamma=0} \\
&= \frac{M!}{s^{M+1}} f_{\gamma_{sd}}(0) \prod_{i=1}^{M} f_{\xi_{min,i}}(0)
\end{aligned}
\qquad (3.42)
$$

Since $f_{\gamma_{sd}}(0)$ and $f_{\xi_i}(0)$ are constants with respect to s, the PDF of γ_{ub} is obtained by applying the ILT on the above as

$$f_{\gamma_{ub}}(\gamma) = \gamma^M f_{\gamma_{sd}}(0) \prod_{i=1}^{M} f_{\xi_{min,i}}(0) \qquad (3.43)$$

The corresponding outage probability or CDF of γ_{ub} is obtained by integrating the above as.

$$p_{out} = \frac{1}{(M+1)\bar{\gamma}_{sd}} \prod_{i=1}^{M} \left(\frac{K_{sr_i}+1}{\bar{\xi}_{sr_i} e^{K_{sr_i}}} + \frac{K_{r_id}+1}{\bar{\xi}_{r_id} e^{K_{r_id}}} \right) \gamma^{M+1} \qquad (3.44)$$

3.2.2.2 Asymmetric channel II:

Similarly, in asymmetric channel II, the outage performance can be expressed as

$$p_{out} = Pr\left[\gamma_{ub} < \gamma\right] \qquad (3.45)$$

where $\gamma_{ub} = \xi_{sd} + g_{max}$, $g_{max} = \max(g_{min,1}, g_{min,2}, ..., g_{min,M})$ and $g_{min,i} = \min(\gamma_0 \xi_{sr_i}, \gamma_0 \gamma_{r_id})$.

As the previous in (3.42), the LT of the random variable of γ_{ub} over i.n.d fading channel can be written as

$$\mathcal{L}\left(f_{\gamma_{ub}}(\gamma)\right) = \frac{M!}{s^{M+1}} f_{\gamma_{sd}}(0) \prod_{i=1}^{M} f_{g_{min,i}}(0) \qquad (3.46)$$

The PDF of γ_{ub} is obtained by applying the ILT on the above as

$$f_{\gamma_{ub}}(\gamma) = \gamma^M f_{\gamma_{sd}}(0) \prod_{i=1}^{M} f_{g_{min,i}}(0) \qquad (3.47)$$

The corresponding outage probability or CDF of γ_{ub} is obtained by integrating the above as

$$p_{out} = \frac{1}{(M+1)\bar{\gamma}_{sd}} \prod_{i=1}^{M} \left(\frac{K_{sr_i}+1}{\bar{\xi}_{sr_i} e^{K_{sr_i}}} + \frac{1}{\bar{\gamma}_{r_id}} \right) \gamma^{M+1} \qquad (3.48)$$

3.2.3　Simulation Results

In this section, analytical and Monte-Carlo simulation results are presented. Since the channel are i.n.d, we set different means for different S-R$_i$/R$_i$-D links. In the Rician fading channel, the Rician factor K_{ab} is uniformly distributed in [2,3] and the mean $\bar{\gamma}_{ab}$ of NLOS components are uniformly distributed in [0,1]. The LOS components are derived for a given value of K_{ab} and $\bar{\gamma}_{ab}$. The number of relay nodes is set to 4.

Fig. 3.5 shows the lower bound of outage probability of repetition-based AF relaying over the symmetric (Rician fading or Rayleigh fading) and two different asymmetric fading channels. As expected,

due to the presence of LOS signal, the outage performance over Rician fading channel outperforms all other fading scenarios. On the other hand, due to the absence of LOS signals, Rayleigh fading channel has poorer outage performance than all other fading scenarios. On the other hand, asymmetric channel I provides better outage performance than the asymmetric channel II. It is because S-R link experiences LOS signal in asymmetric channel I, so, there is lower chance to amplify the noise by relay nodes in the 2nd phase. However, for the asymmetric channel II, S-R is a NLOS situation, there is a higher chance to amplify the noise by relay nodes and send it to the destination.
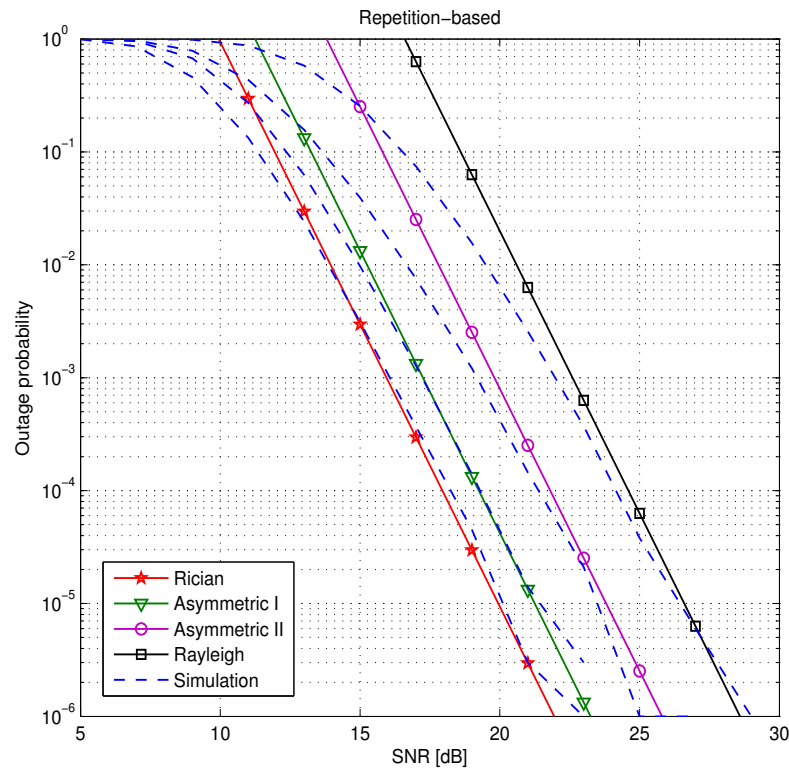

Figure 3.5: The outage probability of repetition-based relaying over Rayleigh fading, Rician fading, asymmetric channel I and asymmetric channel II.

Fig. 3.6 shows the lower bound of outage probability of opportunistic AF relaying for the same scenario. It plays the same role as previous when outage performance compared between asymmetric channel I and asymmetric channel II. However, when outage is compared between repetition-based AF relaying and opportunistic AF relaying, later provides better outage performance and the gain is about 7 dB.

3.2.4   Conclusions

In this section, the outage performance of opportunistic AF relaying over asymmetric and i.n.d fading environments has been investigated. The knowledge of asymmetric channel can be identified through the positioning information of nodes and corresponding signal strength between the nodes. A lower bound of the outage probability has been derived and validated through Monte-Carlo simulation results. We show that the outage performance of AF relaying is better when the relay is in LOS situation with respect to the source rather than to the destination for any number of relay nodes in the environment.
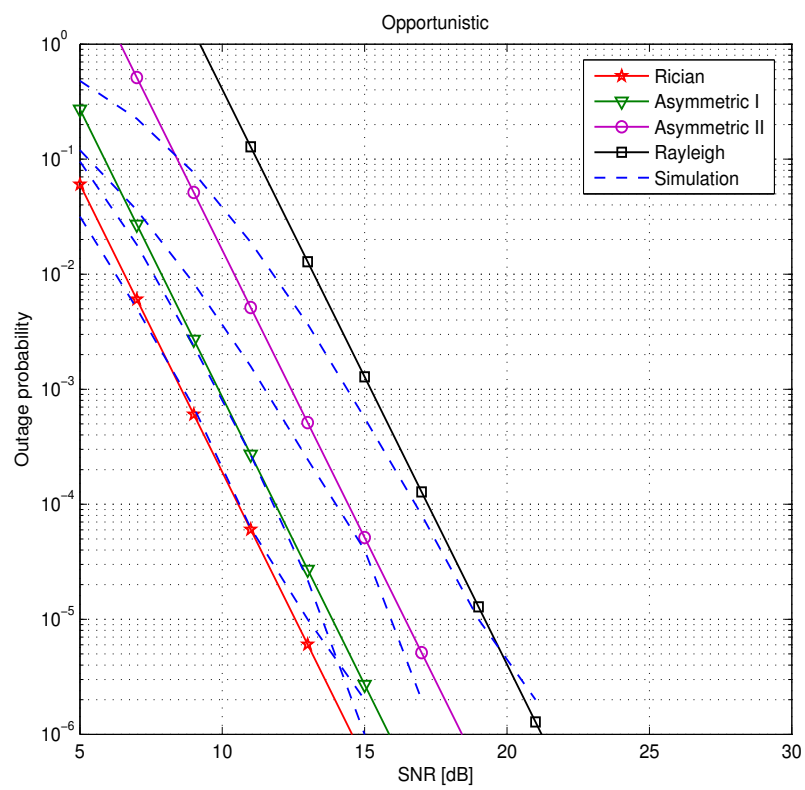
Figure 3.6: The outage probability of opportunistic relaying over Rayleigh fading, Rician fading, asymmetric channel I and asymmetric channel II.

4 LOCATION-AIDED RELAY SELECTION STRATEGIES

4.1 Impact of Mobility and Inaccurate Path Loss Model Parameters on Relay Selection

In wireless networks, the performance of data transmissions is depending on the distance between transmitter and receiver nodes as well as on the number of collocated nodes and their activity patterns. Neighbor nodes can cause performance degradation due to interference and collision. Furthermore, when there is a large distance between the transmitter and receiver, rate adaptation schemes switch to a more robust modulation scheme, which decreases the transmission rate. As shown in [LTN+07] this reduction in transmission rate can significantly reduce the network capacity, and thereby also transmissions with high rate may be affected. By introducing relaying techniques, nodes located between a transmitter and receiver pair can be exploited to provide a multihop path with shorter links. The shorter links between nodes may form a more reliable path to the destination node, which allows to achieve a higher throughput, see references [ZC05] [MYP+07] [NP07].

Existing work, such as the coopMAC protocol [LTN+07] is targeted at stationary wireless networks. As shown in [LTN+07], mobility outdates information about potential helper nodes, which causes performance to decrease to the same level as if relaying was not considered. Even with low mobility (max 1 m/s, 60 s pauses), the gain compared to standard 802.11 without relaying is less than 10%. The Harbinger protocol described in [ZV05] copes better with mobility. The protocol assumes that nodes are aware of their position and that the position of the destination is contained in the packet header. By letting the contention time depend on a receiving node's distance to the destination, the receiving node closest to the destination will act as the relay and the packet is forwarded towards the destination. However, since the relay nodes are chosen on a per-hop basis, the chosen path is not necessarily the best path. A slightly different approach is taken with the CCMAC protocol [HT08], which aims at improving throughput for uplink transmissions in the region near the access point (AP) by allowing simultaneous source to relay transmissions.

In this work we consider the scenario where mobile users primarily need to make downlink transmissions. Audio or video streaming are examples of applications leading to such traffic patterns. In such downlink scenarios we will therefore focus on *centralized two-hop relay selection* where transmissions from the AP may be direct or via a two-hop relay path. As in the coopMAC protocol, we rely on maintaining an up-to-date view on the potential relay nodes, but for the downlink case, only the AP needs to have an updated view.

The AP's ability to determine the best path depends on the accuracy of the AP's view on the links properties in the network. This view is updated by periodic collection of link quality or position information measurements, as described in more detail later. The age and availability of link measurements in relation to the movement speed of the mobile devices (MDs) is expected to impact the accuracy of the choice of path. In addition to these factors, also the number of nodes is expected to influence the path selection. In this work we will investigate how the path selection is impacted by these factors.

4.1.1 Scenario Description

We consider downlink transmissions from a fixed AP to MDs in an IEEE 802.11 network. Data transmissions can be done directly to the destination MD or as a two-hop transmission via any intermediate relay node, as sketched in Fig. 4.1. A relayed transmission is only considered if it provides a better transmission quality than a direct transmission. In this work the goodness of a transmission is determined in terms of the achieved bit error rate (BER).

That is, the relayed transmission path is chosen if the condition in (4.1) is satisfied:

$$BER_{\mathrm{AP},r_{opt},\mathrm{D}} < BER_{\mathrm{AP,D}} \qquad (4.1)$$

Where $BER_{\mathrm{AP},r_{opt},\mathrm{D}}$ is the BER of the two-hop path that delivers the lowest BER according to:

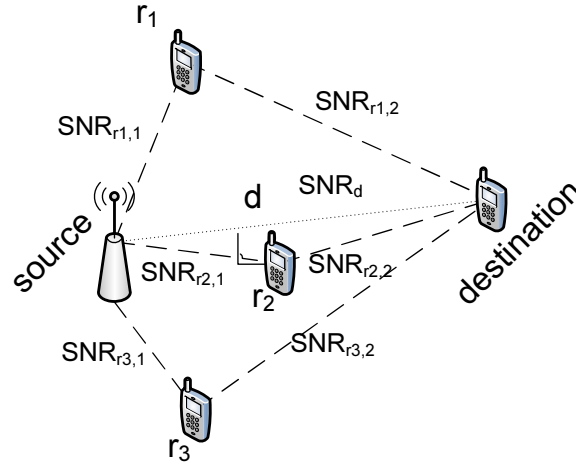$$r_{opt} = \arg\min_{r}(1 - (1 - BER_{\mathrm{AP},r}) \cdot (1 - BER_{r,\mathrm{D}})) \qquad (4.2)$$

Figure 4.1: Example of possible direct and two-hop paths.

where $BER_{\mathrm{AP},r}$ and $BER_{r,\mathrm{D}}$, are the BER of the first hop from the AP to the relay r and second hop from the relay r to the destination D, respectively. Notice that this approach does not ensure that the chosen relay path delivers a higher throughput than the direct path, due to the store and forward behavior of the relay node. However, the lower BER increases reliability of the transmission.

For both schemes the procedures used to collect measurements are envisioned as L2 protocol extension. Further, since old measurements may be misleading due to mobility of the MDs, it is assumed that a parameter denoted α_{store} exists in the AP, which expires measurements when their *storage time* exceeds α_{store}.

We can further define the age of a measurement as the elapsed time since the hello broadcast of the latest measurement for that link was initiated. The age of a link measurement is a stochastic process that is influenced mainly by the hello broadcast generating process. A random jitter is added to the inter-event time for hello broadcasts, which ensures that hello transmissions from different MDs are not in sync. Further, since the MDs' movements are independent of each other, the mobility model is assumed to be ergodic.

4.1.2 SNR-based Relay Selection Scheme

In order for the AP to make this decision it needs to estimate the BER of the network links. The BER is estimated from the measurements of link signal to noise ratio (SNR), which are obtained from MDs and collected by the AP.

By letting all MDs broadcast *hello* messages periodically with average interval duration $\mu_{\mathrm{hello}}[\mathrm{s}]$, other devices within receiving range are able to measure the received signal strength (RSS) and thereby the SNR of the hello broadcast. This measurement is assumed to represent the link state at this moment in time. Further, all nodes are using the same fixed transmission power. The hello message is a IEEE 802.11 MAC frame without payload (20 octets), since only the MAC address is needed for the receiver to identify the broadcast source. Notice that hello broadcasts may be lost if collisions occur.

Whenever an MD overhears a hello broadcast and thereby obtains an SNR measurement, it assembles a measurement frame and sends it to the AP using a unicast transmission. Due to the small frame size, RTS/CTS is not applied but standard 802.11 retransmissions are used if needed. The measurement frame is envisioned as being a MAC control frame that carries the MAC address of the hello broadcast source (6 octets) and the SNR measurement (2 octets), which amounts to a frame size of 28 octets when adding this information to the standard 802.11 control frame layout [IEE07]. Hereby N hello broadcasts lead to $N \cdot (N - 1)$ measurement transmissions to the AP, in the case where all nodes receive all hello-broadcasts. The actual amount of measurement transmissions may vary due to losses and possible retransmissions. As this approach generates many individual transmissions that contribute to the overhead future work

could consider to accumulate a bulk of measurements before initiating a transmission to the AP.

The AP identifies the link from which the measurement has been obtained from the MAC addresses of the broadcast node and measurement node. Notice that it is assumed that links are symmetric.

Having obtained SNR measurements from links between devices in the network, the AP now chooses the best path according to eq. (4.1).

4.1.3 Location-based Relay Selection

The idea behind this scheme is that by knowing the locations of the MDs in the network, the path-loss, SNR and in turn the BER can be estimated with propagation models by assuming fixed transmit power and approximating noise floor and propagation properties of the environment. Locations are obtained by letting all MDs transmit location measurements periodically with interval μ_{loc} to the AP using unicast transmissions. Similarly to the case with hello broadcasts for the SNR measurement based scheme, the initial transmission time is chosen for each node uniformly random in the interval $[0, \mu_{\text{loc}}]$. Further, the following location measurement transmissions are offset with a uniform random jitter in the interval $[-0.1 \cdot \mu_{\text{loc}}, 0.1 \cdot \mu_{\text{loc}}]$ to avoid transmissions being in sync. The measurement frame is a MAC control frame that carries the longitude (4 octets) and latitude (4 octets) of the node. Assuming the longitude and latitude are given as a degree decimal fraction and the circumference of the earth is $40000km$, the precision that is supported by this format is approximately $\frac{40000km}{2^{4\cdot8}} = 0.01m$. The frame size amounts to 28 octets when adding longitude and latitude information to the standard 802.11 control frame layout [IEE07]. This is the same size as the SNR measurement frame.

Having collected the MD locations, first the path-loss is estimated with this path-loss model from [DRX98]:

$$\overline{PL}(d) \ [dB] = PL(d_0) \ [dB] + 10n \log_{10}\left(\frac{d}{d_0}\right) \tag{4.3}$$

where $\overline{PL}(d)$ is the path loss in dB at the receiver, d is the distance between transmitter and receiver, $PL(d_0)$ is the path loss in dB at a reference distance $d_0 = 1m$, and n is the path loss exponent. As the value of n is scenario dependent and its exact value is typically not known in advance, we will investigate the sensitivity to inaccurate estimates of this parameter in section 4.1.6.2.

Given a specific transmit power level P_{tx}, the calculated path-loss $\overline{PL}(d)$ and assumed noise floor N_{floor}, the SNR is calculated as:

$$SNR = P_{\text{tx}} + \overline{PL}(d) - N_{\text{floor}} - X[dB] \tag{4.4}$$

where X is a random variable representing shadowing due to obstacles in the environment. Initially we will assume $X = 0$, however in NLOS situations that we will investigate later in this section it will be necessary to guess the attenuation. This is covered in section 4.1.6.2. Having determined the SNR, the expected BER can now be calculated using theoretical expressions from reference [Pro95].

4.1.4 Evaluation Methodology

For evaluation we consider simulations of mobility and the wireless network followed by a combined performance evaluation as sketched in Fig. 4.2.

First a simulation of node mobility is generated based on the random waypoint mobility model. The outcome is a trace of the movements of all nodes. Now the ns-2 simulation[2] is executed, based on the mobility trace and the scenario specific parameters listed in Table 4.1. We use the *802.11ext* module to simulate realistic 802.11a behavior. This ns-2 version includes a Nakagami fading model which has been parametrized according to Table 4.1 with model parameters $\Gamma = n$ and $m = \frac{(K+1)^2}{2K+1}$ to approximate a Ricean fading environment.

---

[2]The ns-2 simulation is based on [CSEJ$^+$07], which has been updated with the author's patch from October 21, 2008.
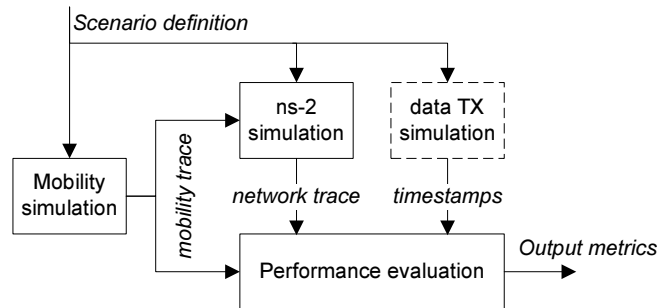
Figure 4.2: Simulation overview.

For evaluating the SNR and location based algorithms, we use two different custom ns-2 agents for generating and collecting measurements. For the SNR based algorithm the agent in each MD periodically generate broadcasts and forward overheard broadcasts to the AP, as described in section 4.1.2. For the location-based algorithm, the agent makes each MD transmit a measurement frame containing its location periodically as described in section 4.1.3. We assume that MDs are able to obtain their own location coordinate $(x + \varepsilon_{\text{pos}}, y + \varepsilon_{\text{pos}})$ where ε_{pos} is a zero mean gaussian error with standard deviation σ_{pos} representing the localization inaccuracy.

The outcome of the ns-2 simulation is a trace file that for every node describes when hello and measurement frames are received. Another trace file that specifies destination node and timestamp for the data transmissions is generated based on the defined transmission interval parameter μ_{tx}. The destination node is chosen randomly between all MDs for each transmission.

Scenario size	$100m \, x \, 100m$
No. of mobile devices	10
Mobility model	Random Waypoint (speed: $2 - 8m/s$)
Rice K-value	6 (based on [DL94])
Path loss exponent n	2.9 (based on [DRX98] for outdoor measurements.)
Modulation scheme	BPSK (6 Mbit/s in 802.11a)
Noise floor	-86 dBm
Transmission power	100 mW

Table 4.1: Scenario parameters.

In this work the measurement collection and data transmissions are simulated separately in ns-2 and matlab, to make the implementation simpler and thus allow for rapid prototyping. The considered solution does therefore not take into account the mutual influence of the data transmissions and the measurement collection and a future work item is to take this interaction into account.

4.1.5   Performance Evaluation

In order to evaluate the performance of the proposed location measurement based path selection scheme, we compare the performance of this scheme to the following three schemes: the SNR measurement based scheme from reference [NMS10], the case where the *direct* path is always used, and the *ideal* case where exact and updated link state information is always available. We consider the following metrics:

4.1.5.1 Avg. BER

This metric describes the average BER that is obtained for the data transmission for each of the considered schemes. The BER is calculated from the SNR using theoretical expressions from [Pro95] given the BPSK modulation scheme and the Ricean fading model (K=6). The SNR that is needed to estimate the

BER is calculated using the following steps: 1) Node positions at transmission instants are obtained from the mobility model and the link distances are calculated as the shortest distance between all node pairs. Based on link distances, the path loss and SNR are calculated using eq. (4.3) and eq. (4.4) and hereafter the BER is estimated using using theoretical expressions from e.g. reference [Pro95].

4.1.5.2 Signaling channel utilization

This metric gives the overhead spent on obtaining and collecting measurements as a fraction of channel capacity. First, the transmission time t_{tx} of hello and measurement frames is calculated as a function of the number of MAC PDU bits N_{MPDU} according to the IEEE 802.11a specifications in [IEE07]:

$$t_{tx} = t_{symbol} \left\lceil \frac{N_{MPDU} + N_{service} + N_{tail}}{N_{DBPS}} \right\rceil + t_{training} + t_{signal} \qquad (4.5)$$

Here N_{MPDU} represents $N_{hello} = 20 \cdot 8$ bits for hello broadcasts and $N_{meas} = 28 \cdot 8$ bits for SNR and location measurements.

Now the signaling channel utilization is estimated as in eq. (4.6) and eq. (4.7), where N is the number of MDs.

$$U_{snr} = \frac{N \cdot (t_{tx}(N_{hello}) + (N-1) \cdot t_{tx}(N_{meas}))}{\mu_{hello}} \qquad (4.6)$$

$$U_{loc} = \frac{N \cdot t_{tx}(N_{loc})}{\mu_{loc}} \qquad (4.7)$$

The actual signaling channel utilization may vary slightly due to possible collisions and retransmissions.

4.1.6   Results and Discussion

4.1.6.1 Signaling Overhead of Relay Selection Schemes

Initially, we compare the overhead in terms of the channel utilization used for signaling for the SNR-based and location-based relaying schemes.
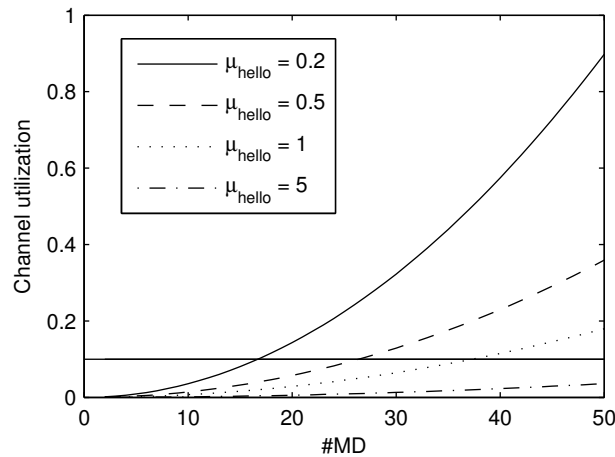

Figure 4.3: Utilization of channel for obtaining and collecting SNR measurements (Data rate is 6Mbit/s).

In Fig. 4.3 the channel utilization spent for obtaining and collecting SNR measurements for different hello broadcast intervals and node densities is shown. This has been calculated using eq. (4.6). As capacity should be used for data transmission and not spent as overhead for measurement collection, a utilization of more than 10% is considered unacceptable. In the plot we see that this limit is exceeded at slightly less than 40 MDs with $\mu_{hello} = 1s$. In vehicular scenarios where even faster updates are needed,

we see that for $\mu_{\text{hello}} = 0.5s$ and $\mu_{\text{hello}} = 0.2s$ the utilization exceeds the 10% limit for just 25 and 18 MDs, respectively. This result emphasizes the need for a more efficient relay path selection scheme.

Turning our attention to the proposed location-based scheme, we see from the channel utilization plots shown in Fig. 4.4 that the used overhead is much lower for this scheme compared the the SNR-based scheme. The curves are calculated using eq. (4.7). Here, the 2% utilization is never exceeded in the plot, even when we have 50 MDs with measurement intervals of just $\mu_{\text{hello}} = 0.2s$, which lead to a utilization of 90% for the SNR measurement based scheme. This is mainly due to the fact that the utilization of the location based scheme grows linearly with the number of MDs whereas the growth is almost quadratic for the SNR based scheme.
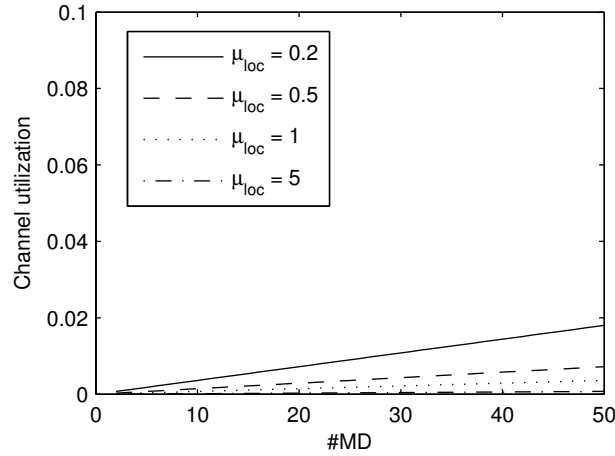

Figure 4.4: Utilization of channel for obtaining and collecting location measurements (Data rate is 6Mbit/s). Notice this plot shows only $0 - 0.1$ on the y-axis.

4.1.6.2 Results for the SNR Based Algorithm

The results have been created using the parameters and settings listed in Table 4.1 and Table 4.2. The default parameters for the ns-2 802.11ext model have been used if not explicitly specified in the tables. The errorbar in the results show the overall mean and 95% confidence intervals for the mean values obtained in each simulation run.

Simulation time	$360s$
No. of simulation runs	15
Hello interval μ_{hello}	$5 \pm \text{uniform}(0..0.5)s$
Location interval μ_{loc}	$f(N, \mu_{\text{hello}})$
Transmission interval μ_{tx}	0.5 s (exponentially distributed)
Storage time α_{store}	20 s

Table 4.2: Simulation parameters in addition to Table 4.1.

The first results in Fig. 4.5 show the achieved BER for varying number of MDs. We see that increasing the number of MDs does not have a practical impact on the relative performance of the ideal and measurement based schemes. However compared to the always direct scheme, the measurement based and ideal schemes are gaining better BER performance. This demonstrates that when the node density increases, further relay transmissions via short links are possible, which in turn leads to reduced BER.

The next set of results shown in Fig. 4.6 show the impact on the measurement based scheme of varying the hello interval μ_{hello} compared to the ideal and direct schemes.

In Fig. 4.6 we see that for $\mu_{\text{hello}} < 5s$, the achieved BER of the measurement based scheme is very close to the ideal scheme. As μ_{hello} increases, the measurement based scheme tends towards the direct
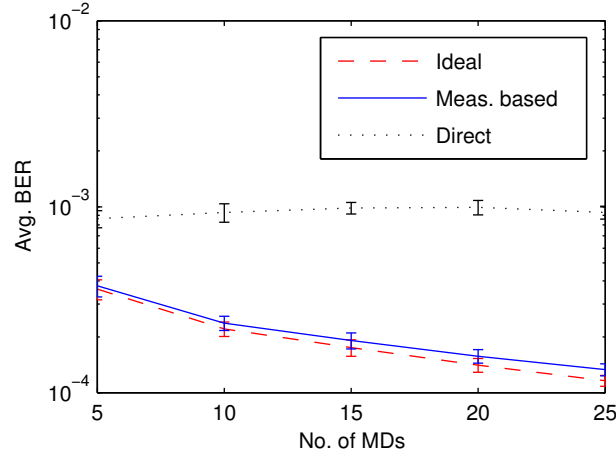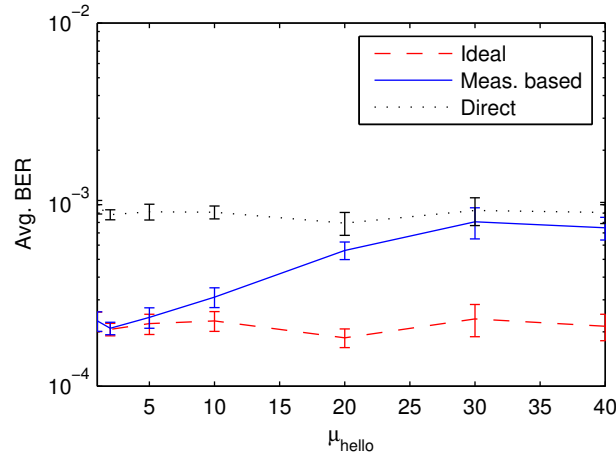
Figure 4.5: Achieved avg. BER for varying no. of MDs.

scheme. It is also noteworthy that the BER never seems to increase above the level of the direct scheme. This can be explained by the fact that all measurements that are older than a predefined storage threshold are deleted and thus, they do not lead to an uncorrect decision. By applying such storage threshold the entries with the stale information are effectively discarded.

Figure 4.6: Achieved avg. BER for varying μ_{hello}.

We now analyse how the mobility model impacts the path selection. Fig. 4.7 shows the achieved BER when the speed of the mobile devices is increased. The x-axes in both figures represent the average speed according to Table 4.3. Fig. 4.7 clearly shows that increasing the mobility speed leads to a significantly worse BER peformance than the direct scheme. This is of course highly undesirable, as the AP would be better off by using only direct transmissions. One obvious solution would be to increase the hello broadcast rate, as this would reduce the age of measurements. A downside to this is that the signaling overhead increases linearly with the hello broadcast rate. Increasing the broadcast rate is therefore costly in terms of capacity. We therefore investigate if limiting the storage time with the α_{store} parameter can improve this situation without increasing the signaling overhead.

The results in Fig. 4.8 show the achieved avg. BER for the mobility model with parameters specified by ID 3 in Table 4.3, which has a significantly worse performance than the direct scheme in Fig. 4.7. In Fig. 4.8 we see that setting $\alpha_{\text{store}} = 2s$ the resulting avg. BER is slightly lower than the direct scheme. Hereby we have shown that by proper setting of the α_{store} parameter it is possible to enhance performance without additional signaling overhead for a given scenario. As $\mu_{\text{hello}} = 5s$ in the considered scenario, setting $\alpha_{\text{store}} = 2s$ entails that the AP does not always have knowledge of a link, but measurements are

	Speed [m/s]		
ID	min	max	avg.
1	0.5	2	1.25
2	2	8	5
3	5	15	10
4	10	20	15

Table 4.3: Minimum and maximum speed used for the RWP mobility model and the corresponding ID and average speed.
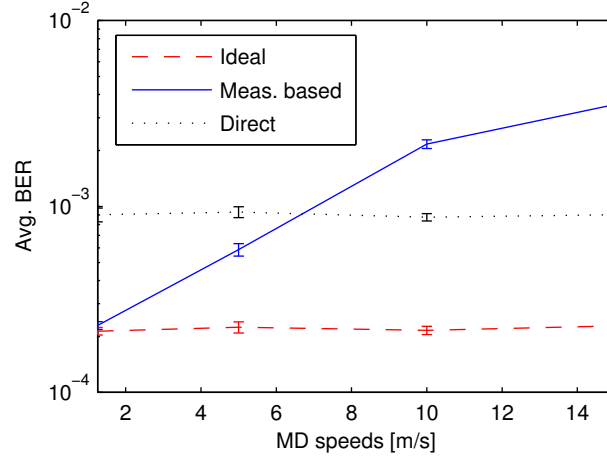

Figure 4.7: Achieved avg. BER for varying mobility speed.

only used when they are fresh, i.e. less than 2 seconds old. Further, as we consider symmetric links, both measurements from the two MDs of a link contribute to the AP's knowledge of a link. this means that the fraction of time where the AP has knowledge of a specific link, lies in the interval between $\frac{2}{5}$ and $\frac{4}{5}$, since hello broadcasts are unsyncronized and assumed to be i.i.d.

4.1.6.3 Results for the Location-based Algorithm

Considering now also the location-based relay selection algorithm, Fig. 4.9 shows that for the same measurement rate ($\mu_{\text{hello}} = \mu_{\text{loc}}$) the SNR and location based schemes perform similarly. However, if we instead use the μ_{loc} that satisfies $U_{\text{snr}} = U_{\text{loc}}$ (see eq. (4.6) and eq. (4.7)) the signaling overhead in terms of channel utilization will be the same for the SNR and location based schemes. The performance of the location based scheme will in this case be close to the ideal scheme.

As the accuracy of GPS location estimates depends on uncontrollable factors such as weather and surrounding buildings and therefore may vary, we investigate the achieved performance for different accuracy levels in Fig. 4.10. In this and the following plots the SNR based scheme has been generated for an average movement speed of $5m/s$. The path loss model used for the location based scheme uses the true path loss exponent $n = 2.9$ in this plot. Fig. 4.10 shows that the location measurement based scheme performs close to the ideal scheme for $\sigma_{\text{pos}} < 5m$, while it is still better than the SNR based scheme up to $\sigma_{\text{pos}} < 10m$ and becomes worse than the direct scheme when crossing $\sigma_{\text{pos}} \simeq 13m$. Considering that GPS receivers typically achieve an accuracy of $15m$ [Gar09], a GPS-only localization system may not be accurate enough for location based relaying. A solution would be to consider a hybrid localization approach using both GPS, Galileo and network based localization techniques that have been shown to improve location accuracy in [MSL+08].

Since the path loss exponent cannot be assumed to be known, we investigate the impact of varying the guessed value of n in Fig. 4.11. Interestingly, the performance of the location based scheme is very
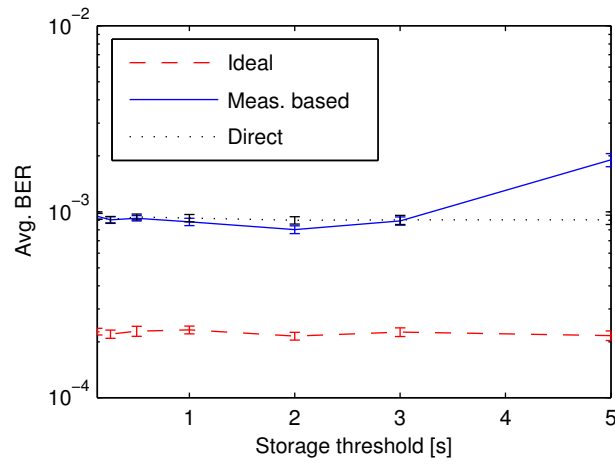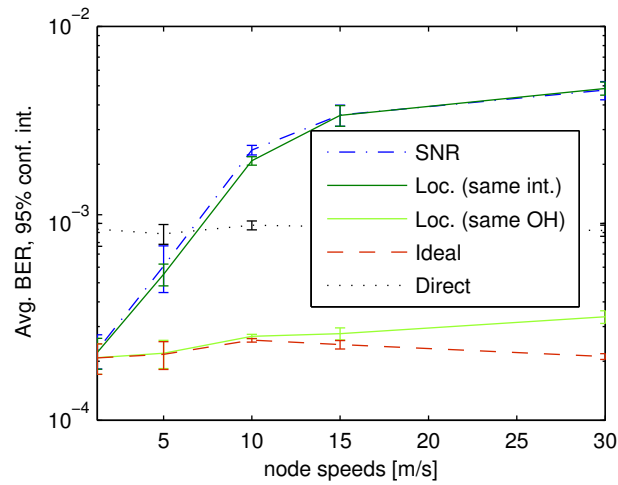
Figure 4.8: Avg. BER for mobility model ID 3.

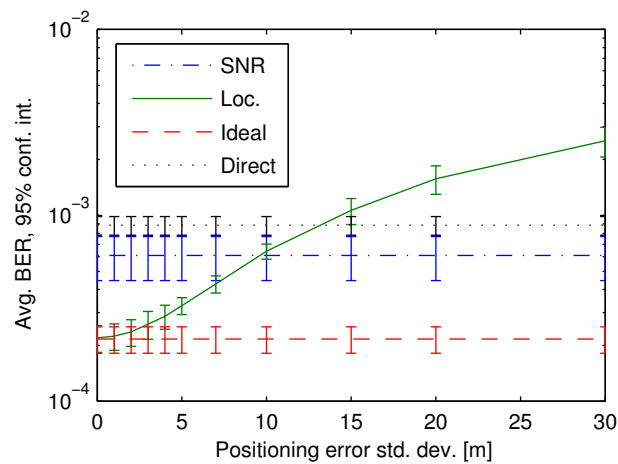Figure 4.9: BER impact of varying node speed.

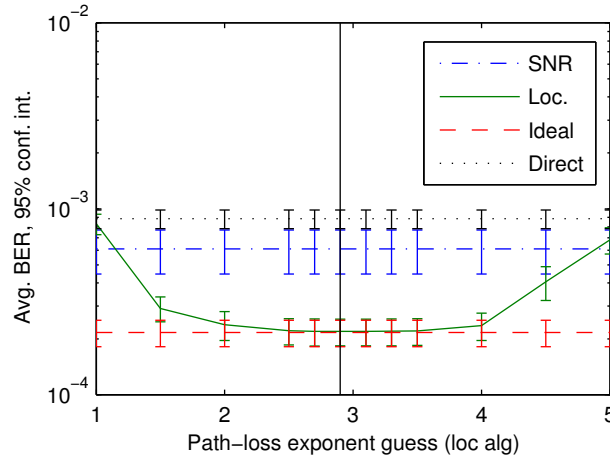Figure 4.10: BER impact of the accuracy of location measurements. Node speed is $5m/s$.

Figure 4.11: BER impact of the accuracy of the used path loss exponent compared to the true value of 2.9. Node speed is $5m/s$.

close to the ideal scheme for values in a relatively wide range of $2 < n < 4$. Correct estimation of the path loss exponent does not seem to be highly important for achieving a near ideal performance with the location based scheme.

There may be cases where the direct propagation path between two nodes is blocked by obstacles. This NLOS condition may occur between two MDs or the AP and an MD. In this work we have introduced a horizontal "wall" that attenuates all crossing transmissions, but does not hinder node movements. In Fig. 4.12 we investigate the impact of varying the wall attenuation for a wall that is placed $0.25m$ below the AP. That is, the AP has LOS to all MDs in the upper half of the scenario and NLOS towards all MDs in approximately the lower half.
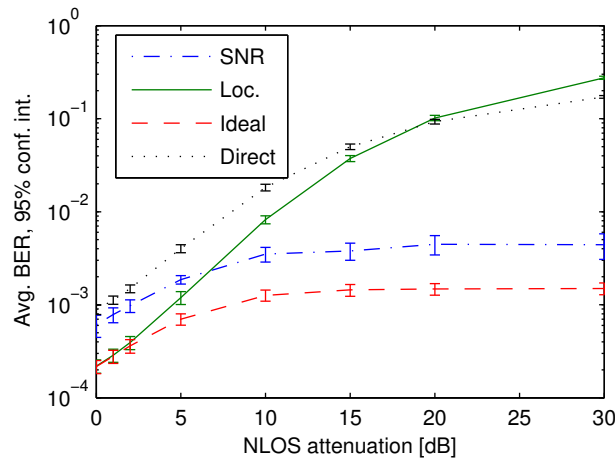
Figure 4.12: BER impact from NLOS caused by horizontal wall for increasing attenuation. Node speed is $5m/s$.

All schemes achieve worse performance for increasing wall attenuation. However, it is clear that the ability to sense the wall attenuation is beneficial. This is clear by noticing that the performance of the ideal and SNR based schemes does not degrade as much as the location based and direct schemes. When transmitting to an MD in the lower half of the scenario, the direct scheme will experience the attenuation for all transmissions from the AP to such nodes, whereas the ideal and SNR based schemes can take the attenuation into account when selecting a relay node. Since the location based schemes uses only the path loss model for predicting link states, the wall attenuation is not taken into account and the relay can even be chosen in such unfortunate way that the wall is crossed in both the AP-relay and relay-destination

transmissions. This can be seen in Fig. 4.12, where the BER of the location based scheme even exceeds the direct scheme.

Assuming that the AP has access to a spatial map of obstructions that cause NLOS conditions, the performance of the location based scheme can be improved in NLOS conditions. The map could be used to determine if there is LOS between two node positions. For LOS situations the attenuation term X in (4.4) is zero, while for NLOS it will be nonzero. But as the wall attenuation cannot be assumed to be known, we investigate the performance impact of different guesses for the attenuation value. We use a wall attenuation of $13.3dB$ in our simulations, since according to reference [DRX98] this value is typical.

Fig. 4.13 shows that as the NLOS attenuation guess gets close to the true value of $13.3dB$, the avg. BER of the location based scheme decreases. Guesses exceeding the true value do however not cause an increase in the BER. In addition to the wall position $0.25m$ below the AP, we also investigate the situation
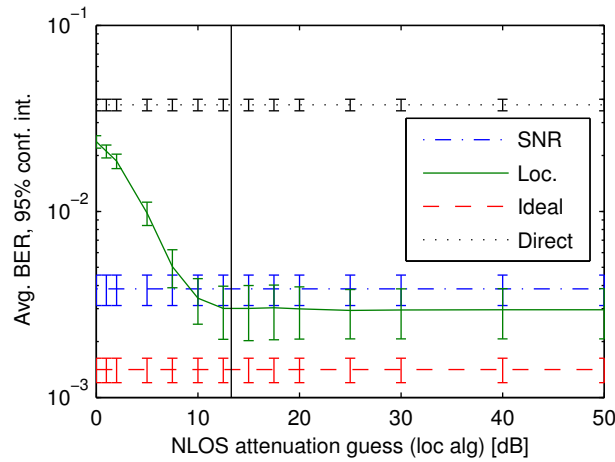

Figure 4.13: BER impact for different guesses of the unknown NLOS attenuation with a true value of $13.3dB$. Wall is close to AP. Node speed is $5m/s$.

where the wall is half-way between the AP and the bottom border of the scenario, which corresponds to $25m$ below the AP. This result is shown in Fig. 4.14. Primarily, we can see that the conditions have become difficult for even the ideal scheme as the BER has shifted a decade up, compared to Fig. 4.13. Further, it can be seen that under- or overestimation of the wall attenuation has a clearly negative impact on performance. So in this case, a priori knowledge of the wall attenuation is needed to obtain good performance. The wall attenuation could be obtained by evaluating both SNR and location measurements in the online system, however this is a topic for future work.

4.1.7   Conclusion

The scenario considered in this work concerns downlink data transmissions in a IEEE 802.11 based wireless network with mobile users. The focus of this work has been on analyzing relay selection schemes when either direct or two-hop relayed transmissions are possible for each data transmissions. Specifically, we have considered an SNR measurement based scheme and a location measurement based scheme and compared their performance. The schemes have been evaluated for the random waypoint mobility model as well as using ns-2 and matlab simulations. Specifically we vary the number of mobile devices, their speed, the measurement frequency, and lastly the measurement storage time threshold. Specifically for the location-based scheme we have investigated the impact of inaccurate path loss model parameters. Results were compared to a scheme that always uses direct transmissions and an ideal scheme that has instant and perfect link state knowledge.

The results show that for relatively fast moving mobile devices ($5-15\ m/s$) the achieved avg. BER performance of the SNR measurement based scheme can get significantly worse than the always direct scheme. Increasing the hello broadcast rate can mitigate this effect, however, at the cost of a linear
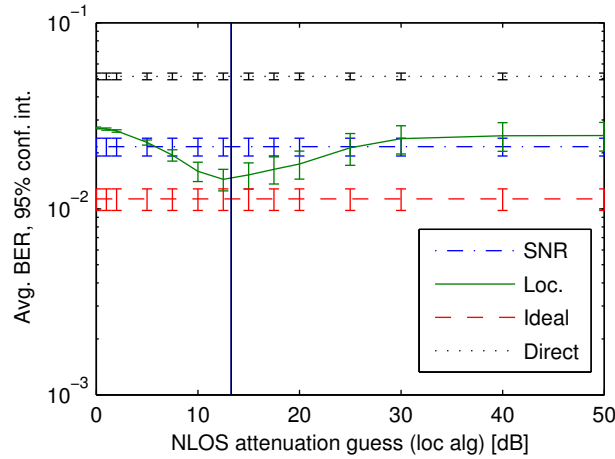
Figure 4.14: BER impact for different guesses of the unknown NLOS attenuation with a true value of 13.3*dB*. Wall is halfway between AP and bottom. Node speed is 5*m/s*.

increase in signaling overhead. We show that by limiting the measurement storage time, i.e. letting the AP use only fresh measurements, we are able to achieve a performance slightly better than or equal to the always direct scheme without increasing the signaling overhead. This result underlines the importance of choosing the storage threshold parameter carefully in scenarios with mobile devices. However, in case of fast moving users, the measurement collection frequency that is required for acceptable performance results in a large signaling overhead.

We therefore proposed a relay path selection scheme based which uses collected location information together with a path loss model for relay selection and thereby creates considerably less signaling overhead. We have shown that due to reduced signaling overhead, this scheme allows considerably higher movement speeds as compared to the SNR measurement based scheme. In the considered case, a four fold increase of the movement speed was possible.

Further we found that the required location measurement accuracy was comparable to the typical accuracy of standard GPS systems. In many cases, a standard GPS system would therefore be usable, however, as the accuracy of GPS in urban/indoor environments is typically worse, a localization systems with a higher accuracy than standard GPS, should be considered for these cases. For example network based localization methods could be exploited to improve the localization accuracy.

As the parameters of the environment are not always known in advance, we have investigated the sensitivity of the location based relaying scheme towards inaccurate settings of parameter in the path loss model. With regard to the path loss exponent, which is typically either unknown and thus guessed from the environment characteristics or estimated as the average over a larger area, we found that estimates within a relatively wide range of ± 1 around the true value resulted in near-optimal results. In the case of a NLOS situation, we found that the relaying performance was severely degraded without a priori knowledge. If on the other hand knowledge of LOS/NLOS between nodes was made available by extending the location based scheme with a spatial map of obstructions, the obtained performance was useful for estimates within $\pm 3dB$ of the true attenuation factor. A hybrid scheme that combines the low overhead from the location based scheme with the sensing ability from the SNR based scheme would therefore be an interesting topic for future work.

4.2   Position Information Based Relay Selection Techniques for Cooperative Communications

4.2.1   *Motivation and Approach*

Applications of positioning (or location) information (PI) of wireless devices are constantly growing. PI can be used for location based services, cognitive radio, handoff services, synchronization and interference cancelation. PI has also been used for routing in wireless ad hoc networks where PI of all nodes

are known by centralized unit [ZR03]. However, centralized unit is unable to update all PI due to its feedback load for large number of network nodes. In order to reduce the load of the network, several wireless standardization committees have recommended to have PI to each future wireless devices individually. The PI at each wireless device may be available through localization algorithms [YDGL08] or from independent systems such as global positioning systems or global navigation satellite systems.

Most of the relay selection processes are based on instantaneous channel gain (ICG) of the source-relay (sr) and relay-destination (rd) links. ICG is a part of channel state information (CSI). The selection based on maximum ICG (MICG) of relay-destination (rd) links is proposed in [BA]. MICG requires M channel estimations to select the highest ICG among M rd links. M is the number of successful decoded relay nodes also known as contention relay nodes. The other method based on optimal ICG (OICG) is provided in [BKRL06b] and becomes a more popular relay selection process. However, it requires a large number of channel estimations resulting in higher network complexity specially when the number of nodes in the network increases [FU08]. The outage performance of the opportunistic and repetition based cooperative relay networks for DF and AF protocols are provided in [XLZY09,ZAL05,HKA07,BSW07].

The objective of this work is to use PI in the relay selection process with very low complexity and good system performance. In this section, we use PI for distributed relay networks to select the best opportunistic relay node. More precisely we propose to use the shortest distance (SD) of rd links in this selection process. The complexity of the proposed scheme is analyzed and compared with MICG and OICG schemes. First, the complexity comparison is provided based on the assumption that PI are available for all nodes. Then, the comparison is provided based on the assumption that PI are estimated by themselves. Finally, the outage and bit error rate (BER) of opportunistic DF relaying are provided in Rayleigh fading channel and compared with existing schemes. We show that the proposed scheme provides the same outage and BER as MICG scheme. However, it provides better outage and BER when compared with OICG scheme.

4.2.2   *Relay Selection by using PI*

The proposed scheme consists of two phases, namely phase I and phase II. We assume that the relay selection process is in phase I. During phase I, the source broadcasts its PI and its data to the destination and the relays. Since distance and PI are closely related, it is easy to find the distances of sr links by using the PI of source and relays. Let d_{sr_i} be the distance between the source and i^{th} relay. We define the set $\mathscr{D}$ to be the set of relays which take place within the distance d_0 of the source and these can decode data of the source. Therefore, the ith relay belongs to the decoded subset, $\mathscr{D}$, of M nodes if it satisfies the following condition i.e.

$$\mathscr{D} \triangleq \{i : d_{sr_i} \leq d_0, i = 1, 2, ..., M\} \tag{4.8}$$

where d_0 is a threshold distance, defined by $d_0 = (\alpha SNR/(2^{2R} - 1))^{1/\nu}$ or equivalently satisfies the relation

$$\frac{1}{2} \log_2 (1 + SNR\lambda) \geq R \tag{4.9}$$

where R is the system data rate, SNR is the transmit signal-to-noise ratio, $\lambda = \alpha d_0^{-\nu}$ is the threshold value at the relays, ν is the channel power decay factor and α is the proportional parameter depending on the transceiver design. The successful decoded relay nodes send their PI to the destination. The destination calculates the distance of $r_i d$ link by using the PI of ith relay and its own. Let say the distances of rd links are $d_{r_1 d}, d_{r_2 d}, ..., d_{r_M d}$ where M is the cardinal of $\mathscr{D}$. The best opportunistic relay node is decided by minimizing the distances of rd links and defined by a subset, $\mathscr{D}$, as

$$\mathscr{D} = \{c : d_{sr_i} \leq d_0, c = \min_i \{d_{r_i d}\}, \ i = 1, 2, \ldots, l\} \tag{4.10}$$

where cardinal of $\mathscr{D}$ is equal to 0 or 1 in opportunistic relaying network. Finally, the destination broadcasts the decision index through a feedback channel. Fig. 4.15 shows the proposed relay selection technique based on PI and SD approach.

Figure 4.15: Proposed relay selection process is based on PI and shortest distance approach.

During phase II, the selected relay sends the decoded data to the destination. By using PI, the best opportunistic relay can be selected without the knowledge of ICG or CSI of the links. So, the proposed scheme does not require any channel estimation complexity for the relay selection process.

4.2.3 Complexity Analysis

In this section, we analyze the complexity of the relay selection schemes based on M competitive relay nodes. The proposed SD approach finds the best relay link by minimizing the l distances of rd links. The maximum complexity of SD scheme is of $\mathcal{O}(M^2)$ when PI is available to the nodes. However, when all nodes estimate their own PI, the additional complexity for estimating PI for M competitive relay nodes is of $\mathcal{O}(M(M+2)) \simeq \mathcal{O}(M^2)$ [YDGL08].

The complexity of MICG and OICG depends on the complexity of channel estimation. In this work, we assume that the channel is estimated in frequency domain through traditional minimum mean square error (MMSE). For this purpose, M channels (source to M relays) estimation are required to determine the decoded relays and M channel coefficients (M relays to destination) are required to find ICG of the M links. The complexity of MMSE to achieve matrix inversion for $2M$ channel estimation is of $\mathcal{O}(2MN_f^3)$ where N_f is the size of the FFT matrix which is very large when compared to M. The complexity of MMSE for FFT operation for $2M$ channel estimation is of $\mathcal{O}(2MN_f \log_2 N_f)$. The actual channel estimation complexity either in time or frequency domains given in [WZN08] is much more than the presented here.

In MICG approach, the best opportunistic relay node is selected by considering maximum ICG of M rd links. The complexity for maximization of M ICG is of $\mathcal{O}(M^2)$ as SD approach. The approximate complexity for MICG scheme is of $\mathcal{O}(MN_f^3) + \mathcal{O}(MN_f \log_2 N_f) + \mathcal{O}(M^2)$ when MMSE is used for the channel estimation.

In OICG approach, the best opportunistic relay node is selected by using max-min approach [BSW07]. The complexity for this max-min approach is of $\mathcal{O}(M^2 \log_2 M)$. The approximate complexity of OICG schemes is of $\mathcal{O}(MN_f^3) + \mathcal{O}(MN_f \log_2 N_f) + \mathcal{O}(M^2 \log_2 M)$ when MMSE is used for the channel estimation. Table 4.4 shows that the proposed scheme has very lower complexity when compared to MICG and OICG schemes in both cases: when PI is available and when PI is estimated by themselves.

Table 4.4: Computational Complexity

	PI	CSI		Optimization
		Matrix inversion	FFT operation	
MD with available PI	-	-	-	$\mathscr{O}(M^2)$
MD with estimated PI	$\mathscr{O}(M(2M+1))$	-	-	$\mathscr{O}(M^2)$
MICG	-	$\mathscr{O}(MN_f^3)$	$\mathscr{O}(MN_f \log_2 N_f)$	$\mathscr{O}(M^2)$
OICG	-	$\mathscr{O}(MN_f^3)$	$\mathscr{O}(MN_f \log_2 N_f)$	$\mathscr{O}(M^2 \log_2 M)$

4.2.4   *Outage performance of Opportunistic Relaying*

In our proposed scheme, the best opportunistic relay node is selected by considering the minimum distance of the *rd* links whereas in MICG scheme it is selected by considering the maximum ICG of the *rd* links. The distances are directly related to the channel gain (loss) by the relation $d_{r_i d}{}^{\nu} \gamma_{r_i d} = \alpha$ in a free path propagation loss [FU08]. It shows that distances and ICG are inversely proportional to each other. Therefore, based on the linear programming problem, we can show that

$$\arg\min_i(d_{r_i d}) = \arg\max_i(\gamma_{r_i d}) \quad i = 1, 2, ..., M \tag{4.11}$$

Since the indexes from min and max approaches are the same, SD and MICG schemes provide the same opportunistic relay node. Both schemes offer the same outage and BER performance. So, if SD is used for relay selection, channel estimation complexity can be avoided totally without any performance degradation. For simplicity, we provide the outage performance based on ICG. The ICG, $\gamma_{r_i d}$, can be obtained by using the distances, $d_{r_i d}$, of $r_i d$ link.

4.2.4.1 Outage Probability in the Absence of Direct Link

In opportunistic relaying, only one relay node is active in phase II which is selected from *l* contention relay nodes. Therefore, the outage probability of SD and MICG in the absence of direct link can be expressed as

$$
\begin{aligned}
p_{SD,MICG}^{sd=0}(\mathscr{O}) &= Pr[I < R] \\
&= \sum_{l=0}^{1} Pr[\mathscr{O} || \mathscr{D}| = l] Pr[|\mathscr{D}| = l]
\end{aligned} \tag{4.12}
$$

where $|\mathscr{D}|$ is the cardinal of $\mathscr{D}$, *I* is the mutual information of the relay network and $Pr[\mathscr{O} || \mathscr{D}| = 0]$ is the probability of outage given that no active relay node is present. The full outage is occurred in the absence of direct and relay links. The conditional probability can be written as

$$Pr[\mathscr{O} || \mathscr{D}| = 0] = 1 \tag{4.13}$$

In opportunistic relying, only one relay node is active in *rd* links. This active relay node is decided by considering the maximum ICG of the *rd* links as

$$\hat{x} = \max(\gamma_{r_i d}) \quad i = 1, 2, ..., M \tag{4.14}$$

$Pr[\mathscr{O} || \mathscr{D}| = 1]$ is the probability of outage given that only one active relay node is active in $\mathscr{C}$ as

$$
\begin{aligned}
Pr[\mathscr{O} || \mathscr{D}| = 1] &= Pr\left[\frac{1}{2} \log_2(1 + SNR\hat{x}) < R\right] \\
&= Pr[\hat{x} < \gamma] \\
&= F_{\hat{x}}(\gamma)
\end{aligned} \tag{4.15}
$$

The cumulative distribution function (CDF) of $\hat{x}$ for MICG scheme in i.i.d Rayleigh fading channel is defined as

$$
\begin{aligned}
F_{\hat{x}}(\gamma) &= Pr\left[\max(\gamma_{r_1d}, \gamma_{r_2d}, ..., \gamma_{r_Md}) < x\right] \\
&= \left(1 - e^{\gamma/\Omega_{rd}}\right)^M
\end{aligned}
\tag{4.16}
$$

Similarly the CDF of OICG in the same scenarios is given by [BSW07, Eq. (20)]

$$
F_{\hat{y}}(\gamma) = \left(1 - e^{-\gamma/\Omega}\right)^M
\tag{4.17}
$$

where $\Omega = \Omega_{sr}\Omega_{rd}/(\Omega_{sr} + \Omega_{rd})$ and $\hat{y} = \max\left(\min\left(\gamma_{sr_i}, \gamma_{r_id}\right)\right)$

The cardinal of $\mathscr{D}$ depends on both *sr* and *rd* links. $|\mathscr{D}| = 0$, if ICG of relays in $\mathscr{D}$ are greater than γ in phase I and below γ in phase II. Therefore, $Pr[|\mathscr{D}| = 0]$ is given as

$$
\begin{aligned}
Pr[|\mathscr{D}| = 0] &= \left(e^{-\gamma/\Omega_{sr}}\right)^M \left(1 - e^{-\gamma/\Omega_{rd}}\right)^M \\
&= \left(e^{-\gamma/\Omega_{sr}} - e^{-\gamma/\Omega}\right)^M
\end{aligned}
\tag{4.18}
$$

Since $|\mathscr{D}|$ is equal to 0 or 1 in opportunistic relaying, $Pr[|\mathscr{D}| = 1]$ is given by

$$
Pr[|\mathscr{D}| = 1] = 1 - \left(e^{-\gamma/\Omega_{sr}} - e^{-\gamma/\Omega}\right)^M
\tag{4.19}
$$

Using (4.13)-(4.19) in (2.14), the outage probability of SD/MICG can be expressed as

$$
\begin{aligned}
p_{SD,MICG}^{sd=0}(\mathscr{O}) = \left(e^{-\gamma/\Omega_{sr}} - e^{-\gamma/\Omega}\right)^M + \\
\left\{1 - \left(e^{-\gamma/\Omega_{sr}} - e^{-\gamma/\Omega}\right)^M\right\} \left(1 - e^{-\gamma/\Omega_{rd}}\right)^M
\end{aligned}
\tag{4.20}
$$

Similarly, by using the above procedure and the help of (4.17) and [HKA07, Eq. (13)], the outage probability of OICG scheme in absence of the direct link can be written as

$$
\begin{aligned}
p_{OICG}^{sd=0}(\mathscr{O}) = \left(e^{-\gamma/\Omega_{sr}} - e^{-\gamma/\Omega}\right)^M + \\
\left\{1 - \left(e^{-\gamma/\Omega_{sr}} - e^{-\gamma/\Omega}\right)^M\right\} \left(1 - e^{-\gamma/\Omega}\right)^M
\end{aligned}
\tag{4.21}
$$

4.2.4.2 Outage Probability in the Presence of Direct Link

In the presence of direct link, if no active relay node is present, the signal can be transmitted through the *sd* link and the outage is occurred if $\gamma_{sd} < \gamma$. Therefore, the conditional probability can be expressed as

$$
\begin{aligned}
Pr[\mathscr{O}||\mathscr{D}| = 0] &= Pr\left[\frac{1}{2}log_2(1 + SNR\gamma_{sd}) < R\right] \\
&= Pr[\gamma_{sd} < \gamma] \\
&= 1 - e^{-\gamma/\Omega_{sd}}
\end{aligned}
\tag{4.22}
$$

In the presence of direct and relay links, the destination performs maximum ratio combining (MRC) of *sd* and *rd* links. Therefore, corresponding conditional probability is given as

$$
\begin{aligned}
Pr[\mathscr{O}||\mathscr{D}| = 1] &= Pr\left[\frac{1}{2}log_2(1 + SNR\gamma_{sd} + SNR\hat{x}) < R\right] \\
&= Pr[\gamma_{sd} + \hat{x} < \gamma] \\
&= F_{\gamma_{sd}+\hat{x}}(\gamma)
\end{aligned}
\tag{4.23}
$$

where γ_{sd} is a exponential random variable and $\hat{x}$ is a random variable with PDF is given as

$$
\begin{aligned}
f_{\hat{x}}(x) &= \frac{d}{dx} Pr[\hat{x} < x] \\
&= \frac{M}{\Omega_{rd}} e^{-x/\Omega_{rd}} \left(1 - e^{-x/\Omega_{rd}}\right)^{M-1}
\end{aligned}
\tag{4.24}
$$

To evaluate (4.23), we use the moment generating function (MGF) of random variable γ_{sd} and $\hat{x}$ which are given as

$$
\begin{aligned}
\mathscr{M}_{\gamma_{sd}}(-s) &= \frac{1}{\Omega_{sd}} \int_0^\infty e^{-sx} e^{-x/\Omega_{sd}} dx \\
&= \frac{1}{\Omega_{sd}s + 1}
\end{aligned}
\tag{4.25}
$$

and

$$
\begin{aligned}
\mathscr{M}_{\hat{x}}(-s) &= \frac{M}{\Omega_{rd}} \int_0^\infty e^{\frac{-(\Omega_{rd}s+1)x}{\Omega_{rd}}} (1 - e^{-x/\Omega_{rd}})^{M-1} dx \\
&= MB(\Omega_{rd}s + 1, M)
\end{aligned}
\tag{4.26}
$$

where B(x,y) is a beta function obtained by substituting $t = e^{-x/\Omega}$ in the above integral. The MFG of $\gamma_{sd} + \hat{x}$ is given as

$$
\begin{aligned}
\mathscr{M}_{\gamma_{sd}+\hat{x}}(-s) &= \frac{MB(\Omega_{rd}s + 1, M)}{\Omega_{sd}s + 1} \\
&= \frac{\Gamma(M+1)\Gamma(\Omega_{rd}s + 1)}{(\Omega_{sd}s + 1)\Gamma(\Omega_{rd}s + M + 1)} \\
&= \sum_{m=0}^{M-1} \binom{M-1}{m} \frac{M(-1)^m}{(\Omega_{rd}s + 1 + m)(\Omega_{sd}s + 1)}
\end{aligned}
\tag{4.27}
$$

By using the partial fraction expansion and applying an inverse LT in (4.27), the PDF of $\gamma_{sd} + \hat{x}$ can be expressed as

$$
f_{\gamma_{sd}+\hat{x}}(x) = \sum_{m=0}^{M-1} \binom{M-1}{m} \frac{M(-1)^m \left(e^{\frac{-x}{\Omega_{sd}}} - e^{\frac{-(m+1)x}{\Omega_{rd}}}\right)}{(m+1)\Omega_{sd} - \Omega_{rd}}
\tag{4.28}
$$

Therefore, the CDF of $\gamma_{sd} + \hat{x}$ is given as

$$
\begin{aligned}
F_{\gamma_{sd}+\hat{x}}(\gamma) = 1 + \sum_{m=0}^{M-1} \binom{M-1}{m} \times \\
\frac{M(-1)^m \left(\frac{\Omega_{rd}}{m+1} e^{\frac{-(m+1)\gamma}{\Omega_{rd}}} - \Omega_{sd} e^{\frac{-\gamma}{\Omega_{sd}}}\right)}{(m+1)\Omega_{sd} - \Omega_{rd}}
\end{aligned}
\tag{4.29}
$$

Similarly CDF of $\gamma_{sd} + \hat{y}$ for OICG is

$$
\begin{aligned}
F_{\gamma_{sd}+\hat{y}}(\gamma) = 1 + \sum_{m=0}^{M-1} \binom{M-1}{m} \times \\
\frac{M(-1)^m \left(\frac{\Omega}{m+1} e^{\frac{-(m+1)\gamma}{\Omega}} - \Omega_{sd} e^{\frac{-\gamma}{\Omega_{sd}}}\right)}{(m+1)\Omega_{sd} - \Omega}
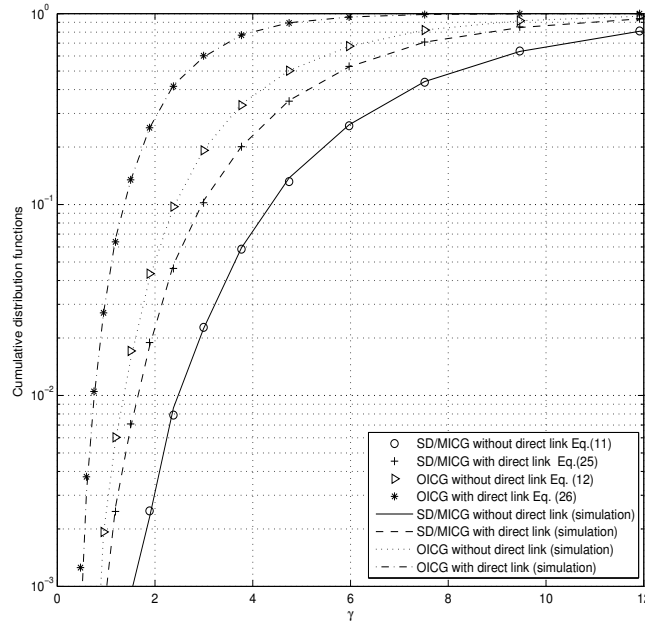\end{aligned}
\tag{4.30}
$$

Figure 4.16: Theoretical and Monte-Carlo simulation of cumulative distribution function of the selection process. The number of iterations is 10000 and parameters are M=6, $\Omega_{sr} = 2.2$, $\Omega_{sd} = 2.4$ and $\Omega_{rd} = 2.6$.

$Pr[|\mathscr{D}| = 0]$ and $Pr[|\mathscr{D}| = 1]$ remain the same as the previous one. By substituting (4.18), (4.19), (4.22) and (4.28) in (2.14), the outage probability can be expressed as

$$
\begin{aligned}
p_{SD,MICG}^{sr=1}(\mathscr{O}) = & \left(1 - e^{-\gamma/\Omega_{sd}}\right)\left(e^{-\gamma/\Omega_{sr}} - e^{-\gamma/\Omega}\right)^M + \\
& \left\{1 - \left(e^{-\gamma/\Omega_{sr}} - e^{-\gamma/\Omega}\right)^M\right\}\left\{1 + \sum_{m=0}^{M-1}\binom{M-1}{m}\times\right. \\
& \left.\frac{M(-1)^m\left(\frac{\Omega_{rd}}{m+1}e^{\frac{-(m+1)\gamma}{\Omega_{rd}}} - \Omega_{sd}e^{\frac{-\gamma}{\Omega_{sd}}}\right)}{(m+1)\Omega_{sd} - \Omega_{rd}}\right\}
\end{aligned}
\tag{4.31}
$$

Similarly, by using the above procedure and the help of (4.30) and [HKA07, Eq. (13)], the outage probability of OICG scheme in presence of direct link can be written as

$$
\begin{aligned}
p_{OICG}^{sr=1}(\mathscr{O}) = & \left(1 - e^{-\gamma/\Omega_{sd}}\right)\left(e^{-\gamma/\Omega_{sr}} - e^{-\gamma/\Omega}\right)^M + \\
& \left\{1 - \left(e^{-\gamma/\Omega_{sr}} - e^{-\gamma/\Omega}\right)^M\right\}\left\{1 + \sum_{m=0}^{M-1}\binom{M-1}{m}\times\right. \\
& \left.\frac{M(-1)^m\left(\frac{\Omega}{m+1}e^{\frac{-(m+1)\gamma}{\Omega}} - \Omega_{sd}e^{\frac{-\gamma}{\Omega_{sd}}}\right)}{(m+1)\Omega_{sd} - \Omega}\right\}
\end{aligned}
\tag{4.32}
$$

The above analysis shows that the diversity of the opportunistic relaying mainly depends on the CDF of the selection process given in (4.16), (4.17), (4.29) and (4.30). Fig. 4.16 shows the CDF of SD/MICG and OICG in presence and absence of direct link. We observed that sd/MICG has higher diversity than OICG scheme in both cases.
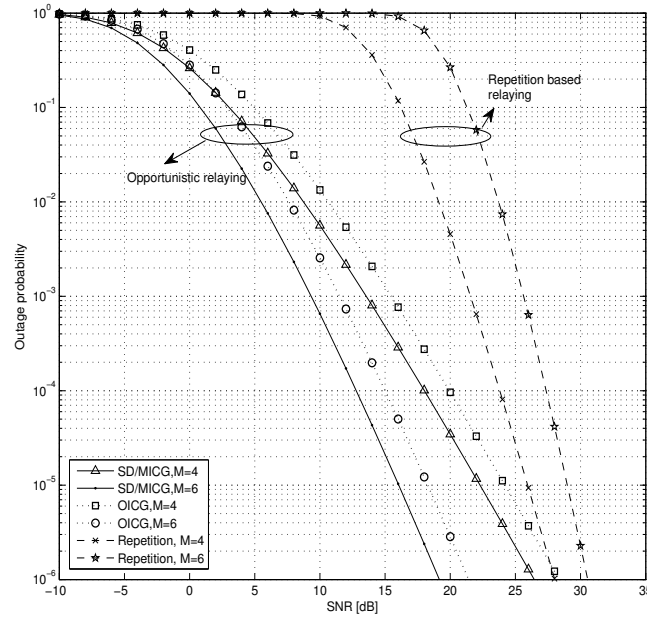
Figure 4.17: Outage probability of opportunistic DF relaying for SD/MICG and OICG schemes and repetition-based relaying for M=4 and 6 with $\Omega_{sr} = 2.2$, $\Omega_{sd} = 2.4$ and $\Omega_{rd} = 2.6$. It is assumed that both direct and relay links are present.

4.2.5   Simulation Results

In this section, we illustrate the outage probability of opportunistic DF relaying for SD/MICG and OICG schemes in Rayleigh fading channel. The BER is also provided in the same simulation scenarios. For this simulation, we assume that d_{sd} is 2 km. The distances, d_{sr_i} and d_{r_id}, are uniformly distributed in $[0,2]$. The transceiver gain, α, is of 5 dB and the power decay factor, ν, is of 2 for free path propagation. The threshold distance, d_0, is obtained from (4.9). The ICG, γ_{r_id}, of r_id link is obtained from corresponding distance, d_{r_id}. Finally, Ω_{sr} and Ω_{rd} are obtained by averaging the M ICG in sr links and M ICG in rd links, respectively.

Fig. 4.17 shows the outage probability for SD/MICG and OICG from (4.31) and (4.32) and repetition-based relaying from [ZAL05, Eq. (4)] in the presence of direct link. Even though opportunistic relaying has only one active relay node, it provides better outage performance than the repetition-based cooperative relaying. The repetition-based relaying has diversity at higher SNR with increase in M. However, the outage performance decreases at low SNR with increase in M. It is mainly because the bandwidth inefficiency is exponential in M. In MICG scheme, the opportunistic relay node is selected by considering the link which has the maximum ICG of rd links whereas in OICG, it is selected by considering the link which has optimum ICG between the sr and rd links. It is seen from the inequality, $\max(\gamma_{r_id}) > \max(\min(\gamma_{sr_i}, \gamma_{r_id}))$, that SD/MICG has more ICG than OICG approach. This ICG increases the mutual information and thus increases the outage performance of SD/MICG than OICG scheme.

Fig. 4.18 shows the outage probability of opportunistic relaying in presence and absence of direct link for SD, MICG and OICG approaches from (4.20), (4.21), (4.31) and (4.32). In this simulation, we use $M = 5$, $R = 1$ bit/sec/Hz and $R = 2$ bit/sec/Hz. Fig. 4.18 shows that the outage in the presence of direct link is better than the absence of the direct link for all schemes. The gain of SD/MICG from OICG at 0.1% outage is about 5 dB in the absence of direct link and the gain is about 2 dB in the presence of direct link. This gain difference is because the outage totaly depends on the selected relay node in the absence of direct link, so their gain difference is prominent. However, in the later case, the outage partly depends on the selected relay due to the presence of direct link. The gain difference between two different data
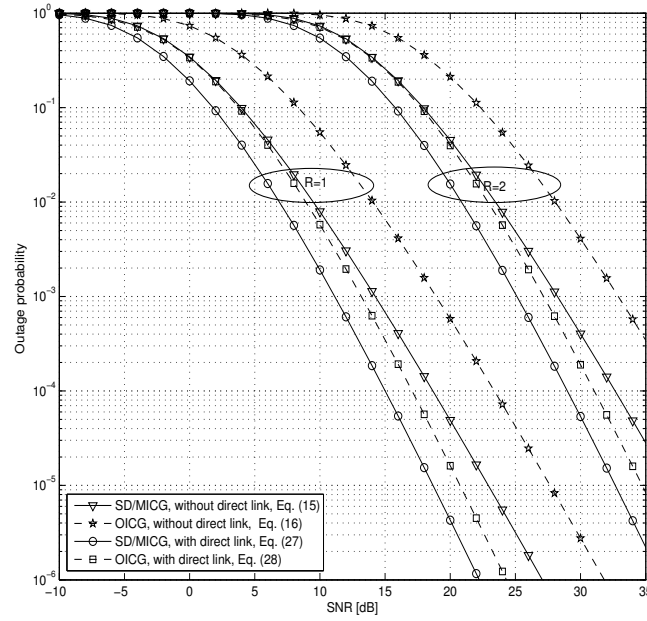
Figure 4.18: Outage probability of opportunistic DF relaying for $M = 5$, and data rate is of $R = 1$ bit/sec/Hz and $R = 2$ bit/sec/Hz.

rates is about 12 dB for all the schemes.

Fig. 4.19 provides the BER of SD, MICG and OICG schemes in presence of direct link, absence of direct link and without cooperative communication. We assume that the number of relay nodes is 12. In Fig. 4.19, we can easily observe that both SD and MICG scheme provide the same BER in both transmission scenarios. It means that the same opportunistic relay node is selected by both SD and MICG techniques. SD/MICG even provides better BER than OICG schemes in the presence and the absence of direct link. On the other hand, SD has very low complexity compared with MICG without any performance loss as shown in section 4.2.3. Therefore, the proposed scheme is very useful for opportunistic relaying networks.

4.2.6   Conclusions

Here, we have used PI to select an opportunistic relay node of DF cooperative network. The opportunistic relay node is selected by considering the link which has the *rd* link with shortest distance. The proposed scheme does not require any channel estimation for the relay selection. The complexity of the proposed scheme is analyzed in two different scenarios: PI is available to the nodes and PI is estimated by themselves. The complexities are compared with MICG and OICG schemes. We have shown that the proposed scheme has very lower complexity and is easier to implement than MICG and OICG schemes. The outage and BER performance are also analyzed in presence and absence of direct link. The proposed scheme provides better outage and BER performance than the OICG scheme.
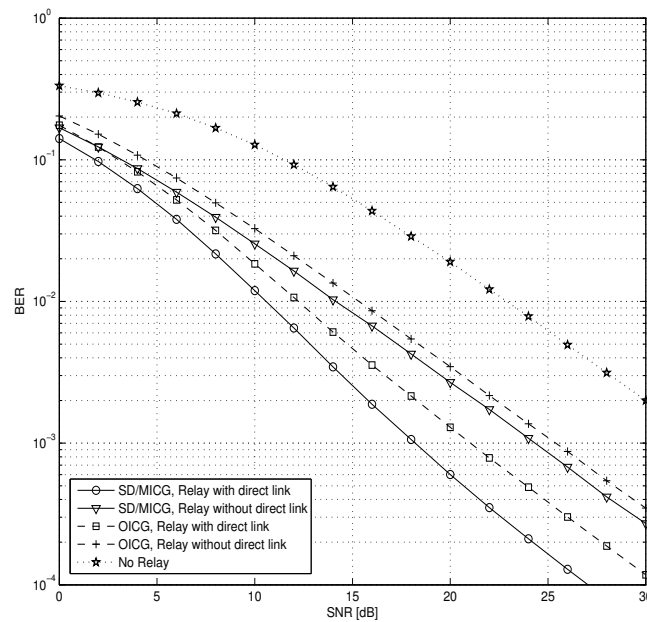
Figure 4.19: BER vs SNR of SD, MICG and OIGC opportunistic DF relaying in the Rayleigh fading channel.

5 SUMMARY AND OUTLOOK

This deliverable provided final results about location-aided cooperative communications carried out in the WHERE project from both the physical layer and the network layer of wireless systems. Performance of various cooperative relaying protocols and multi-hop routing protocols were analytically and experimentally investigated for both AWGN and fading channels. Discussions were also provided about how to efficiently utilize the location information in cooperative networking as well as the impact on overall performance. This work covered two WHERE scenarios, i.e. C1-A and C2. More intensive investigation would be performed in the WHERE continuation about efficient location-aided cooperative relaying as well as the implementation issues. More detailed achievements of this deliverable are summarized as follows:

Chapter 1 presented an brief introduction about three classical relaying protocols, i.e. DF, AF, and CF. Two key issues , i.e., the effect of user mobility and the use of location information in cooperative communication, have been briefly addressed.

Chapter 2 addressed the location-aided DF cooperative relaying in the physical-layer aspect. Specifically, we investigated the outage performance of DF relaying over asymmetric fading channels. New cooperative strategies and multi-link adaptation approaches were proposed for multiuser incremental relaying protocols. Location information was used as a kind of side information that offered average channel gain or imperfect channel knowledge. The impact of location information on the DF performance has been investigated through both analytical analysis and computer simulations.

Chapter 3 addressed the location-aided AF cooperative relaying in the physical layer aspect. Specifically, we investigated the outage performance of AF relaying over asymmetric fading channels. New power allocation strategies have been proposed to improve the average sum-rate and outage performance of two-way AF relaying network. According to the scenario C1-A, the location information was used to obtain parameters such as avg. SNR for various wireless links and mobility information. Both analytical and simulation results have shown the significance of using location information in cooperative AF relaying protocols.

Chapter 4 presented the location-aided relay selection technique that was used to improve the network-layer throughput or physical-layer outage performance. The analysis was conducted by calculating the actual link quality via bit level simulations and using this as a reference to evaluate the performance of both location-based and avg. SNR based relay decision algorithms. Simulation results indicated that high accuracy positioning systems could be used to estimate the link quality sufficiently accurate to match the avg. SNR based approach.

In general, the results of this deliverable should serve as the final input to Task 3.3 of WP3. Besides the above contributions, we plan to conduct a more extensive investigation for location-aided cooperative communications by considering advanced techniques in both the physical layer and network-layer research. Moreover, the investigation will look at emerging wireless systems such as FemtoCell, LTE-advance, wireless backhaul, mobile ad-hoc networks. Location information will be used to support energy-efficient cooperative communications.

REFERENCES

[ARDB08] C. Abou-Rjeily, N. Daniele, and J.C. Belfiore. On the amplify-and-forward cooperative diversity with time-hopping ultra-wideband communications. *IEEE Trans. Communications*, 56(4):630–641, 2008.

[AS64] M. Abramowitz and I. A. Stegun. *Handbook of Mathematical Function*. New York, 1964.

[AVM09] A. Agustin, J. Vidal, and O. Munoz. Protocols and resource allocation for the two-way relay channel with half-duplex terminals. In *Proc. IEEE Int. Conf. Commun. (ICC'09)*, pages 14–18, 2009.

[BA] E. Beres and R. S. Adve. On selection cooperation in distributed network. *Accepted for IEEE Transaction on Wireless Communications*.

[BHW07] A. Bletsas, S. Hyundong, and M. Z. Win. Cooperative communications with outage-optimal opportunistic relaying. *IEEE Transaction on wireless communications*, 6(9):pp.3450–3460, Sept. 2007.

[BKRL06a] A. Bletsas, A. Khisti, D.P Reed, and A. Lippman. A simple cooperative diversity method based on network path selection. *IEEE Journal on Selected Areas in Communications*, 24(3):659–672, 2006.

[BKRL06b] A. Bletsas, A. Khisti, D.P Reed, and A. Lippman. A simple cooperative diversity method based on network path selection. *IEEE Journal on Selected Areas in Communications*, 24:659–672, March 2006.

[BSW07] A. Bletsas, H. Shin, and M. Z. Win. Cooperative communication with outage optimal opportunistic relaying. *IEEE Transactions on Wireless Communications*, 6:3450–3459, 2007.

[CSEJ+07] Q. Chen, F. Schmidt-Eisenlohr, D. Jiang, M. Torrent-Moreno, L. Delgrossi, and H. Hartenstein. Overhaul of IEEE 802.11 modeling and simulation in ns-2. *Proceedings of the 10th ACM Symposium on Modeling, analysis, and simulation of wireless and mobile systems*, 2007.

[DH05] X. Deng and A. M. Haimovich. Power allocation for cooperative relaying in wireless networks. *IEEE Trans. Commun. Letters*, 9(11):994–996, Nov. 2005.

[DHHH00] A. Duel-Hallen, S. Hu, and H. Hallen. Long-range prediction of fading signals. *IEEE Signal Processing Magazine*, 17(3):62–75, May 2000.

[DL94] J.S. Davis and J.P.M.G. Linnartz. Vehicle to Vehicle RF propagation Measurements. *1994 Conference Record of the Twenty-Eighth Asilomar Conference*, 1, 1994.

[DRX98] G. Durgin, TS Rappaport, and H. Xu. Measurements and models for radio path loss and penetration loss inand around homes and trees at 5.85 GHz. *IEEE Transactions on Communications*, 46(11):1484–1496, 1998.

[FU08] M. M. Fareed and M. Uysal. A novel relay selection method for decode-and-forward relaying. In *Canadian Conference on Electrical and Computer Engineering*, pages 000135 – 000140, May 2008.

[Gar09] Garmin. About gps, 2009.

[GC97] A. J. Goldsmith and S. G. Chua. Variable-rate variable-power mqam for fading channels. *IEEE Transactions on Communications*, 45(10):1218–1230, Oct. 1997.

[GCN08]   F. Gao, T. Cui, and A. Nallanathan. Optimal training design for channel estimation in decode-and-forward relay networks with individual and total power constraints. *IEEE Trans. Sig. Process.*, 56(12):5937–5949, Dec. 2008.

[GJ06]   K.S. Gomadam and S. A. Jafar. Impact of mobility on cooperative communication. In *IEEE WCNC*, volume 2, pages 908–913, 2006.

[GM00]   D. Goodman and N. Mandayam. Power control for wireless data. *IEEE Personal Communications*, 7(2):48–54, July 2000.

[HA02]   M. O. Hasna and M. S. Alouini. Performance analysis of two-hop relayed transmission over rayleigh fading channels. In *Proc. IEEE VTC 02'Fall*, pages 1992–1996, 2002.

[Hag88]   J. Hagenauer. Rate-compatible punctured convolutional codes (RCPC codes) and their applications. *IEEE Transactions on Communications*, 36(4):389–400, April 1988.

[HHCK07]   Y. W. Hong, W. J. Huang, F.H. Chiu, and C. C. J. Kuo. Cooperative communications in resource-constrained wireless networks. *IEEE Signal Processing Magazine*, 24(3):47–57, 2007.

[HKA07]   K.-S. Hwang, Y.-C. Ko, and M.-Slim Alouini. Outage probability of cooperative diversity systems with opportunistic relaying based on decode-and-forwards. *IEEE Transactions on Wireless Communications*, 7:5100–5106, 2007.

[HL08]   B. Hegyi and J. Levendovszky. Efficient, distributed, multiple-relay selection procedures for cooperative communications. In *3rd International Symposium on Wireless Pervasive Computing*, pages 170–174, 2008.

[HN02]   T. E. Hunter and A. Nosratinia. Cooperation diversity through coding. In *Proceedings IEEE International Symposium Information Theory (ISIT 2002), Lausanne, Switzerland*, page 220, 2002.

[HSL05]   T. Himsoon, W. Su, and K.J.R Liu. Differential transmission for amplify-and-forward cooperative communications. *IEEE Signal Processing Letters*, 12(9):597–600, 2005.

[HT08]   Z. Hu and C.K. Tham. CCMAC: coordinated cooperative MAC for wireless LANs. In *Proceedings of the 11th international symposium on Modeling, analysis and simulation of wireless and mobile systems*, pages 60–69. ACM New York, NY, USA, 2008.

[HTHC08]   Y. Han, S. H. Ting, C. K. Ho, and W. H. Chin. High rate two-way amplify-and-forward half-duplex relaying with OSTBC. In *Proc. IEEE VTC 08'Spring*, pages 2426–2430, 2008.

[HZL08]   C. K. Ho, R. Zhang, and Y. Liang. Two-way relaying over ofdm: Optimized tone permutation and power allocation. In *Proc. IEEE Int. Conf. Commun. (ICC'08)*, pages 3908–3912, 2008.

[IEE07]   IEEE 802.11-2007, wireless lan medium access control (mac) and physical layer (phy) specifications, june 2007., June 2007.

[IHL07]   A.S. Ibrahim, Z. Han, and K. J. Ray Liu. Distributed energy-efficient cooperative routing in wireless networks. In *IEEE Proc. GLOBECOM 2007*, pages 4413–4418, 2007.

[ISSL08]   A.S. Ibrahim, A. K. Sadek, W. Su, and K. J. Ray Liu. Cooperative communications with relay-selection: When to cooperate and whom to cooperate with? *IEEE Transactions on Wireless Networks*, 7(7):2814–2827, 2008.

[Jr.50]   J. F. Nash Jr. Equilibrium points in n-person games. *Proceedings of the National Academy of Sciences of the United States of America*, 36(1):48–49, January 1950.

[KS09]   M. Katz and S. Shamai. Relaying protocols for two colocated users. *IEEE Transactions on Information Theory*, 52:2329 – 2344, 2009.

[KT08]   I. Krikidis and J. Thompson. Amplify-and-Forword with partial realy selection. *IEEE Communications Letters*, 12:235–237, Apr. 2008.

[LBC+05]   J. Luo, R. S. Blum, L. J. Cimini, L. J. Greenstein, and A. M. Haimovich. Decode-and-forward cooperative diversity with power allocation in wireless networks. In *IEEE Global Telecommunications Conference, GLOBECOM*, pages 5–9, Nov. 2005.

[LC06]   D.K. Lee and K.M. Chugg. A pragmatic approach to cooperative communication. In *IEEE Proceedings MILCOM 2006*, pages 1–7, 2006.

[Lee94]   L.H. C. Lee. New rate-compatible punctured convolutional codes for viterbi decoding. *IEEE Transactions on Communications*, 42(12):3073–3079, December 1994.

[LLG06]   L. Lai, K. Liu, and H. E. Gamal. The three-node wireless network: achievable rates and cooperation strategies. *IEEE Trans. Info. Theo.*, 52(3):805 – 828, Mar. 2006.

[LTN+07]   P. Liu, Z. Tao, S. Narayanan, T. Korakis, and S.S. Panwar. CoopMAC: A cooperative MAC for wireless LANs. *IEEE Journal on Selected Areas in Communications*, 25(2):340, 2007.

[LTW04a]   J. N. Laneman, D. N. C. Tse, and G. W. Wornell. Cooperative diversity in wireless networks: Efficient protocols and outage behavior. *IEEE Transactions of Information Theory*, 50:3062–3080, 2004.

[LTW04b]   J. N. Laneman, D. N. C. Tse, and G. W. Wornell. Cooperative diversity in wireless networks: Efficient protocols and outage behaviour. *IEEE Transactions on Information Theory*, 50(12):3062–3080, Dec 2004.

[LV05]   C. Lee and S. Vishwanath. Cooperative communication strategies for sensor networks. In *IEEE Proc. IEEE MILCOM 2005*, volume 2, pages 698–704. IEEE, 2005.

[LVZD07]   Y. Li, B. Vucetic, Z. Zhou, and M. Dohler. Distributed adaptive power allocation for wireless relay networks. *IEEE Transaction on Wireless Communications*, 6(3):948–958, March 2007.

[MSL+08]   C. Mensing, S. Sand, M. Laaraiedh, B. Uguen, B. Denis, M. Garcia, J. Casajus, T. Pedersen, G. Steinboeck X. Yin, B.H. Fleury, S. Mayrargue, and D. Slock. Where d2.1 - performance assessment of hybrid data fusion and tracking algorithms. Technical report, ICT-217033 WHERE, 2008.

[MYP+07]   S. Moh, C. Yu, S.M. Park, H.N. Kim, and J. Park. CD-MAC: Cooperative diversity MAC for robust communication in wireless ad hoc networks. In *IEEE International Conference on Communications, 2007. ICC'07*, pages 3636–3641, 2007.

[MYT08]   Y. Ma, N. Yi, and R. Tafazolli. Bit and power loading for ofdm-based three-node relaying communications. *IEEE Trans. Signal Process.*, 56(7):3236–3247, 2008.

[NHCL05]   Fan Ng, Juite Hwu, Mo Chen, and Xiaohua Li. Asynchronous space-time cooperative communications in sensor and robotic networks. In *Proc. IEEE Intl Conf. Mechatronics and Automation 2005*, pages 1624–1629, 2005.

[NHH04a]   A. Nosratinia, T. E. Hunter, and A. Hedayat. Cooperative communication in wireless net-works. *IEEE Communications Magazine*, 42(10):74–80, Oct 2004.

[NHH04b]   A. Nosratinia, T.E. Hunter, and A. Hedayat. Cooperative communication in wireless net-works. *IEEE Communications Magazine*, 42(10):74–80, OCT 2004.

[NMS10]   J. J. Nielsen, T. K. Madsen, and H-P. Schwefel. Mobility impact on centralized selection of mobile relays. In *Proceedings of the 6th IEEE Consumer Communications And Networking Conference CCNC 2010*. IEEE, 2010.

[NP07]   S. Narayanan and S.S. Panwar. To Forward or not to Forward–that is the Question. *Wireless Personal Communications*, 43(1):65–87, 2007.

[NVT08]   Seunghoon Nam, Mai Vu, and Vahid Tarokh. Relay selection methods for wireless cooper-ative communications. In *CISS*, pages 859–864, 2008.

[OAS07]   F. Atay Onat, D. Avidor, and S.Mukherjee. Two-hop relaying in random networks with limited channel state information. In *Proc. 4th IEEE SECON 2007*, pages 570–579, 2007.

[PAR08]   R.C. Palat, A. Annamalai, and J.H. Reed. Log-likelihood-ratio based selective decode and forward cooperative communication. In *Proc. IEEE VTC 2008*, pages 615–618, 2008.

[Pro95]   J.G. Proakis. Digital Communications Third Edition. *McGrawHill Inc, New York, USA*, 1995.

[PY07]   P. Popvski and H. Yomo. Physical network coding in two-way wireless relay channels. In *Proc. IEEE Int. Conf. Commun. (ICC'07)*, pages 707–712, 2007.

[Rap01]   T. Rappaport. *Wirelss communications: principle and practice*. Prentice-Hill, Englewood Cliffs, NJ, 2nd edition, 2001.

[Rei08]   A. Reichman. Cooperative communication overview. In *IEEE International Conference on Microwaves, Communications, Antennas and Electronic Systems (COMCAS-2008)*, pages 1–6, 2008.

[Ros09]   P. Rost. *Opportunities, Benefits, and Constraints of Relaying in Mobile Communication Systems*. PhD thesis, Technical University of Dresden, June 2009.

[RW07]   B. Rankov and A. Wittneben. Spectral efficient protocols for half-duplex fading relay chan-nels. *IEEE Journal on Selec. Areas in Commun.*, 25(2):379–389, Feb. 2007.

[SEA03a]   A. Sendonaris, E. Erkip, and B. Aazhang. User cooperation diversity - part i: System description. *IEEE Transcations on Communications*, 51(11):1927–1938, Nov 2003.

[SEA03b]   A. Sendonaris, E. Erkip, and B. Aazhang. User cooperation diversity - part ii: Imple-mentation aspects and performance analysis. *IEEE Transcations on Communications*, 51(11):1939–1948, Nov 2003.

[SEA03c]   A. Sendonaris, E. Erkip, and B. Aazhang. User cooperation diversity-part I: System de-scription. *IEEE Transactions on Communications*, 51(1):1927–1938, November 2003.

[SG02]   S.Zhou and G.B. Giannakis. Optimal transmitter eigen-beamforming and space-time block coding based on channel mean feedback. *IEEE Transactions on Signal Processing*, 50(10):2599–2613, Oct 2002.

[SGL06]   A. Scaglione, D.L. Goeckel, and J.N. Laneman. Cooperative communications in mobile ad hoc networks. *IEEE Signal Processing Magazine*, 23(5):18–29, 2006.

[Sha61]   C. E. Shannon. Two-way communication channels. In *Proc. 4th Berkeley Symp. Probability and Statistics*, volume 1, pages 611–644, 1961.

[SKS09]   H. Suraweera, G. Karagiannidis, and P. Smith. Performance analysis of the dual-hop asymmetric fading channel. *IEEE Transactions on Wireless Communications Letters*, 8:2783–2788, 2009.

[SLL+09]   H.A. Suraweera, R.H.Y. Louie, Y. Li, G.K. Karagiannidis, and B. Vucetic. Two hop amplify-and-forward transmission in mixed Rayleigh and Rician fading channels. *IEEE Communications Letters*, 13(4):227–229, April 2009.

[SSA06]   H. A. Suraweera, P. J. Smith, and J. Armstrong. Outage probability of cooperative relay networks in nakagami-m fading channels. *IEEE Communications Letters*, 10(12):834–836, December 2006.

[SSL05]   A. K. Sadek, W. Su, and K. J. R. Liu. Clustered cooperative communications in wireless networks. In *IEEE Proc. IEEE GLOBECOM 2005*, volume 3, pages 1157–1161, 2005.

[SSL07a]   A. K. Sadek, W. Su, and K. J. R. Liu. Multinode cooperative communications in wireless networks. *IEEE Transactions Signal Processing*, 55(1):341–355, 2007.

[SSL07b]   A. K. Sadek, W. Su, and K. J. R. Liu. Multinode cooperative communications in wireless networks. *IEEE Transaction on Signal Processing*, 55(1):341–355, Jan. 2007.

[SSL08]   W. Pam Siriwongpairat, A. K. Sadek, and K. J. Ray Liu. Cooperative communications protocol for multiuser ofdm networks. *IEEE Transactions on Wireless Communications*, 7(7):2430–2435, 2008.

[SW08]   B.J. Sepko and Lee Wookwon. A study on effect of interference in cooperative communication. In *IEEE Proc. IEEE Symposium on Radio and Wireless 2008*, pages 651–654, 2008.

[SWL06]   A. K. Sadek, Y. Wei, and K. J. R. Liu. When does cooperation have better performance in sensor networks? In *IEEE Proc. IEEE SECON 2006*, pages 188–197, 2006.

[WCG06]   T. Wang, A. Cano, and G. B. Giannakis. Link-adaptive cooperative communications without channel state information. In *IEEE Proc. IEEE MILCOM 2006*, pages 1–7, 2006.

[WSL+07]   Z. Wen, X. Shen, F. Lin, T. Luo, and G. Yue. Impact of mobility on ber in wireless cooperative networks. In *IEEE Proc. IEEE Intl. Workshop on Anti-counterfeiting, Security and Identification 2007*, pages 302–305, 2007.

[WZN08]   Y. Wu, X. Zhu, and A. K. Nandi. Low complexity adaptive Turbo frequency-domain channel estimation for single-carrier multi-user detection. *IEEE Transaction on Wireless Communicaiton*, 7:4094–237, Nov. 2008.

[XLZY09]   F. Xu, F. C. M. Lau, Q. F. Zhou, and D. W. You. Outage peformance of cooperative communication systems using opportunistic relaying and selection combining receiver. *IEEE Singal Processing Letters*, 16:113–116, 2009.

[YDGL08]   J. Youssef, B. Denis, C. Godin, and S. Lesecq. Reducing the complexity order of position estimators with combined radiolocation measurements. In *Canadian Conference on Electrical and Computer Engineering*, 2008.

[YH07]   L. Yi and J. Hong. A new cooperative communication mac strategy for wireless ad hoc networks. In *IEEE Proc. 6th IEEE/ACIS 2007*, pages 569–574, 2007.

[YL05]   M. Yu and J. Li. Is amplify-and-forward practically better than decode-and-forward or vice versa? In *IEEE ICASSP 2005*, pages 365–368, 2005.

[ZAL05]   Y. Zhao, R. Adve, and T. J. Lim. Outage probability at arbitrary SNR with cooperative diversity. *IEEE Communications Letters*, 9:700–703, 2005.

[ZAL06]   Y. Zhao, R. Adve, and T. J. Lim. Symbol error rate of selection Amplify-and-Forward relay systems. *IEEE Communications Letters*, 10:757–759, 2006.

[ZC05]   H. Zhu and G. Cao. rDCF: A relay-enabled medium access control protocol for wireless ad hoc networks. In *Proceedings IEEE INFOCOM 2005. 24th Annual Joint Conference of the IEEE Computer and Communications Societies*, volume 1, 2005.

[ZCZ$^+$09] G. Zhang, L. Cong, L. Zhao, K. Yang, and H. Zhang. Competitve resource sharing based on game theory in cooperative relay networks. *ETRI Journal*, 31(1):89–91, February 2009.

[ZMT08]   Y. Zhang, Y. Ma, and R. Tafazolli. Modulation-adaptive cooperation schemes for wireless networks. In *VTC08' Spring*, May 2008.

[ZR03]   M. Zorzi and R.R. Rao. Geographic random forwarding (geraf) for ad hoc and sensor networks: multihop performance. *IEEE Transactions on Mobile Computing*, 2(4):337–348, 2003.

[ZV05]   B. Zhao and M. C. Valenti. Practical relay networks: a generalization of hybrid-ARQ. *IEEE Journal on Selected Areas in Communications*, 23(1):7–18, 2005.

[ZZC$^+$07] Z. Zhou, S. Zhou, J.H. Cui, Jun-Hong, and S. Cui. Energy-efficient cooperative communication based on power control and selective relay in wireless sensor networks. In *IEEE Proc. MILCOM 2007*, pages 1–7, 2007.

[ZZS$^+$04] J. Zhang, Q. Zhang, C. Shao, Y. Wang, and Z. Zhang. Adaptive optimal transmit power allocation for two-hop non-regenerative wireless relaying system. In *VTC Spring*, pages 1213–1217, May 2004.

[ZZZ09]   Y. Zou, B. Zheng, and J. Zhu. Outage analysis of opportunistic cooperation over Rayleigh fading channels. *IEEE Transactions on Wireless Communications*, 8(6):3077–3085, June 2009.